AD-A182 119 RADIATIVE AND CONVECTIVE HEAT TRANSFER OVER ABLATING COMPOSITE FLAT SURFA (U) ADVANCED TECHNOLOGIES AND TESTING LABS GREENSBORO NC D Y GOSWAMI 22 APR 87 1/2

UNCLASSIFIED AFOSR-TR-87-0818 F49620-86-C-0118 F/G 20/13 NL

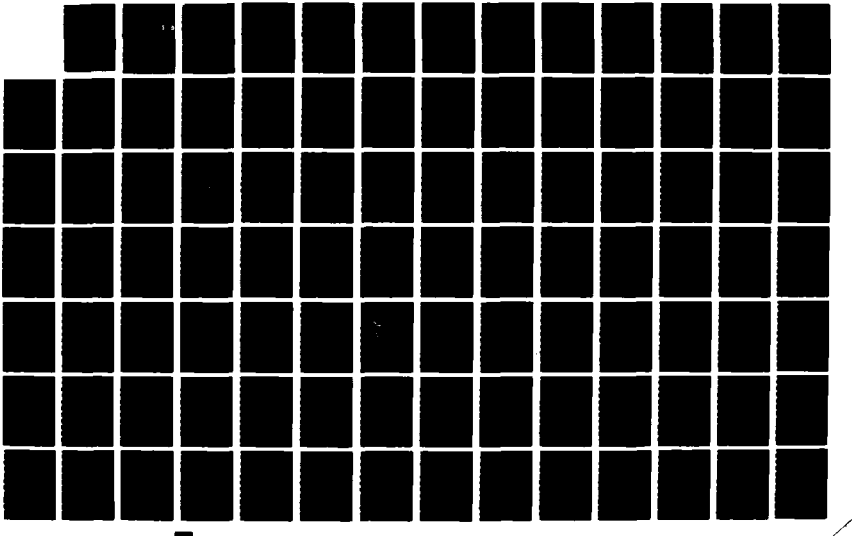

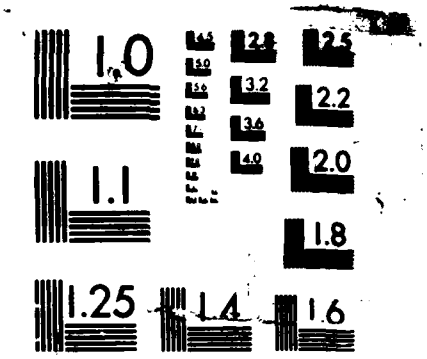

MICROCOPY RESOLUTION TEST CHART

RADIATIVE AND CONVECTIVE HEAT TRANSFER OVER ABLATING COMPOSITE FLAT SURFACE IN HYPERSONIC FLOW REGIME

Advanced Technologies & Testing Laboratories
2109 Kylemore Dr.
Greensboro, N.C. 27406

Dr. D. Yogi Goswami, Principal Investigator

April 1987

Final Report for period September 1, 1986 to March 1, 1987
Contract # F49620-86-C-0118

Dr. Anthony Amos, Program Manager

Air Force Office of Scientific Research
Building 410
Bolling AFB, DC 20332-6448

ADA 182119

REPORT DOCUMENTATION PAGE

1a. REPORT SECURITY CLASSIFICATION Unclassified	1b. RESTRICTIVE MARKINGS
2a. SECURITY CLASSIFICATION AUTHORITY	3. DISTRIBUTION / AVAILABILITY OF REPORT Approved for public release Distribution unlimited
2b. DECLASSIFICATION / DOWNGRADING SCHEDULE	
4. PERFORMING ORGANIZATION REPORT NUMBER(S) AF-7	5. MONITORING ORGANIZATION REPORT NUMBER(S) AFOSR-TR- 87-0818
6a. NAME OF PERFORMING ORGANIZATION Advanced Technologies and Testing Laboratories, Inc 6b. OFFICE SYMBOL (If applicable)	7a. NAME OF MONITORING ORGANIZATION Air Force Office of Scientific Research/NA Directorate of Aerospace Sciences
6c. ADDRESS (City, State, and ZIP Code) 2109 Kylemore Dr., Greensboro, N.C. 27406	7b. ADDRESS (City, State, and ZIP Code) Bld 410 Building 410, Bolling AFB, DC 20332-6448
8a. NAME OF FUNDING / SPONSORING ORGANIZATION Air Force Office of Scientific Research 8b. OFFICE SYMBOL (If applicable) AFOSR/NA	9. PROCUREMENT INSTRUMENT IDENTIFICATION NUMBER F49620-86-C-0118
8c. ADDRESS (City, State, and ZIP Code) Building 410 Bolling AFB DC 20332-6448	10. SOURCE OF FUNDING NUMBERS PROGRAM ELEMENT NO. 61102F PROJECT NO. ~~2302~~ 3005 TASK NO. B1 WORK UNIT ACCESSION NO.

11. TITLE (Include Security Classification)
Radiative and Convective Heat Transfer Over Ablating Composite Flat Surface in Hypersonic Flow Regime

12. PERSONAL AUTHOR(S)
Goswami, D. Y.

13a. TYPE OF REPORT	13b. TIME COVERED	14. DATE OF REPORT (Year, Month, Day)	15. PAGE COUNT
Final	FROM 9-1-86 TO 2-28-87	1987, April, 22	102

16. SUPPLEMENTARY NOTATION

17. COSATI CODES			18. SUBJECT TERMS (Continue on reverse if necessary and identify by block number)
FIELD	GROUP	SUB-GROUP	
20	11		Radiative ; Convective; Heat transfer; Absoption; Scattering; Hypersonic flow; Ablation, Radiative Properties

19. ABSTRACT (Continue on reverse if necessary and identify by block number)

A computer program was developed for predicting the convective and radiative heat transfer to the surface of a flat plate with hypersonic boundary layer flow and with injection of absorb--ing, emitting and scattering particles due to ablation. The program was used to study the heat transfer rate as a function of wall and freestream temperatures and Mach number of the flow. The results were also obtained to study the effect of injection of absorbing and scattering particles in the boundary layer on the heat flux as a function of wall and free-stream temperatures, Mach numbers and particle radiative properties. It is seen that, if there is a strong external incident radiation, the injection of scattering particles reduces the radiative flux by as much as 75% depending on the scattering coefficient of the particles and the particle density in the flow. A review of the published literature shows that the data of the radiative properties of particles is lacking. Also the data of the radiative properties of modern composite materials surfaces is not available.

20. DISTRIBUTION / AVAILABILITY OF ABSTRACT ☒ UNCLASSIFIED/UNLIMITED ☐ SAME AS RPT. ☐ DTIC USERS	21. ABSTRACT SECURITY CLASSIFICATION Unclassified
22a. NAME OF RESPONSIBLE INDIVIDUAL Dr. Anthony Amos	22b. TELEPHONE (Include Area Code) 202-767-4937 22c. OFFICE SYMBOL AFOSR/NA

DD FORM 1473, 84 MAR 83 APR edition may be used until exhausted. All other editions are obsolete.

TABLE OF CONTENTS

ABSTRACT

A computer code was developed for predicting the convective and radiative heat transfer to the surface of a flat plate with hypersonic boundary layer flow and with injection of absorbing, emitting and scattering particles due to ablation. The program was used to study the heat transfer rate as a function of wall and freestream temperatures and Mach Number of the flow. The results were also obtained to study the effect of injection of absorbing and scattering particles in the boundary layer on the heat flux as a function of wall and freestream temperatures, Mach Numbers and particle radiative properties. It is seen that, if there is strong external incident radiation, the injection of scattering particles reduces the radiative flux by as much as 75% depending on the scattering coefficient of the particles and the particle density in the flow.

A review of the published literature shows that the data of the radiative properties of particles is lacking. Also the data on the radiative properties of modern composite material surfaces is not available.

NOMENCLATURE

a_n	A tabulated coefficient dependent on the particle size parameter and refractive index
A	Defined in equation (39)
A_{sc}	Effective absorptivity in the presence of scattering
B	Defined in equation (40)
B_w, B_∞	Diffuse surface radiosity
C	Mass fraction of injected species
D_{ji}	Coefficient of Diffusion of Specie j into specie i
D_p	Diameter of spherical particles
e_b	Black body emissive power
E	Hemispherical radiant flux
ϵ_n	Nth order exponential integral function
G	Defined in equation (10)
H	Stagnation enthalpy
I	Radiation intensity
J	Change in intensity due to absorption, emission, or scattering
K	Coefficient defined by $K^2 = \alpha(\alpha+2\beta)$
l	Prandtl's mixing length
m	Coefficient defined in equation (26)
m	Real part of the complex refractive index m(1-ix)
P	Pressure
Pr	Prandtl number
P_n	Nth order Legendre polynomial
Q_c	Convective heat flux at the plate surface
Q_R	Radiative heat flux
Q_T	Total heat flux due to convection and radiation

R	Volumetric density of spontaneous radiation
R_f	Reflectivity
Re_x	Local Reynolds number
S	Scattering function
T	Temperature
u	x- component of velocity
v	y- component of velocity
x	Distance parallel to the plate surface
y	Distance normal to the plate surface
Z	Particle size parameter

Greek Letters

α	Absorption coefficient
β	Extinction coefficient
γ	Scattering coefficient
δ	Coefficient defined in equation (28)
δ_x	Boundary layer thickness
θ	Polar angle between the incident ray and the scattered ray
μ	Cosine of the angle between the direction of propagation and the x- axis
μ_{eff}	Effective viscosity
ρ	Density
φ	Azimuthal angle
ω	Solid angle
$\Omega'\Omega'$	Tabulated parameters relating γ_λ and β_λ of the particles
τ	Optical coordinate
τ_o	Optical thickness

Subscripts

a	Pertaining to absorption
e	Pertaining to emission
eff	Effective property
s	Pertaining to scattering of beam initially in the direction of propagation
s'	Pertaining to scattering of beams from all directions into the direction of propagation
x	Pertaining to location x
w	Pertaining to wall
∞	Pertaining to freestream
λ	Monochromatic or wavelength dependent property

INTRODUCTION

Prediction of radiative and convective heat transfer to the surface of a hypersonic space vehicle is very important in the design and development of such vehicles. The predicted heat flux at the surface gives an important boundary condition for the analysis of heat transfer through the skin to the inside of the vehicle. However, this is a complicated problem especially when the medium of the boundary layer participates in the radiative heat transfer. If the aerodynamic heating is so high that the vehicle surface material ablates, the problem becomes even more complicated, since the mass injection due to ablated material not only affects the flow in the boundary layer, it also affects the radiative transfer because the particles of injected mass absorb, emit and scatter thermal radiation. The ablation phenomenon can be used as a tool for structural cooling. And if intense incident radiation is expected, such as from a nuclear blast or a laser weapon, the injected particles can be used to scatter and reflect the incident radiation away from the vehicle surface. This can also be achieved by injecting particles with high back scattering coefficients, into the boundary layer.

This study was undertaken to develop a computer code for predicting convective and radiative heat transfer to the surface with hypersonic boundary layer flow and with injection of absorbing emitting and scattering particles into the boundary layer. This was done by incorporating a radiative heat transfer analysis developed by the author [1] into a turbulent boundary layer code developed by Patankar and Spalding [2]. The mass injection into the boundary layer was added into the computer code to study the effect of ablation [3].

The computer program developed in this project was used to predict the

radiative and convective heat transfer rates to a flat surface from the boundary layer and from an external radiative source. The heat transfer rates were studied as a function of wall and free stream temperatures and Mach Number of the flow. Then the results were also obtained to study the effect of injection of absorbing and scattering particles in the boundary layer on this heat flux to the surface, as a function of wall and free stream temperatures, Mach Numbers and particle radiative properties. It is seen that if there is strong incident radiation (we assumed 1,000 Btu/ft^2-sec.) the injection of scattering particles reduces the radiative heat transfer by as much as 1% to 75% depending on the scattering coefficient of the particles and the particle density (or volume fraction). This happens without much change in the temperatures in the boundary layer because the reduction in the incident radiation is mostly due to reflection to the outside rather than absorption. If there is no incident radiation from an external source and the thermal radiation is mainly due to high free-stream temperatures, the injection of scattering particles is not effective in reducing the radiative heat flux, because the scattering particles themselves emit thermal radiation at the boundary layer temperatures and offset any reduction by scattering. However, the injection from the surface reduces the temperature gradient at the surface thereby reducing the convective heat transfer and hence the total heat transfer to the surface.

The results from this study give a boundary condition for heat flux to the surface of a vehicle which can be used to predict the heat transfer and temperatures inside a composite material wall of a space vehicle. The results for conditions other than those presented, can be obtained by running the computer code developed in this study. It must, however, be pointed out that this study has some limitations which must be improved and

it raises some questions that must be addressed. A limitation of this development is the way it models ablation. The ablation process is modeled simply as injection of mass into the boundary layer, without any consideration of the enthalpy of ablation process and the various species obtained and the surface modification due to ablation. A review of the literature conducted in this study shows that the data on the radiative properties (absorption and scattering coefficients) of particles is almost non-existent. Also, the data on the radiative properties of modern composite material surfaces is not available. Another question that this study raises is how the surface ablation of the composite material affects the surface roughness which then affects the drag and the convective heat transfer to the surface. It is hoped that the deficiencies in the computer modeling and the other question raised in this study can be tackled in the Phase II of the project.

THEORETICAL DEVELOPMENT

In order to analyze the radiative and convective heat transfer in a turbulent boundary layer over a wall with surface ablation, the problem is formulated as follows:

Figure 1 shows the flow situation and the choice of coordinate system. The problem is formulated as a steady turbulent boundary layer flow of air past a flat plate at zero angle of attack. Effect of ablation is modeled as mass injection from the wall into the boundary layer. There is assumed to be no shock layer present in order to keep it purely boundary layer problem. However, output from a shock analysis could be used as input to this boundary layer problem in order to effect a solution to the entire flow field.

The governing equations for steady, two-dimensional, radiating, turbulent flow are:

(a) the conservation of mass

$$\frac{\partial}{\partial x}(\rho u) + \frac{\partial}{\partial y}(\rho v) = 0 \tag{1}$$

(b) the conservation of X-momentum

$$\rho u \frac{\partial u}{\partial x} + \rho v \frac{\partial u}{\partial y} = \frac{\partial}{\partial y}\left(\mu_{eff.} \frac{\partial u}{\partial y}\right) - \frac{dP}{dx} \tag{2}$$

(c) the conservation of energy

$$\rho u \frac{\partial H}{\partial x} + \rho v \frac{\partial H}{\partial y} = \frac{\partial}{\partial y}\left\{ \frac{\mu_{eff}}{Pr_{eff}} \frac{\partial H}{\partial y} + \mu_{eff}\left(1 - \frac{1}{Pr_{eff}}\right)\frac{1}{2}\frac{\partial u^2}{\partial y}\right\} - DIV\ Q_R \tag{3}$$

the concentration equation for the jth specie:

$$\rho u \frac{\partial C_j}{\partial x} + \rho v \frac{\partial C_j}{\partial y} - \frac{\partial}{\partial y}\left(\rho D_{ji} \frac{\partial C_j}{\partial y}\right) = 0 \tag{4}$$

where u, v, p, H and C represent the time averaged values of the fluctuating turbulent quantities. μ_{eff} and Pr_{eff} are called "effective" transport properties and refer to the turbulent and laminar contributions to shear and heat flux respectively. Expressions for these quantities are given in Appendix A. Since the flow is steady at zero angle of attack, it is quite easy to show that

$$\frac{dp}{dx} = 0 \text{ for the flat plate}$$

The last term in the equation (3), $\text{div}Q_R$, is called the <u>radiation source term</u>. In a high speed, viscous boundary layer, locally the temperature gradients in the Y-direction will be far greater than the temperature gradients in the X-direction. For this reason, a one dimensional radiative transport regime is assumed.

Therefore,

$$\text{div } Q_R = \frac{d}{dy}(Q_R) = \int_0^{\infty} \frac{dQ_{R_\lambda}}{dy} d\lambda \qquad (5)$$

This term can be calculated using a simplified analysis developed by Goswami and Vachon [1] and described in the next section.

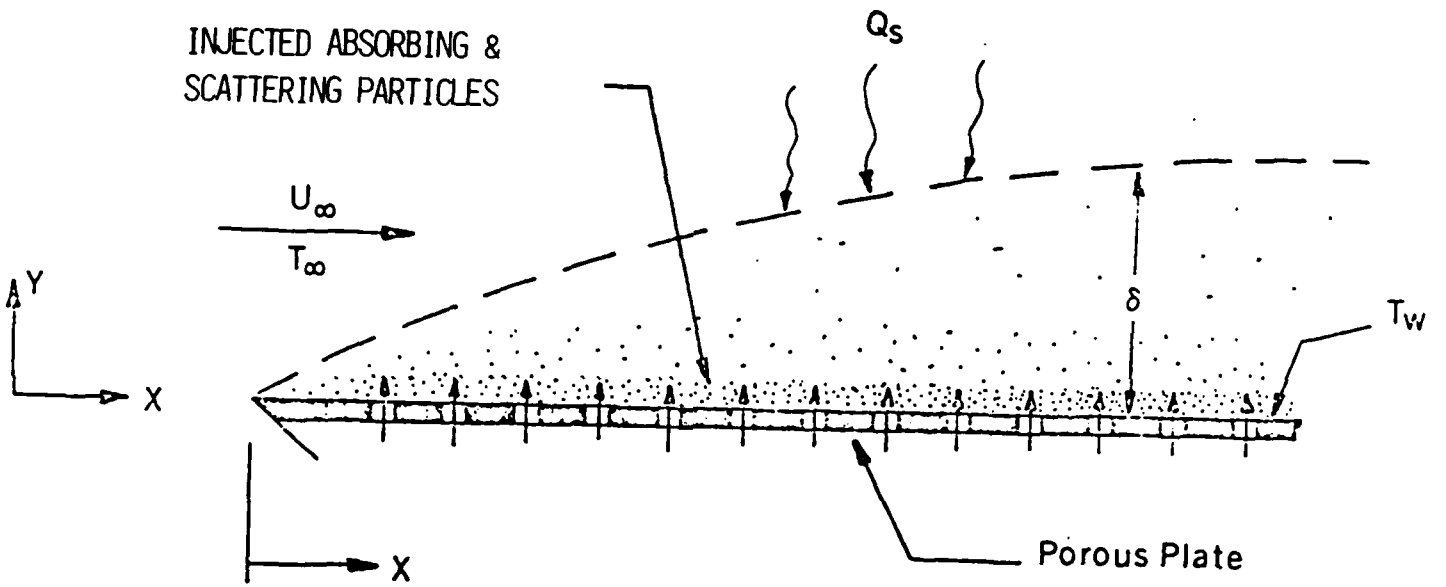

FIG. 1 SCHEMATIC OF A FLAT PLATE WITH MASS INJECTION

RADIATIVE HEAT TRANSFER ANALYSIS

This section describes the general equations of radiotive heat transfer in absorbing, emitting and scattering medium and also describes the development of a simplified analysis of the above problem. The simplified analysis was first developed by Goswami and Vachon [1] and was called as effective absorptivity analysis. Since then, the approach has become accepted in the scientific community and is now known as "SCALING" [4-6].

A. General Equations of Radiative Transfer

In order to formulate the equation for the radiative flux vector in an absorbing, emitting and scattering medium, it is necessary to develop the expression for the intensity of radiation, I_λ, within the medium. To this end, the development of Sparrow and Cess [7] is referred to.

Referring to Figure 2, the intensity of radiation within the medium, $I_\lambda(x,\theta)$, can be considered to be composed of two contributions, i.e., $I_\lambda^+(x,\theta)$ directed in the positive x direction and $I_\lambda^-(x,\theta)$ directed in the negative x direction, such that:

$$I_\lambda(x,\theta) = I_\lambda^+(x,\theta) - I_\lambda^-(x,\theta) \tag{6}$$

To find expressions for I_λ^+ and I_λ^-, a radiation balance is performed on a volume element of the medium as shown in Figure 2. As a monochromatic beam of intensity $I_\lambda^+(x, \theta)$ passes through the volume element, its intensity is changed by an amount dI_λ^+. This change consists of:

1. Attenuation of I_λ^+ due to absorption within the element by an amount $J_\lambda.a$;
2. Attenuation of I_λ^+ due to scattering by suspended particles in the medium or by the molecules of the medium by an amount $J_\lambda.s$;
3. Augmentation of I_λ^+ by an amount $J_\lambda.s'$ as a result of energy scattered into the beam from other directions;
4. Augmentation of I_λ^+ due to emission from the elemental volume by an amount $J_\lambda.e$.

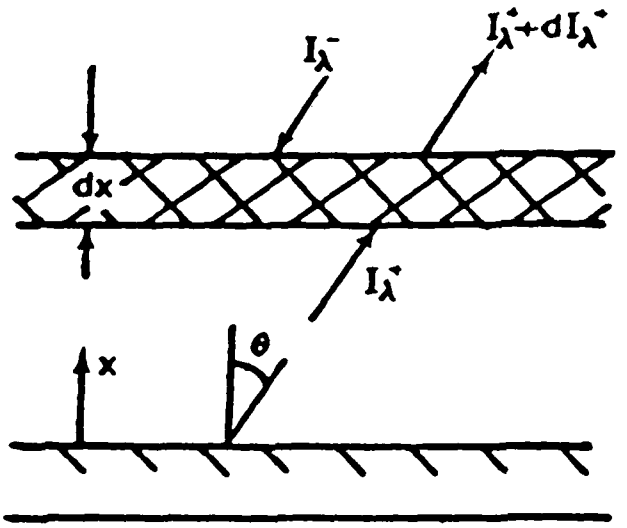

FIGURE 2. RADIATION BALANCE IN AN ELEMENTAL VOLUME

Therefore, dI_λ^+ can be written as:

$$dI_\lambda^+ = J_{\lambda,a} - J_{\lambda,s} + J_{\lambda,s'} + J_{\lambda,e} \tag{7}$$

Substituting the expressions for the term on the right hand side of equation (7), Sparrow and Cess [7] obtained the equation for I_λ^+ as

$$\mu \frac{dI_\lambda^+(\tau_\lambda,\mu,\phi)}{d\tau_\lambda} = -I_\lambda^+(\tau_\lambda,\mu,\phi) + \frac{\alpha_\lambda}{\pi\beta_\lambda} e_{b\lambda}(\tau_\lambda) + \frac{\gamma_\lambda}{4\pi\beta_\lambda} G_\lambda(\tau_\lambda) \tag{8}$$

In the same manner, they obtained the equation for I_λ^- as:

$$\mu \frac{dI_\lambda^-(\tau_\lambda,\mu,\phi)}{d\tau_\lambda} = -I_\lambda^-(\tau,\mu,\phi) + \frac{\alpha_\lambda}{\pi\beta_\lambda} e_{b\lambda}(T) + \frac{\gamma_\lambda}{4\pi\beta_\lambda} G_\lambda(\tau_\lambda) \tag{9}$$

where

$$G_\lambda(\tau_\lambda) = \int_0^{2\pi}\int_{-1}^{1} I_\lambda(\mu',\phi')S(\mu',\phi';\mu,\phi)\, d\mu' d\phi' \tag{10}$$

β_λ in the above equation is called the extinction coefficient ($\beta_\lambda=\alpha_\lambda+\gamma_\lambda$) and τ_λ is called the dimensionless optical thickness given by

$$\tau_\lambda = \int_0^x \beta_\lambda dx \tag{11}$$

Equations (8) and (9) are the equations of transfer. The boundary conditions for these equations depend on the particular problem at hand. In the case of an absorbing and emitting medium, equations (8) and (9) are simplified considerably.

In such a case

$$\beta_\lambda = \alpha_\lambda \qquad \text{and} \qquad \tau_\lambda = \int_0^x \alpha_\lambda dx$$

and (8) and (9) become

$$\mu \frac{dI_\lambda^+}{d\tau_\lambda} = -I_\lambda^+ + \frac{e_{b\lambda}}{\pi} \tag{12a}$$

$$\mu \frac{dI_\lambda^-}{d\tau_\lambda} = -I_\lambda^- + \frac{e_{b\lambda}}{\pi} \tag{12b}$$

The monochromatic radiation in the X-direction is given by

$$Q_{R\lambda}(\tau_\lambda) = \int_{4\pi} I_\lambda(\tau_\lambda,\mu,\phi)\ \mu d\omega \tag{13}$$

for a one dimensional radiative transfer case, the boundary conditions for equations (8), (9) and equations (12) can be written as:

$$\begin{aligned} &\text{at} \quad \tau_\lambda = 0 \qquad I_\lambda^+(\tau_\lambda,\mu) = I_\lambda^+(0,\mu) \\ &\text{at} \quad \tau_\lambda = \tau_{0\lambda} \qquad I_\lambda^-(\tau_\lambda,\mu) = I_\lambda^-(\tau_{0\lambda},-\mu) \end{aligned} \tag{14}$$

The expression for Q_R for absorbing, emitting and scattering media becomes

$$\begin{aligned} Q_{R\lambda}(\tau_\lambda) = {} & 2\pi\int_0^1 I_\lambda^+(0,\mu)e^{-\tau_\lambda/\mu}\ \mu d\mu - 2\pi\int_0^1 I_\lambda^-(\tau_{0\lambda},-\mu)e^{-(\tau_{0\lambda}-\tau_\lambda)/\mu}\mu d\mu \\ & + 2\int_0^{\tau_\lambda}\left[\frac{\alpha_\lambda}{\beta_\lambda}e_{b\lambda}(t) + \frac{\gamma_\lambda}{4\beta_\lambda}G_\lambda(t)\right]\epsilon_2(\tau_\lambda - t)dt \\ & - 2\int_{\tau_\lambda}^{\tau_{0\lambda}}\left[\frac{\alpha_\lambda}{\beta_\lambda}e_{b\lambda}(t) + \frac{\gamma_\lambda}{4\beta_\lambda}G_\lambda(t)\right]\epsilon_2(t-\tau_\lambda)dt \end{aligned} \tag{15}$$

where ϵ_n are the exponential integral functions defined by

$$\epsilon_n(t) = \int_0^1 \mu^{n-2} e^{-t/\mu} \, d\mu \tag{16}$$

Similarly for an absorbing and emitting medium, we have from (12), (13) and (14)

$$\begin{aligned} Q_{R\lambda}(\tau_\lambda) = {} & 2\pi \int_0^1 I_\lambda^+(0,\mu) e^{-\tau_\lambda/\mu} \mu \, d\mu - 2\pi \int_0^1 I_\lambda^-(\tau_{0\lambda},-\mu) e^{-(\tau_{0\lambda}-\tau_\lambda)/\mu} \mu \, d\mu \\ & + 2 \int_0^{\tau_\lambda} e_{b\lambda}(t) \, \epsilon_2(\tau_\lambda - t) dt - 2 \int_{\tau_\lambda}^{\tau_{0\lambda}} e_{b\lambda}(t) \, \epsilon_2(t - \tau_\lambda) dt \end{aligned} \tag{17}$$

and

$$\begin{aligned} -\frac{dQ_{R\lambda}}{d\tau_\lambda} = {} & 2\pi \int_0^1 I_\lambda^+(0,\mu) e^{-\tau_\lambda/\mu} \, d\mu + 2\pi \int_0^1 I_\lambda^-(\tau_{0\lambda},-\mu) e^{-(\tau_{0\lambda}-\tau_\lambda)/\mu} \, d\mu \\ & + 2\pi \int_0^{\tau_{0\lambda}} e_{b\lambda}(t) \, \epsilon_1(|\tau_\lambda - t|) dt - 4 \, e_{b\lambda}(t) \end{aligned} \tag{18}$$

Equations (8), (9), and (14) are quite difficult to solve numerically and result in a very complex computer program.

An alternative analysis has been developed using a different approach which results in considerable simplification in the radiative transfer analysis for an absorbing, emitting, and scattering medium. This development is described in the next section.

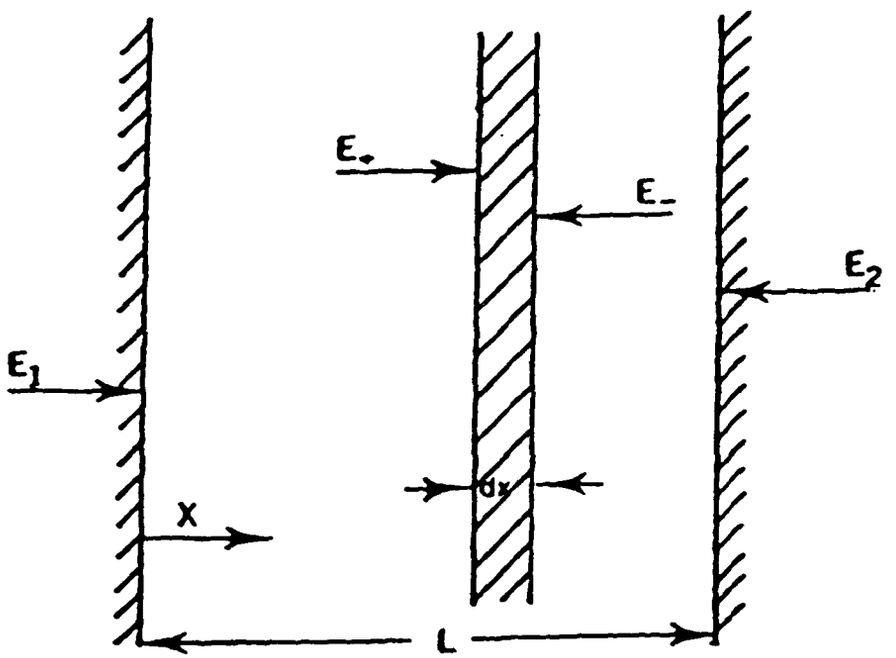

FIGURE 3 COORDINATE SCHEME FOR RADIATIVE HEAT TRANSFER BETWEEN TWO INFINITE PARALLEL PLATES

B. Effective Absorptivity Analysis

It can be seen from the previous section that by assuming the scattering coefficient γ_λ to be zero, and therefore $\beta_\lambda = \alpha_\lambda$, the equations 8, 9, and 15 can be simplified considerably to become equations 12a, 12b and 17 respectively. The simplified equations 12 and 17 neglect scattering. If, however, an expression for the absorption coefficient can be found that includes the effect of scattering, then equations 12 and 17 will describe radiative heat transfer in an absorbing, emitting and scattering medium. This is precisely what is done in the Effective Absorptivity Analysis described below:

Consider a case of radiative heat transfer between two infinite parallel plates with an intervening medium of an absorbing, emitting and scattering gas (Figure 3). Consider a thin layer of the gas in the medium. Assume the radiant heat flux vector to be in the form of a difference of two fluxes in the X-direction flowing in opposite directions. The differential equations for the intensity of radiation I_λ^+ and I_λ^-, as derived earlier can be written as:

$$\mu \frac{dI_\lambda^+(\mu,x)}{dx} = -\beta_\lambda I_\lambda^+(\mu,x) + \frac{\gamma_\lambda}{4\pi}\int_{4\pi} I_\lambda(\mu',x)S(\mu',\mu)d\omega' + \frac{\alpha_\lambda e_{b\lambda}}{\pi}$$

$$\mu \frac{dI_\lambda^-(\mu,x)}{dx} = -\beta_\lambda I_\lambda^-(\mu,x) + \frac{\gamma_\lambda}{4\pi}\int_{4\pi} I_\lambda(\mu',x)S(\mu',\mu)d\omega' + \frac{\alpha_\lambda e_{b\lambda}}{\pi}$$

Integration of (B) over a hemisphere gives:

$$\int_{2\pi_+} \frac{d}{dx}(I_\lambda^+\mu)d\omega = -\alpha_\lambda \int_{2\pi_+} I_\lambda^+(\mu,x)d\omega - \gamma_\lambda \int_{2\pi_+} I_\lambda^+(\mu,x)d\omega \qquad (19)$$

$$+ \frac{\gamma_\lambda}{4\pi}\int_{2\pi_+} d\omega \int_{4\pi} I_\lambda(\mu',x)S(\mu',\mu)d\omega' + 2\alpha_\lambda e_{b\lambda}$$

Here $\int_{2\pi_+}$ represents integration over hemispherical solid angle (Figure 3) such that μ, measured from the positive normal, varies from 1 to 0 and $\int_{2\pi_-}$ represents integration over a hemispherical solid angle such that μ measured from the positive normal varies from 0 to -1.

The second term on the right hand side of (19) can be written as

$$-\gamma_\lambda \int_{2\pi_+} I_\lambda^+(\mu,x)d\omega = -\gamma_\lambda \int_{2\pi_+} I_\lambda^+(\mu',x)d\omega'$$

$$= -\frac{\gamma_\lambda}{4\pi}\int_{2\pi_+}\left[I_\lambda^+(\mu',x)\int_{4\pi} S(\mu,\mu')d\omega\right]d\omega'$$

$$\left[\because \frac{1}{4\pi}\int_{4\pi} S(\mu,\mu')d\omega = 1\right] \qquad (20)$$

$$= -\frac{\gamma_\lambda}{4\pi}\int_{4\pi} d\omega \int_{2\pi_+} I_\lambda^+(\mu',x)S(\mu,\mu')d\omega'$$

Substituting (18) in (19), we get the right hand side equal to

$$-\alpha_\lambda \int_{2\pi_+} I_\lambda^+(\mu,x)d\omega - \frac{\gamma_\lambda}{4\pi}\left[\int_{2\pi_+} d\omega \int_{2\pi_+} I_\lambda^+(\mu',x)S(\mu,\mu')d\omega\right.$$

$$\left. + \int_{2\pi_-} d\omega \int_{2\pi_+} I_\lambda^+(\mu',x)S(\mu,\mu')d\omega'\right] + \frac{\gamma_\lambda}{4\pi}\left[\int_{2\pi_+} d\omega \int_{2\pi_+} I_\lambda(\mu',x)S(\mu,\mu')d\omega'\right.$$

$$\left. + \int_{2\pi_+} d\omega \int_{2\pi_-} I_\lambda(\mu',x)S(\mu,\mu')d\omega'\right] + 2\alpha_\lambda e_{b\lambda}$$

Noting that integration of I_λ on $2\pi_+$ will be the same as integration of I_λ^+ on $2\pi_+$, equation (19) becomes

$$\frac{d}{dx}\int_{2\pi_+} I_\lambda \mu d\omega = -\alpha_\lambda \int_{2\pi_+} I_\lambda(\mu,x)d\omega - \frac{\gamma_\lambda}{4\pi}\int_{2\pi_-} d\omega \int_{2\pi_+} I_\lambda(\mu',x)S(\mu,\mu')d\omega' \qquad (21)$$

$$+ \frac{\gamma_\lambda}{4\pi}\int_{2\pi_+} d\omega \int_{2\pi_-} I_\lambda(\mu',x)S(\mu,\mu')d\omega' + 2\alpha_\lambda e_{b\lambda}$$

Equation (21) can be written in compact form as:

$$\frac{dE_{\lambda+}}{dx} = -(\alpha_\lambda + \delta_{\lambda_+}\gamma_\lambda)m_{\lambda_+}E_{\lambda_+} + \delta_{\lambda_-}\gamma_\lambda m_{\lambda_-}E_{\lambda_-} + \frac{R_\lambda}{2} \tag{22a}$$

Similarly, from (8b) one can get:

$$\frac{dE_{\lambda-}}{dx} = (\alpha_\lambda + \delta_{\lambda_-}\gamma_\lambda)m_{\lambda_-}E_{\lambda_-} - \delta_{\lambda_+}\gamma_\lambda m_{\lambda_+}E_{\lambda_+} + \frac{R_\lambda}{2} \tag{22b}$$

Equations (22a) and (22b) are the differential equations for the fluxes E_{λ_+} and E_{λ_-}. In these equations, the terms are defined as follows:

$$E_{\lambda_+} = \int_{2\pi_+} I_\lambda \mu d\omega \tag{23}$$

$$E_{\lambda_-} = \int_{2\pi_-} I_\lambda \mu d\omega \tag{24}$$

R_λ = Spectral volumetric density of spontaneous radiation.

$$= 4\alpha_\lambda e_{b\lambda} \tag{25}$$

and

$$m_{\lambda_+} = \frac{\int_{2\pi_+} I_\lambda(\mu,x)d\omega}{\int_{2\pi_+} I_\lambda(\mu,x)\mu d\omega} \tag{26}$$

$$m_{\lambda_-} = \frac{\int_{2\pi_-} I_\lambda(\mu,x)d\omega}{\int_{2\pi_-} I_\lambda(\mu,x)\mu d\omega} \tag{27}$$

$$\delta_{\lambda_+} = \frac{\int_{2\pi_-} d\omega \int_{2\pi_+} I_\lambda(\mu',x)S(\mu,\mu')d\omega'}{4\pi \int_{2\pi_+} I_\lambda(\mu',x)d\omega'} \tag{28}$$

$$\delta_{\lambda_-} = \frac{\int_{2\pi_+} d\omega \int_{2\pi_-} I_\lambda(\mu',x)S(\mu,\mu')d\omega'}{4\pi \int_{2\pi_-} I_\lambda(\mu',x)d\omega'} \tag{29}$$

If I_λ is isotropic within the limits of the hemispherical angle m_{λ_+} and m_{λ_-} turn out to be equal [8].

$$m_{\lambda_+} = m_{\lambda_-} = m_\lambda = 2$$

while the coefficients δ_{λ_+} and δ_{λ_-} for the axisymmetrical characteristic curves of arbitrary shape are also found to be equal to one another and are determined from the following:

$$\delta_{\lambda_+} = \delta_{\lambda_-} = \delta_\lambda = \frac{1}{8\pi^2} \int_{2\pi^+} d\omega \int_{2\pi_-} S(\mu,\mu')d\omega' \qquad (30)$$

From (22a) and (22b)

$$\frac{d(E_{\lambda_+} + E_{\lambda_-})}{dx} = \frac{d\epsilon_\lambda^+}{dx} = -2(\alpha_\lambda+2\delta_\lambda\gamma_\lambda)E_{\lambda_+}+2(\alpha_\lambda+2\delta_\lambda\gamma_\lambda)E_\lambda + R_\lambda$$

$$= -2(\alpha_\lambda+2\delta_\lambda\gamma_\lambda)\epsilon_\lambda^- + R_\lambda$$

and

$$\frac{d(E_{\lambda_+} - E_{\lambda_-})}{dx} = \frac{d\epsilon_\lambda^-}{dx} = -2\alpha_\lambda E_{\lambda_+} - 2\alpha_\lambda E_{\lambda_-}$$

$$= -2\alpha_\lambda\epsilon_\lambda^+$$

$$\frac{d\epsilon_\lambda^+}{dx} = -2(\alpha_\lambda + 2\delta_\lambda\gamma_\lambda)\epsilon_\lambda^- + R_\lambda$$

$$\frac{d\epsilon_\lambda^-}{dx} = -2\alpha_\lambda\epsilon_\lambda^+$$

from (31) and (32) one obtains

$$\frac{d^2\epsilon_\lambda^-}{dx^2} - 4K_\lambda^2\epsilon_\lambda^- = -2\alpha_\lambda R_\lambda \qquad (33)$$

where

$$K_\lambda^2 = \alpha_\lambda(\alpha_\lambda + 2\delta_\lambda\gamma_\lambda) \tag{34}$$

The solution of this equation is found to be

$$c_\lambda^- = Ae^{2K_\lambda x} + Be^{-2K_\lambda x} + \frac{\alpha_\lambda R_\lambda}{2K_\lambda^2} \tag{35}$$

and

$$c_\lambda^+ = -\frac{K_\lambda}{\alpha_\lambda}\left[Ae^{2K_\lambda x} - Be^{-2K_\lambda x}\right] \tag{36}$$

Therefore E_{λ_+} and E_{λ_-} are obtained as

$$E_{\lambda_+} = \frac{A}{2}\left(1 - \frac{K_\lambda}{\alpha_\lambda}\right)e^{2K_\lambda x} + \frac{B}{2}\left(1 + \frac{K_\lambda}{\alpha_\lambda}\right)e^{-2K_\lambda x} + \frac{\alpha_\lambda R_\lambda}{4K_\lambda^2} \tag{37}$$

$$E_{\lambda_-} = -\frac{A}{2}\left(1 + \frac{K_\lambda}{\alpha_\lambda}\right)e^{2K_\lambda x} + \frac{B}{2}\left(\frac{K_\lambda}{\alpha_\lambda} - 1\right)e^{-2K_\lambda x} - \frac{\alpha_\lambda R_\lambda}{4K_\lambda^2} \tag{38}$$

Boundary conditions for the layer are

$$E_{\lambda_+}\Big|_{x=x_1} = E^+_{\lambda x_1} \quad \text{and} \quad E_{\lambda_-}\Big|_{x=x_2} = E^-_{\lambda x_2}$$

Substitution of these conditions in (37) and (38) gives A and B as

$$A = \frac{2\left(1-\frac{K_\lambda}{\alpha_\lambda}\right)e^{-2K_\lambda x_2}E^+_{\lambda x_1} + 2\left(1+\frac{K_\lambda}{\alpha_\lambda}\right)e^{-2K_\lambda x_1}E^-_{\lambda x_2} - \frac{\alpha_\lambda R_\lambda}{2K_\lambda^2}\left[\left(1-\frac{K_\lambda}{\alpha_\lambda}\right)e^{-2K_\lambda x_2} - \left(1+\frac{K_\lambda}{\alpha_\lambda}\right)e^{-2K_\lambda x_1}\right]}{\left(1-\frac{K_\lambda}{\alpha_\lambda}\right)^2 e^{2K_\lambda(x_1-x_2)} - \left(1+\frac{K_\lambda}{\alpha_\lambda}\right)^2 e^{-2K_\lambda(x_1-x_2)}} \quad (39)$$

$$B = \frac{2E^+_{\lambda x_1} - A\left(1-\frac{K_\lambda}{\alpha_\lambda}\right)e^{2K_\lambda x_1} - \frac{\alpha_\lambda R_\lambda}{2K_\lambda^2}}{\left(1+\frac{k_\lambda}{\alpha_\lambda}\right)e^{-2K_\lambda x_1}} \quad (40)$$

Transmissivity of the layer from x_1 to x_2 is

$$D = \frac{E_{\lambda_+}\Big|^{x=x_2}_{E^-_{\lambda x_2}=0}}{E^+_{\lambda x_1}} = \frac{1}{E^+_{\lambda x_1}}\left[\frac{A_D}{2}\left(1-\frac{K_\lambda}{\alpha_\lambda}\right)e^{2K_\lambda x_2} + \frac{B_D}{2}\left(1+\frac{K_\lambda}{\alpha_\lambda}\right)e^{-2K_\lambda x_2} + \frac{\alpha_\lambda R_\lambda}{4K_\lambda^2}\right] \quad (41)$$

where

$$A_D = \frac{2\left(1-\frac{K_\lambda}{\alpha_\lambda}\right)e^{-2K_\lambda x_2}E^+_{\lambda x_1} - \frac{\alpha_\lambda R_\lambda}{2K_\lambda^2}\left[\left(1-\frac{K_\lambda}{\alpha_\lambda}\right)e^{-2K_\lambda x_2} - \left(1+\frac{K_\lambda}{\alpha_\lambda}\right)e^{-2K_\lambda x_1}\right]}{\left(1-\frac{K_\lambda}{\alpha_\lambda}\right)^2 e^{2K_\lambda(x_1-x_2)} - \left(1+\frac{K_\lambda}{\alpha_\lambda}\right)^2 e^{-2K_\lambda(x_1-x_2)}} \quad (42)$$

and

$$B_D = \frac{2E^+_{\lambda x_1} - A_D\left(1-\frac{K_\lambda}{\alpha_\lambda}\right)e^{2K_\lambda x_1} - \frac{\alpha_\lambda R_\lambda}{2K_\lambda^2}}{\left(1+\frac{K_\lambda}{\alpha_\lambda}\right)e^{-2K_\lambda x_1}} \quad (43)$$

Reflectivity "R_f" of the layer is

$$R_f = \frac{E_\lambda - \Big|_{E^-_{\lambda x_2}=0}^{x=x_1}}{E^+_{\lambda x_1}} = \frac{1}{E^+_{\lambda x_1}} \left[-\frac{A_D}{2}\left(1 + \frac{K_\lambda}{\alpha_\lambda}\right) e^{2K_\lambda x_1} - \frac{B_D}{2}\left(1 - \frac{K_\lambda}{\alpha_\lambda}\right) e^{-2K_\lambda x_1} - \frac{\alpha_\lambda R_\lambda}{4K_\lambda} \right] \tag{44}$$

Absorptivity "A_{sc}" = 1 - D - R_f

$$= 1 - \frac{1}{E^+_{\lambda x_1}} \left[\frac{A_D}{2} \left\{ \left(1 - \frac{K_\lambda}{\alpha_\lambda}\right) e^{2K_\lambda x_2} - \left(1 + \frac{K_\lambda}{\alpha_\lambda}\right) e^{2K_\lambda x_1} \right\} + \frac{B_D}{2} \left\{ \left(1 + \frac{K_\lambda}{\alpha_\lambda}\right) e^{-2K_\lambda x_2} - \left(1 \mp \frac{K_\lambda}{\alpha_\lambda}\right) e^{-2K_\lambda x_1} \right\} \right] \tag{45}$$

Equation (45) is the expression for absorptivity which includes the effect of scattering. This is given the name "effective absorptivity in the presence of scattering."

Recalling that

$$\text{Absorptivity } A(x) = 1 - e^{-\alpha_\lambda x} \tag{46}$$

an effective absorption coefficient $\alpha_{\lambda_{sc}}$ can be obtained from the effective absorptivity of a layer of thickness $(x_2 - x_1)$ from the relation

$$A_{sc} = 1 - e^{-\alpha_{\lambda sc}(|x_2 - x_1|)} \tag{47}$$

$\alpha_{\lambda_{sc}}$ thus calculated is the coefficient which takes into account the effect of scattering. Absorption coefficients calculated by this method are used

in the calculation of heat radiation from equations (17) and (18):

$$Q_{R_\lambda}(\tau_\lambda) = 2\pi \int_0^1 I_\lambda^+(o,\mu) e^{-\tau_\lambda/\mu} \mu d\mu - 2\pi \int_0^1 I_\lambda^-(\tau_{o\lambda},-\mu) e^{-(\tau_{o\lambda}-\tau_\lambda/\mu} \mu d\mu$$

$$+ 2\int_0^{\tau_\lambda} e_{b\lambda}(t) \epsilon_2(\tau_\lambda - t)dt - 2\int_{\tau_\lambda}^{\tau_{o\lambda}} e_{b\lambda}(t)\epsilon_2(t-\tau_\lambda)dt \qquad (17)$$

and

$$\frac{dQ_{R_\lambda}}{d\tau_\lambda} = 2\pi \int_0^1 I_\lambda^+(o,\mu) e^{-\tau_\lambda/\mu} d\mu + 2\pi \int_0^1 I_\lambda^-(\tau_{o\lambda},-\mu) e^{-(\tau_{o\lambda}-\tau_\lambda/\mu} d\mu$$

$$+ 2\int_0^{\tau_{o\lambda}} e_{b\lambda}(t)\epsilon_1(|\tau_\lambda - t|) - 4e_{b\lambda}(\tau_\lambda) \qquad (18)$$

τ_λ in these equations is

$$\tau_\lambda = \int_0^x \alpha_{\lambda sc} dx \qquad (48)$$

It should be noted that the above equations (17 and (18) are for an absorbing and emitting medium. By substituting the coefficient α_{sc} calculated from (45) and (47) for the regular absorption coefficient α_λ, these equations will describe the radiation transfer for an absorbing, emitting, and scattering medium.

Assume that the wall surface is black with respect to radiation, and that any radiation incident on the edge of the boundary layer has a wavelength distribution identical to a perfect radiator, and furthermore, that radiation emitted from the surface or at the edge of the boundary layer is emitted diffusely. Then

$$I_\lambda^+(0,\mu) = \frac{B_{w_\lambda}}{\pi} = \frac{e_{b_{w_\lambda}}}{\pi} \quad , \qquad I_\lambda^-(\tau_{0\lambda},-\mu) = \frac{B_{-\lambda}}{\pi} = \frac{e_{b-_\lambda}}{\pi} \tag{49}$$

where $B_{w\lambda}$ and $B_{\infty\lambda}$ are the surface radiosities. It follows immediately that

$$2\pi\int_0^1 I_\lambda^+(0,\mu)\, e^{-\tau_\lambda/\mu}\, \mu d\mu = 2e_{b_{w_\lambda}} c_3(\tau_\lambda) \tag{50}$$

$$2\pi\int_0^1 I_\lambda^-(\tau_{0_\lambda},-\mu)\, e^{-(\tau_{0_\lambda}-\tau_\lambda)/\mu}\, \mu d\mu = 2e_{b_{-_\lambda}} c_3(\tau_{0_\lambda}-\tau_\lambda) \tag{51}$$

$$2\pi\int_0^1 I_\lambda^+(0,\mu)\, e^{-\tau_\lambda/\mu}\, d\mu = 2e_{b_{w_\lambda}} c_2(\tau_\lambda) \tag{52}$$

$$2\pi\int_0^1 I_\lambda^-(\tau_{0_\lambda},-\mu)\, e^{-(\tau_{0_\lambda}-\tau_\lambda)/\mu}\, d\mu = 2e_{b_{-_\lambda}} c_2(\tau_{0_\lambda}-\tau_\lambda) \tag{53}$$

Now equation (5) becomes

$$-\text{div } Q_R = \int_0^\infty 2a_{\lambda_{SC}} \Big\{ e_{b_{w_\lambda}} c_2(\tau_\lambda) + e_{b_{-_\lambda}} c_2(\tau_{0_\lambda}-\tau_\lambda) + \int_0^{\tau_{0\lambda}} e_{b_\lambda}(t)\, c_1(|\tau_\lambda - t|)\, dt - 2e_{b_\lambda}(\tau_\lambda) \Big\}\, d\lambda \tag{53}$$

Scattering Function

The scattering function $S_\lambda(\theta', \phi'; \theta, \phi)$, sometimes called phase function, characterizes the directional distribution of the scattered energy, such that

$$S_\lambda(\theta', \phi'; \theta, \phi) \frac{d\omega}{4\pi}$$

represents the probability that radiation in the frequency interval d_λ centered at λ and from a direction $(\theta'\phi')$ will be deflected in a direction (θ, ϕ) within a solid angle "d_ω". Figure 4 shows a coordinate scheme for the scattering function. The integral of this quantity over all the solid angles should, therefore, be equal to 1.

$$\text{i.e.} \qquad \frac{1}{4\pi} \int_{4\pi} S_\lambda(\theta', \phi'; \theta, \phi)\, d\omega = 1$$

Scattering by a single particle is called "single scattering." If a relatively few particles exist in the volume, the scattering can still be characterized by "single scattering" but will have an amplitude proportional to the number of particles in the volume. As the number of particles is increased, each particle is subjected to increased radiation scattered by other particles. This type of scattering is characterized by "multiple scattering."

Analytical determination of the scattering function is made by solving Maxwell's Equations for the propagation of electromagnetic waves with the appropriate boundary conditions. The problem was first solved by Gustav Mie. The development and results were reviewed in detail by Van De Hulst (8) and will not be given here. According to Mie's theory, for homogeneous spheres, the scattering function may be expressed as a function of the size parameter "Z" and the refractive index "$\bar{m}$-ix" of the sphere with respect to

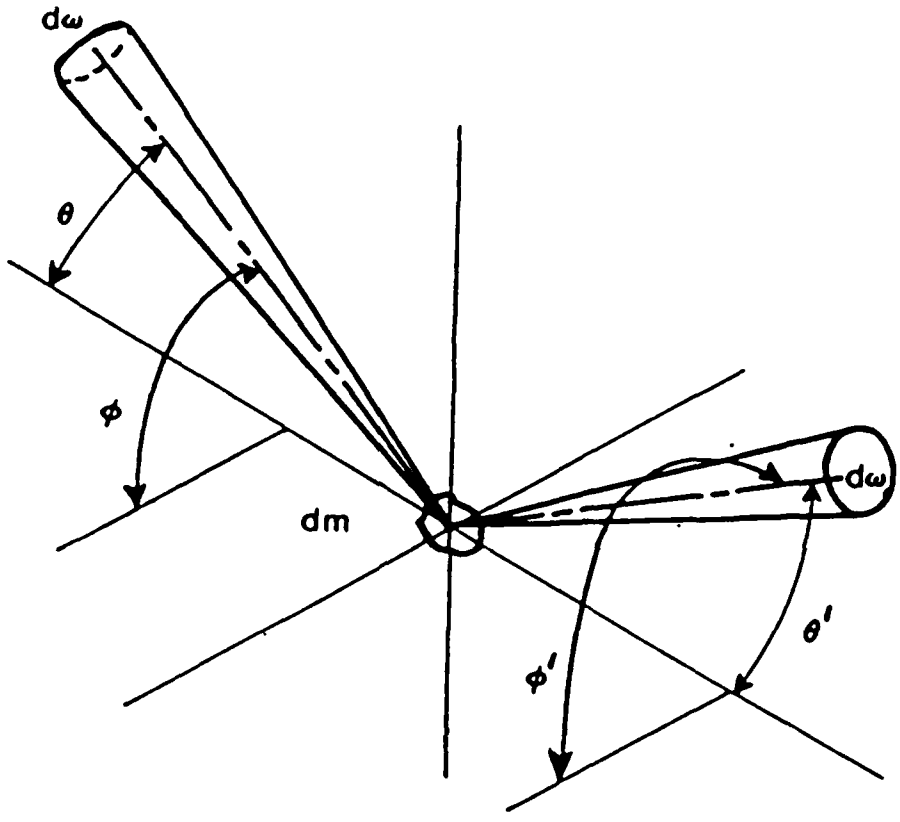

FIGURE 4. COORDINATE SCHEME FOR SCATTERING FUNCTION

the surrounding medium.

$$Z = \frac{\pi D_p}{\lambda} \tag{55}$$

where

D_p = Diameter of the particle

λ = Wavelength of radiation

For values of Z<<1, a simpler formulation developed by Rayleigh holds and for large values of Z, principles of geometrical optics are often utilized. The computation of the scattering function is thus frequently classified as below:

$Z << 1$ Rayleigh scattering

$Z \approx 1$ Mie scattering

$Z >> 1$ Geometrical scattering

When the scattered radiation is spread equally in all directions, it is known as isotropic scattering.

$$S_\lambda(\theta', \phi'; \theta, \phi) = 1 \tag{56}$$

The scattering function for RAyleigh scattering can be written in the form

$$S_\lambda(\theta', \phi'; \theta, \phi) = \frac{3}{4}(1+\cos^2\theta) \tag{57}$$

Here θ represents the polar angle between the incident ray and the scattered ray.

In this study, <u>axially symmetric scattering</u> functions have been used. An axially symmetric scattering function is defined as describing the condition in which the intensity of radiation scattered from a pencil of rays incident on an elemental volume is axially symmetric with respect to the direction of the incident pencil. A further requirement is that the scattered intensity be independent of the direction of the incident pencil

with respect to the axis of the system. Thus for the case of a particle with an axially symmetric scattering function, the function may be tabulated as a function of a single angle (usually the angle between the scattered ray and the forward direction of the incident pencil of rays). The assumption of axially symmetric scattering function has been shown to be a reasonable assumption for random orientation of particles by Love and Beattie [9]. They presented measurements for clouds of aluminum particles, iron, glass, and silica particles. A typical plot of the experimentally obtained scattering function is given in Figure 5.

In this study, the work of Chu, Churchill and Clark [10] was used to compute the scattering functions. They prepared their values for real refractive index and axially symmetric scattering. The extinction and scattering coefficients were taken from the work of Chromey [11] and are presented in Figures 6 and 7.

Chu, Churchill and Clark [10] have published a table of coefficients to be used in a Legendre Polynomial representation of the scattering function for spheres having real refractive indices ranging from $\bar{m} = 0.9$ to $\bar{m} = 2.0$ and $\bar{m} = \infty$ and for values of Z from 1 to 30. In their representation, the scattering function is expressed as

$$S(\theta) = 1 + \sum_{n=1}^{n=\infty} a_n P_n(\text{Cos}\theta) \qquad (58)$$

where $S(\theta)$ is the axially symmetric scattering function, a_n are tabulated coefficients dependent on the particle size parameter "Z" and the refractive index "$\bar{m}$." $p_n(\text{Cos}\,\theta)$ are the nth order Legendre Polynomials with the argument $\text{Cos}\theta$ and θ is a polar angle.

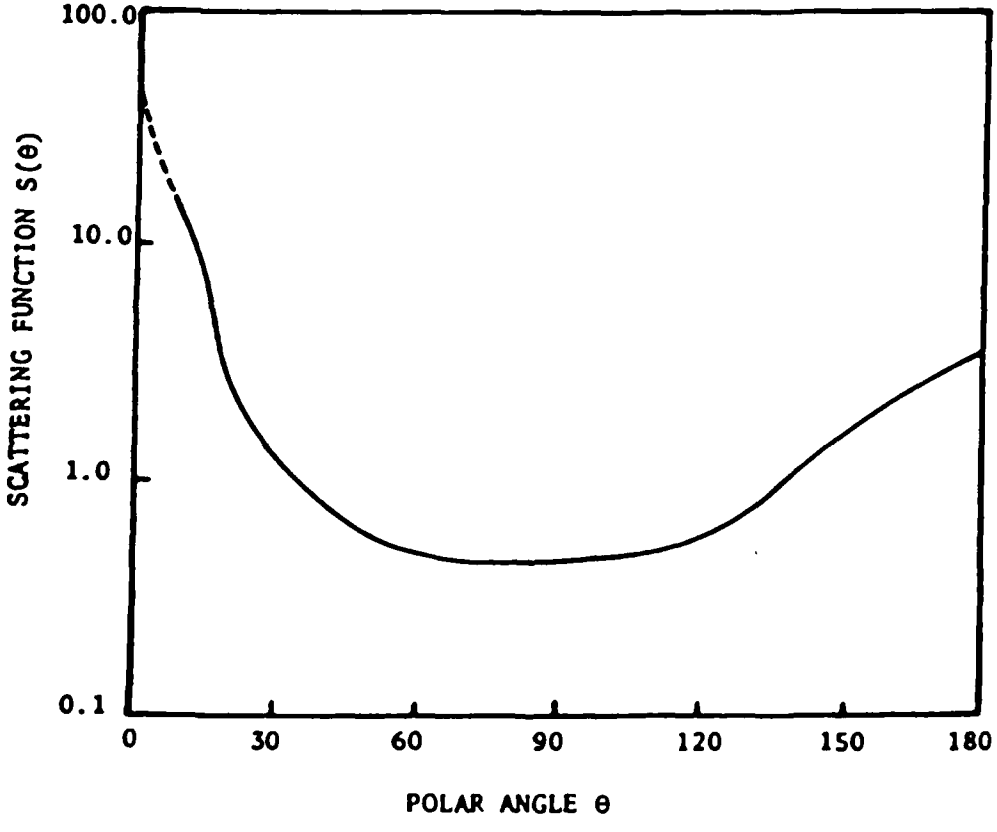

FIGURE 5. A TYPICAL PLOT OF ANGULAR DISTRIBUTION OF SCATTERING FUNCTION [7]

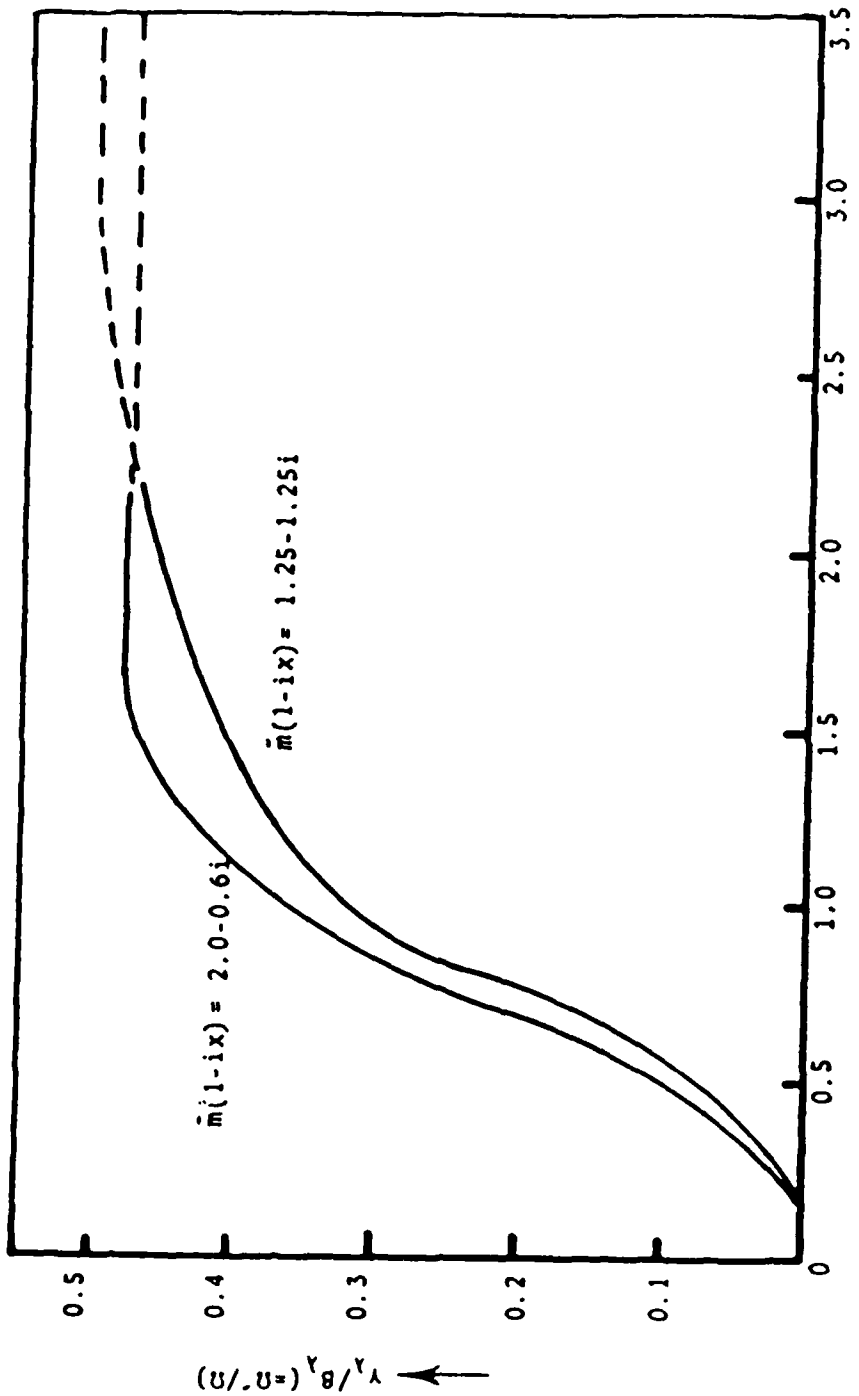

FIGURE 6. THE PARAMETER $\gamma_\lambda/\beta_\lambda$ AS A FUNCTION OF PARTICLE SIZE PARAMETER Z

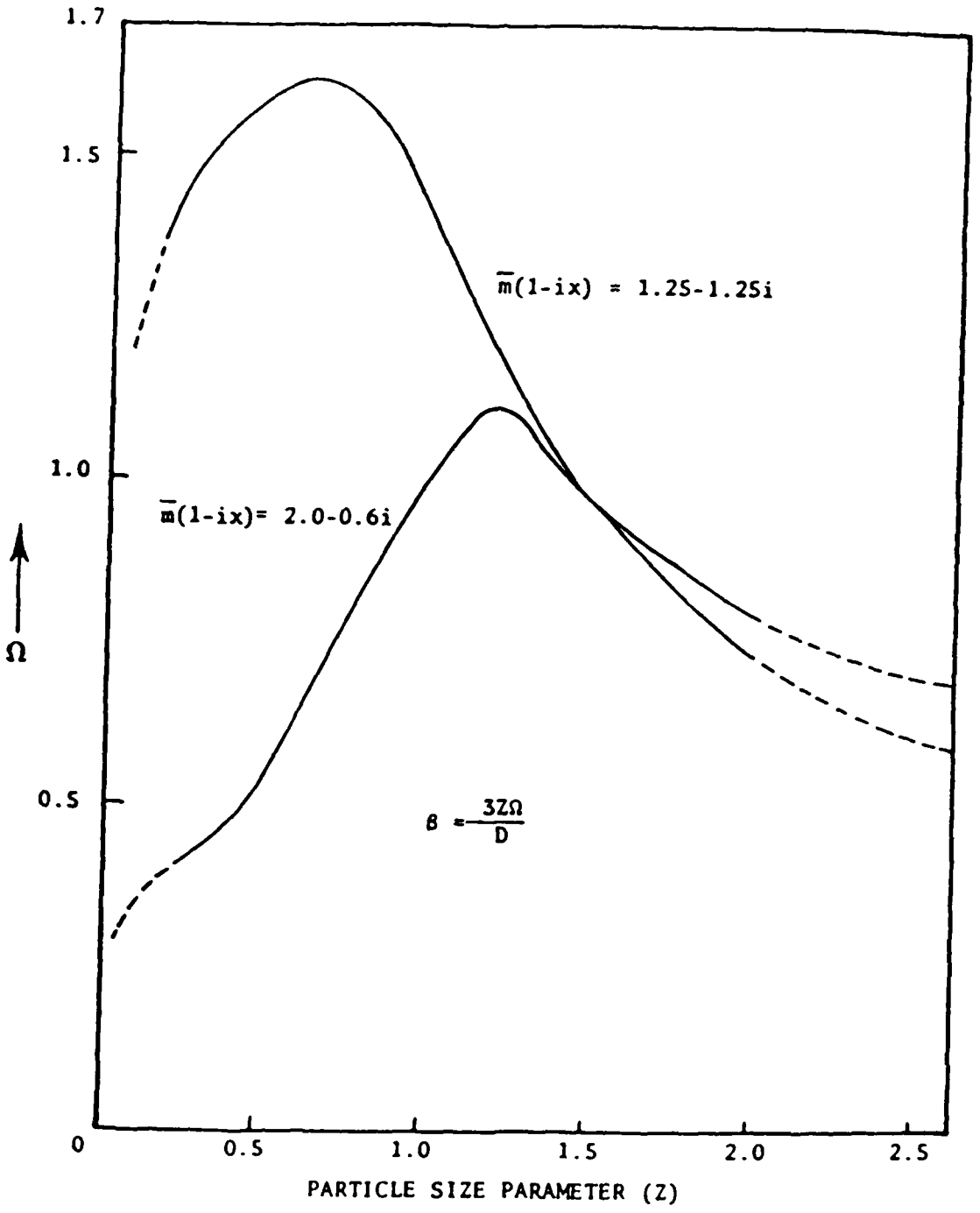

FIGURE 7. EXTINCTION COEFFICIENT AS A FUNCTION OF SIZE PARAMETER

Now the scattering function can be written as:

$$S_\lambda(\mu,\mu') = \frac{1}{2\pi}\int_0^{2\pi} S_\lambda(\theta)\, d\phi'$$

$$S_\lambda(\mu,\mu') = 1 + \frac{1}{2\pi}\sum_{n=1}^{n=\infty} a_n \int_0^{2\pi} P_n(\cos\theta)\, d\phi' \qquad (60)$$

$$S_\lambda(\mu,\mu') = 1 + \sum_{n=1} a_n\, P_n(\mu,\mu') \qquad (61)$$

$$P_n(\mu,\mu') = \frac{1}{2\pi}\int_0^{2\pi} P_n(\cos\theta)\, d\phi' \qquad (62)$$

Chromey (9) has tabulated values of parameters which are denoted as Ω and Ω' for particle size parameter Z from Ø.2 to 2.Ø in increments of Ø.2 and for refractive index "m(1-ix)"

for m = Ø.5Ø, Ø.75, 1.ØØ, ---------, 3.ØØ

x = Ø.Ø, Ø.1, Ø.2, ----------, 1.Ø

The following relationships exist between and and the extinction and scattering coefficients:

$$\frac{\gamma_\lambda}{\beta_\lambda} = \frac{\Omega'}{\Omega} \qquad (63)$$

$$\beta_\lambda = \frac{3Z\Omega}{D_p} \qquad (64)$$

Radiative Properties of Surfaces & Particles

Radiative properties that have importance in the high speed vehicle development include:

1. Emittance and reflectance of vehicle skin surface
2. Absorption coefficient and scattering coefficient of particles that can be injected into the boundary layer as coolants.
3. Absorption and scattering coefficients of ablation products of vehicle sheathing
4. Scattering functions of coolant particles and products of ablation.

A computer literature search was conducted to compile the published data of radiative properties of materials important to this study. The available data is being presented in this report. There is very little data available on the radiative properties of materials of interest. Most of the data available is for the emissivity and reflectivity of surfaces of metals [1-9]. The data for absorption and scattering properties of particles is almost nonexistent. Goubareff, et. al. [12] compiled the thermal radiation properties data available in the fifties and before. The data reported was mostly for metals, alloys and building materials. Toulukian and DeWitt [13] also compiled the radiative properties of metals and alloys. Unfortunately, most of the data reported in References 1 and 2 is old and there is considerable disparity between data taken by different investigators for the same materials. Blau and Francis [14] presented measured data of the spectral emittance of stainless steel and platinum and inconel surfaces coated with silicon monoxide for a wavelength range of 2 to 14 microns. They also showed the effects of surface oxidation which can change the spectral properties by as much as 300%. The data is presented in Appendix A. Neuer and Warner [15] also showed the effect of surface

oxidation for steel. Keegan, et. al. [16] presented measured data on the diffuse spectral reflectance of beryllium, steel, aluminum and platinum over a wavelength range of .2 to 2.1 microns. This data is also presented in Appendix A. Peletskij, et. al. [17] presented data on the total hemispherical emittance of titanium. The more recent studies on radiative properties of metallic materials are presented in References 18 and 19. Ramanathan [18] compared some recent measurements with theoretical predictions. The data for copper, silver, and aluminum is presented in the Appendix A. Makino, et al. [19] evaluated theoretically the spectral and total emissivities of cobalt, chromium and nickel. Their calculated values for cobalt compared well with the measured values. Therefore, their data for cobalt, nickel and chromium is presented in the Appendix A.

Radiative properties of surfaces of ceramics and other heat resisting materials are presented in References 20 to 27. DeWitt and associates [20, 21] presented measured values of spectral emissivity of silicon carbide, silicon nitride and tantalium. These values are given in the Appendix A. Wilson [22] reported data of spectral and total reflectivity and emissivity of ablation chars and carbon and zirconia for temperatures of 2100'K to 3700'K. This data is also presented in Appendix A. Douglas [23] has presented the radiative properties of a Mylar-aluminum laminate. Khrustaler and Rakor [24, 25] presented measured data for total hemispherical and total directional emissivity for Nobium, Molybdenum and tantalum. The most recent data of radiative properties of ceramic materials was presented by Makino, et. al. [26, 27, 28]. They presented spectral and total properties of surfaces of white ceramics (Al_2O_3, ZrO_2), black ceramics (Si_3N_4, SiC) and metallic ceramics (TiC and TiN). Their data as well as data from references 23 and 24 is presented in the Appendix A.

Shafey and Kunitomo [29, 30] and Kunitomo, et. al. [31] have presented theoretical and experimental studies of the absorption and scattering properties of particles of pigments and related these properties to the reflectance of painted layers containing those pigments. While the data presented is not of much importance to our study, some of the ideas presented in their papers are.

The data that is lacking the most in the literature is for the absorption and scattering properties of particles and clouds of particles. References 32 and 33 presented the radiative properties of clouds of soot generated by fires. While this data is not directly useful in this study, it may become useful if a method of thermal protection is developed based on this. Therefore, selected data from these references is given in the Appendix A. Reference 34 to 36 presented some useful data on the radiative properties of particles. Nagy and Lenoir [34] presented absorption and scattering coefficients of aluminum oxide particles of sizes 6 and 12 microns in the wavelength range of 2 to 12 microns. Sanders and Lenoir [35] presented measurements of back scattering and extinction efficiency of graphite and aluminum oxide particles. Love and Beattie [36] also presented measured data for clouds of aluminum, iron, glass and silica particles. Some selected data from these references in presented in the Appendix A.

RESULTS

Based on the theoretical development described earlier in this report, a computer program was developed that solves the turbulent boundary layer flow equations for mass injection of the absorping, emitting and scattering particles in the boundary layer. This was done by modifying an earlier code developed by the author. This earlier code [1] involved the inclusion of radiative heat transfer analysis in the Patankar Spalding code for turbulent boundary layer flow. The modification involved the inclusion of concentration of species equation in the boundary layer flow to account for the mass injection and ablation. This modification was taken from another publication by the author (Reference 3). Since both of the above mentioned studies (1, 3) had validated their results separately, and the present study involved merging the two no attempt was made in comparing the present results with any other publication.

The developed computer program was used to obtain results for radiative, convective and total heat transfer to the surface of a flat wall for various combinations of wall temperature, free stream temperature, Mach Number and scattering coefficients of the injected particles. The results were obtained to analyze the effect of injected particles for protecting the wall surface from incident thermal radiation from an external source.

Figure 8 shows the total heat flux in Btu/ft^2-sec. to the surface as a function of the distance from the leading edge of the plate for T_w/T_∞ of 1, 2, 4 and 6. The total heat transfer is the sum of the convective and radiative heat transfer. This figure shows the total heat transfer when there is no external incident radiation. In such a case, the radiative heat transfer is a very small part of the total heat transfer. This can be seen from Figure 9. As seen from this figure the radiative heat transfer is less than .1% of the total heat transfer for T_w/T_∞ equal to 1. The

Fig: 8 TOTAL HEAT TRANSFER AS A FUNCTION OF X

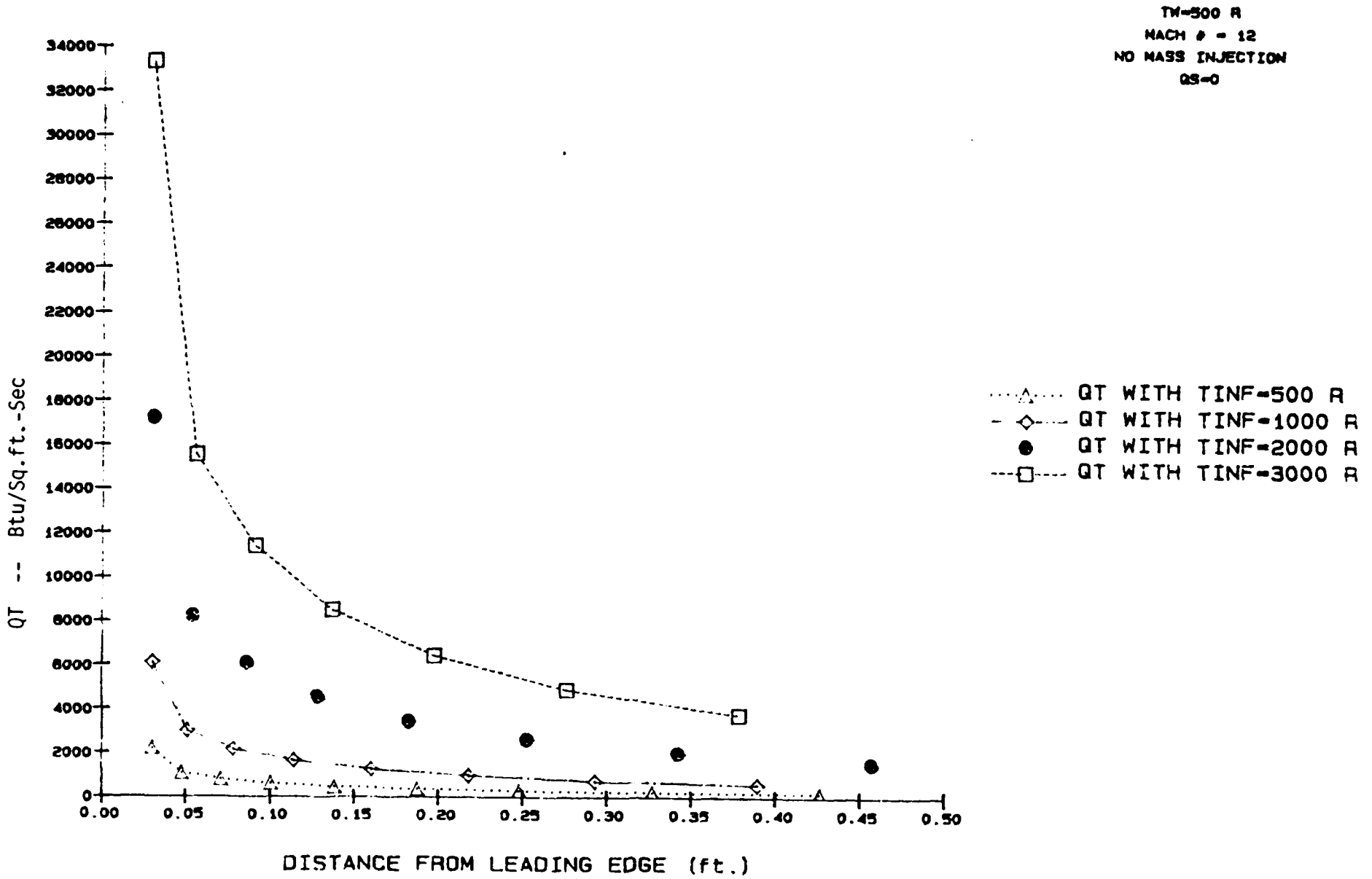

Fig: 9 RADIATIVE AND TOTAL HEAT TRANSFER AS A FUNCTION OF FREE STREAM TEMPERATURE

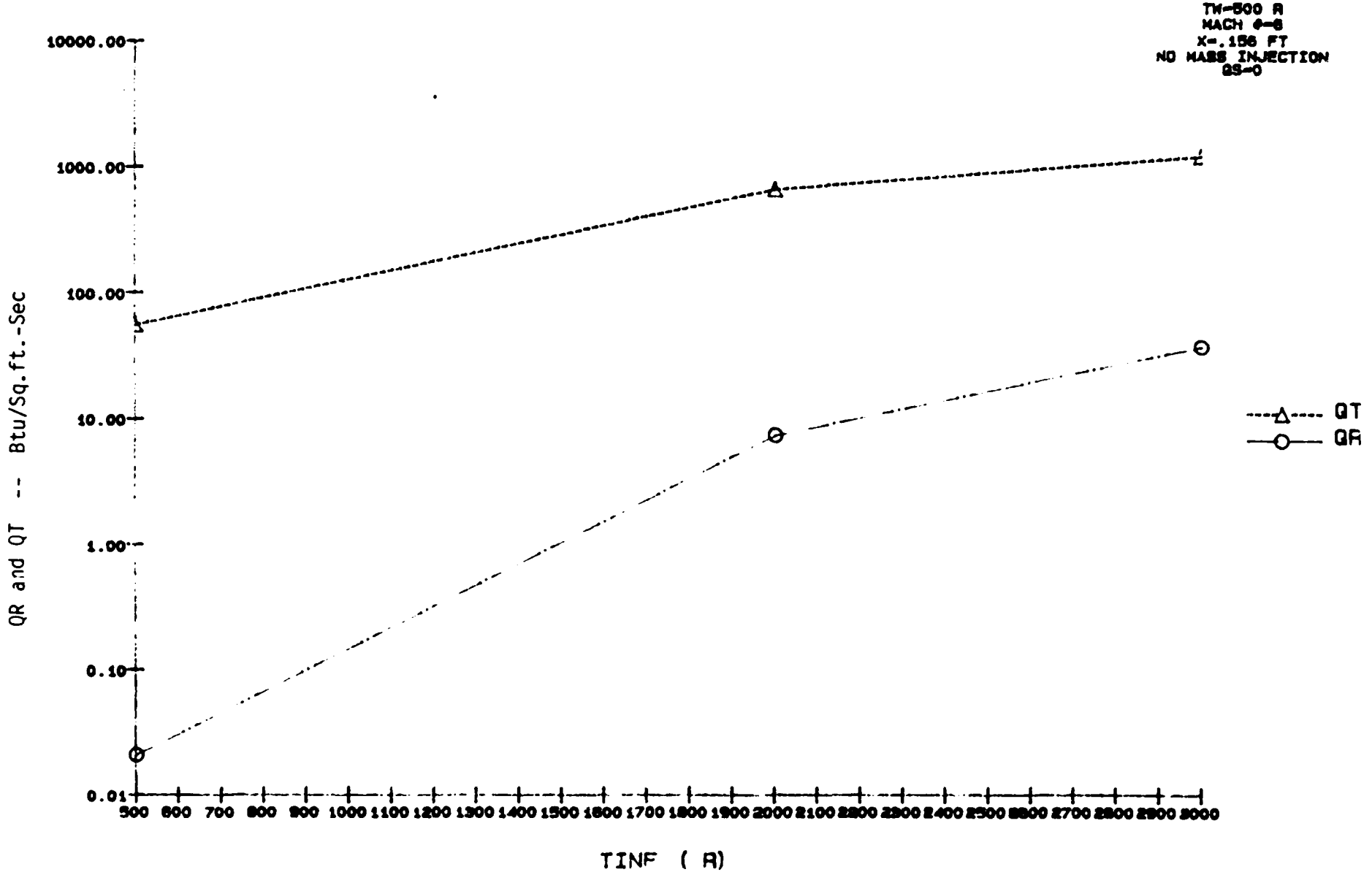

relative fraction of the radiative heat transfer increases as T_∞ increases for the same T_w. At T_w/T_∞ of 6 the percentage of the radiative heat transfer increases to about 5%. Figure 10 shows the radiative heat flux to the surface as a function of the distance from the leading edge for various free stream temperatures. It is seen from these two figures that radiative heat flux is relatively unimportant when the free stream temperatures are not too high. In such a situation any strategy for thermal protection should try to reduce the convective heat flux. However, protection from thermal radiation becomes important when there is a strong external incident radiation source present, such as a nuclear blast or a laser beam. In this study, we have assumed the external radiation source to cause a uniform incident thermal radiation flux of 1000 Btu/ft^2-sec. at the external edge of the boundary layer (Figure 11). Figure 12 shows the effect of Mach Number on the radiative, convective and total heat flux. As seen from this figure, the radiative heat flux is affected very little by the change in Mach Number. However, the convective heat flux increases with Mach Number, thereby increasing the total heat flux. Figure 13 shows a typical temperature profile in the boundary layer in hypersonic flow.

The injection of particles that absorb and scatter thermal radiation reduces the externally incident radiative flux. This is seen from Figures 14 and 15. In these figures the effect of scattering coefficient of the injected particles on the radiative and total heat flux is seen. These figures show very clearly the potential benefits of using this technique for the thermal protection of the vehicle surface by injection of strongly scattering particles. Figure 16 shows the effect of scattering on the radiative heat transfer for different Mach Numbers. It can be seen from this figure that by injection of purely scattering particles it is possible to

Fig: 10 RADIATIVE HEAT TRANSFER AS A FUNCTION OF FREE STREAM TEMPERATURE

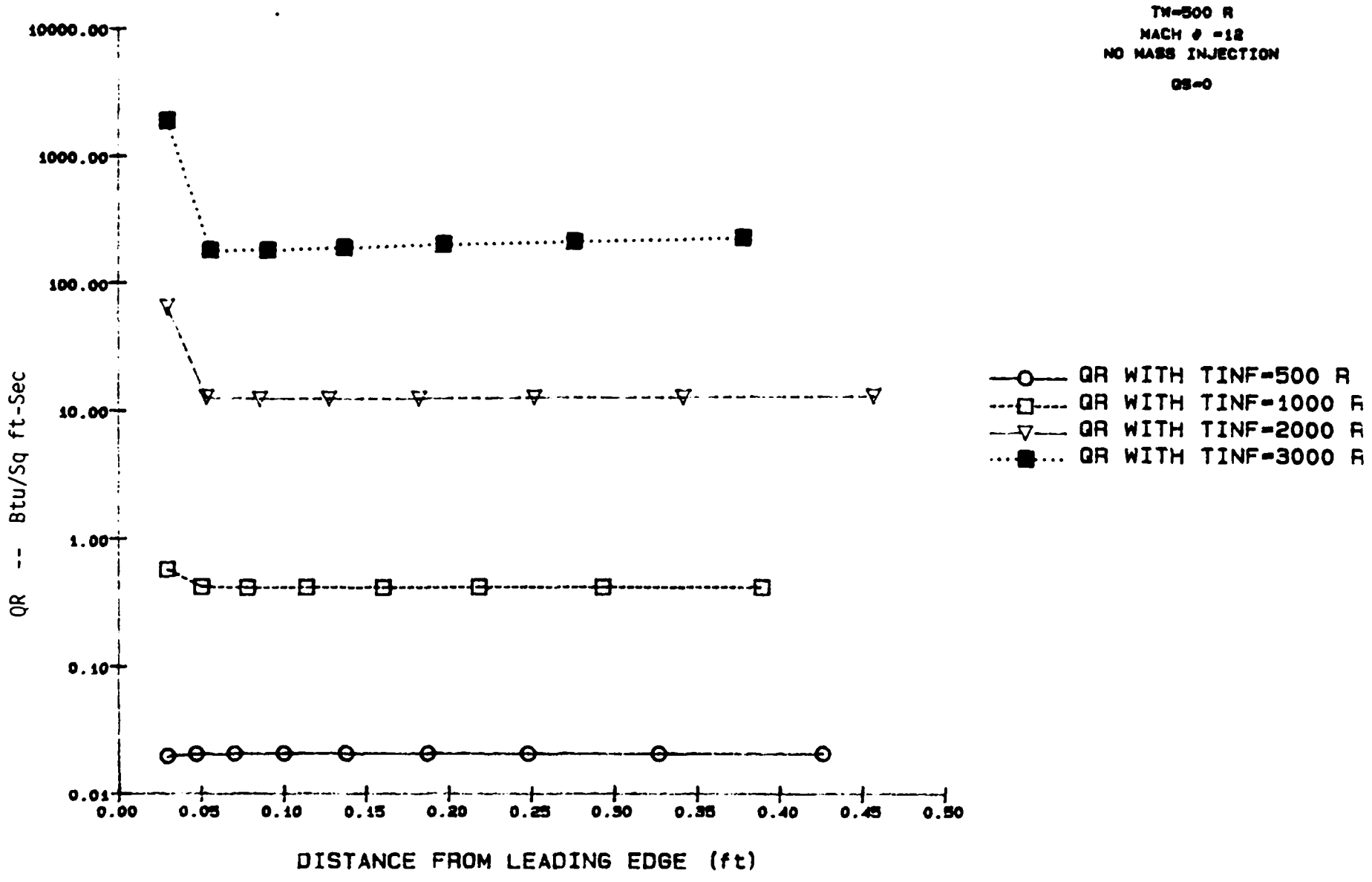

FIGURE 11

RADIATIVE AND TOTAL HEAT TRANSFER AS A FUNCTION OF EXTERNAL INCIDENT RADIATIVE FLUX

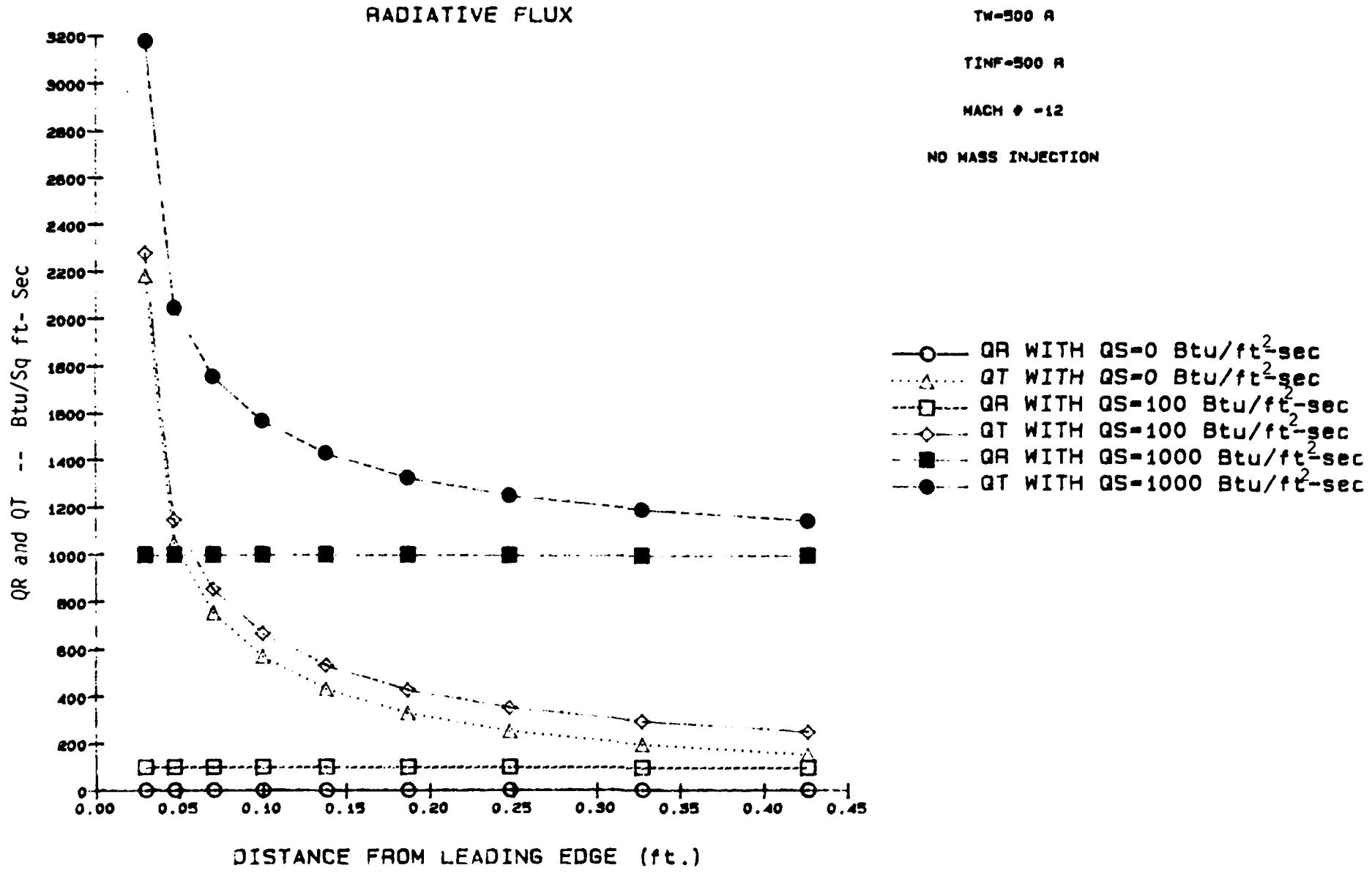

Fig: 12 RADIATIVE AND TOTAL HEAT TRANSFER AS A FUNCTION OF MACH #

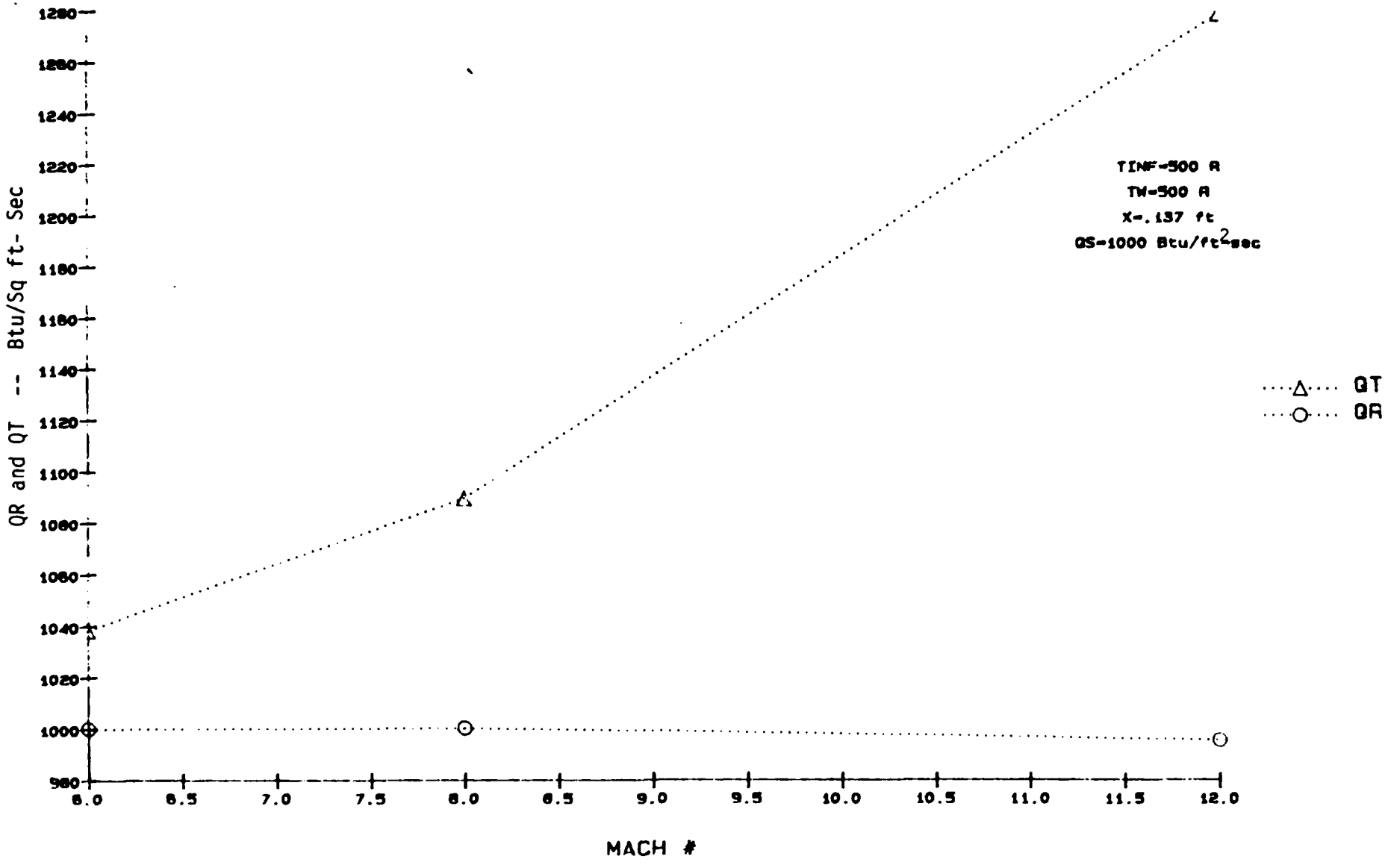

Fig: 13 A TYPICAL TEMPERATURE PROFILE IN THE BOUNDARY LAYER

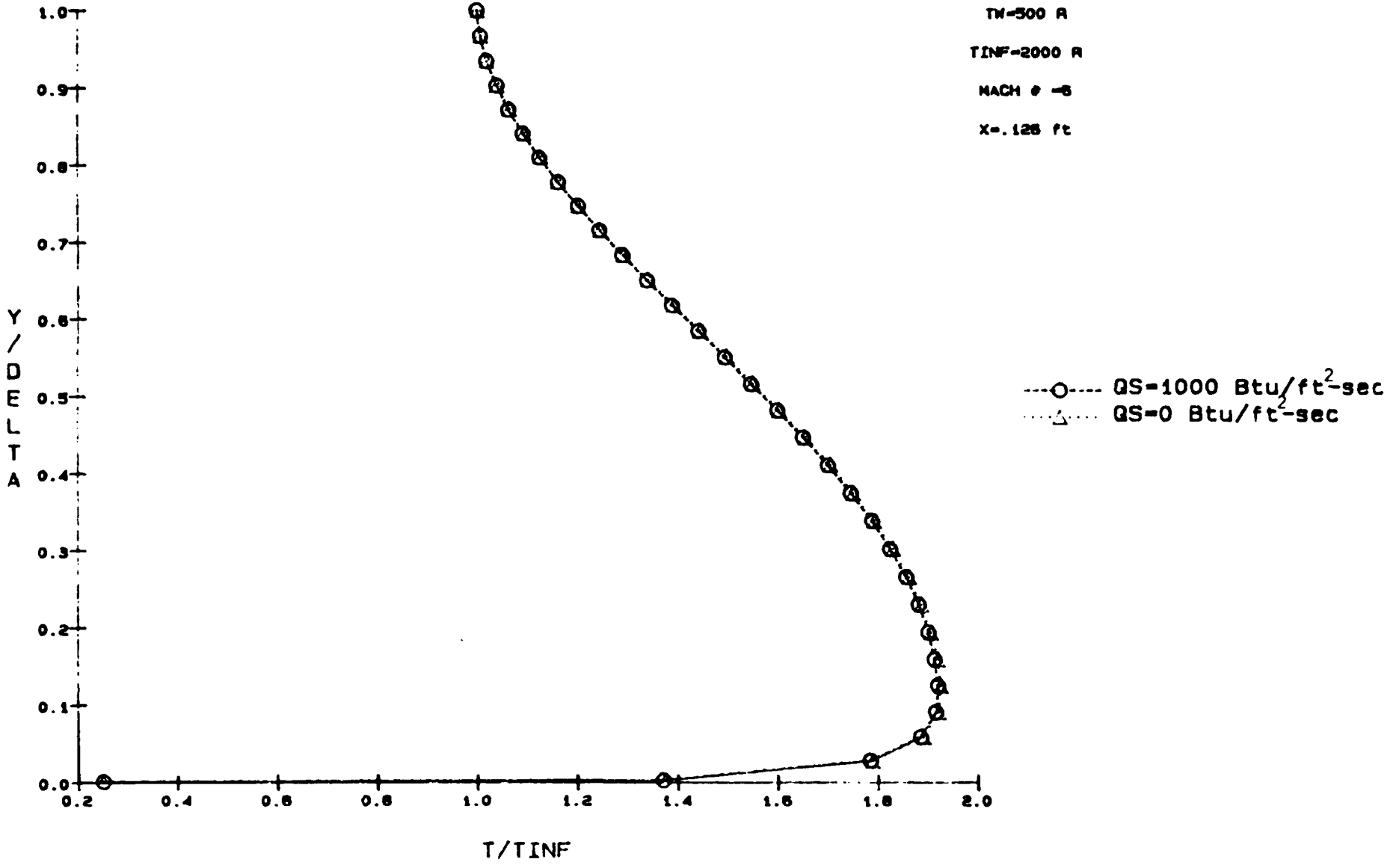

Fig: 14 EFFECT OF SCATTERING COEFFICIENT OF INJECTED PARTICLES ON RADIATIVE AND TOTAL HEAT FLUX

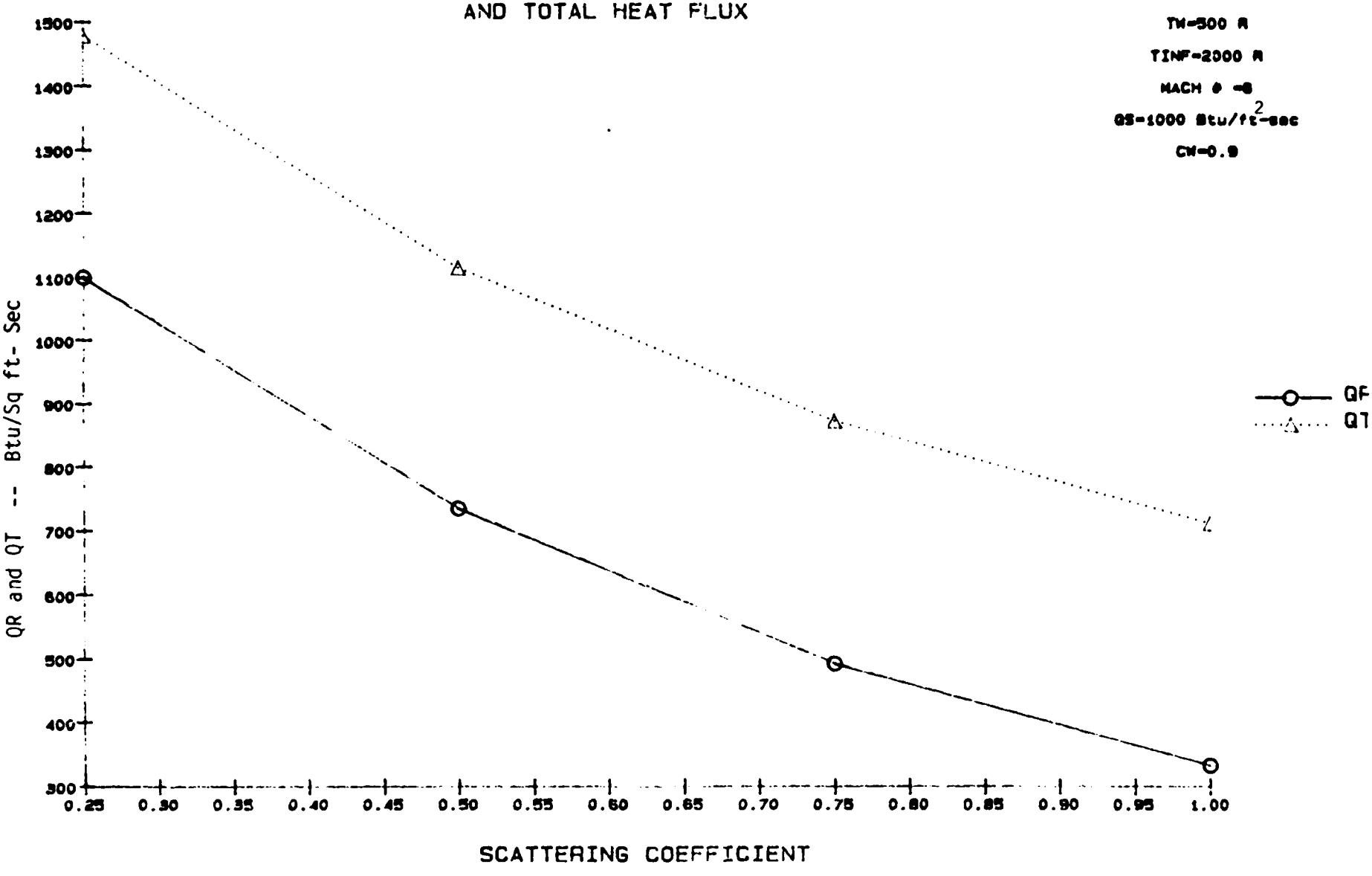

Fig: 15 EFFECT OF SCATTERING COEFFICIENT ON RADIATIVE AND TOTAL HEAT TRANSFER

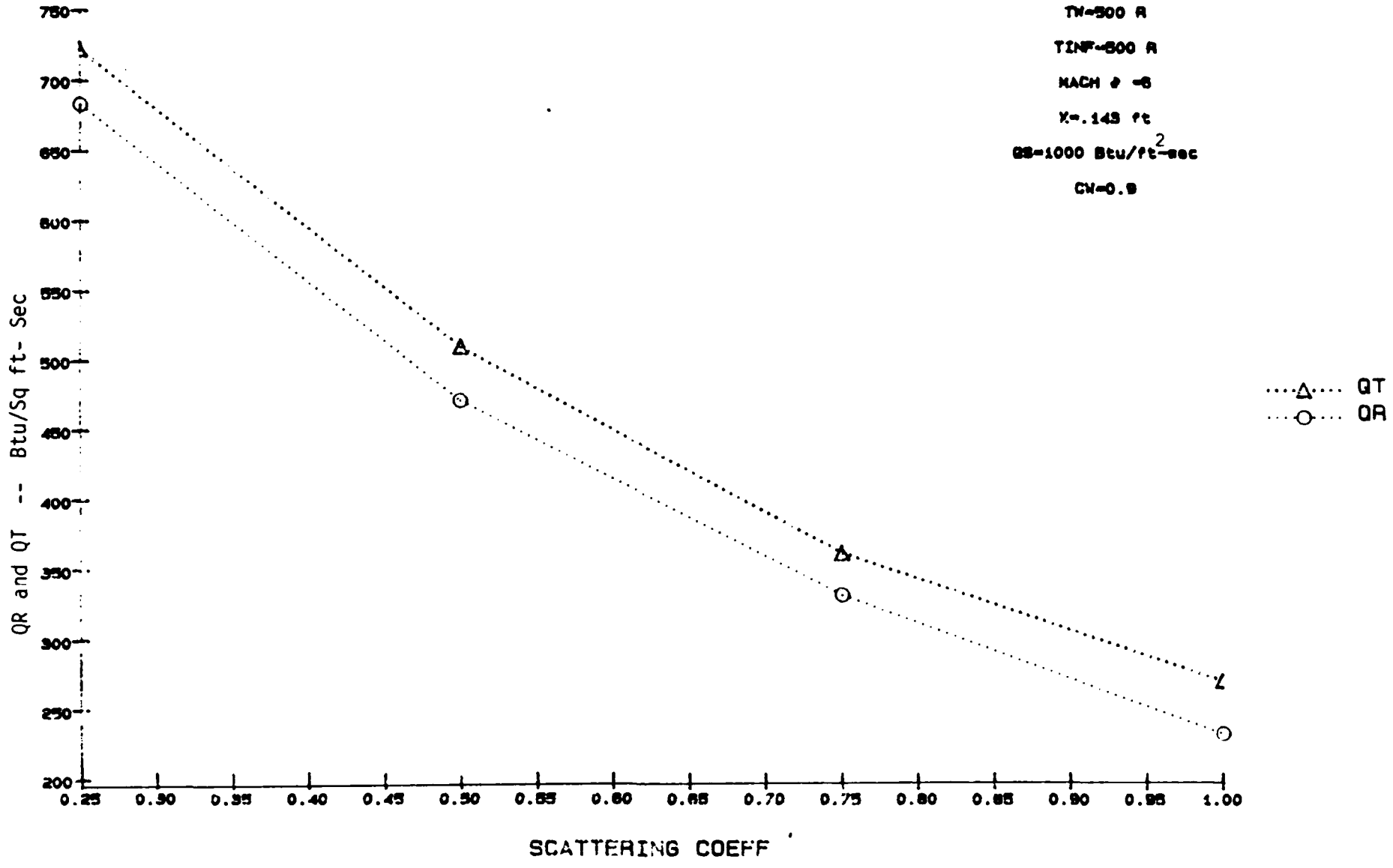

Fig: 16 RADIATIVE HEAT FLUX WITH AND WITHOUT SCATTERING AS A FUNCTION OF MACH #

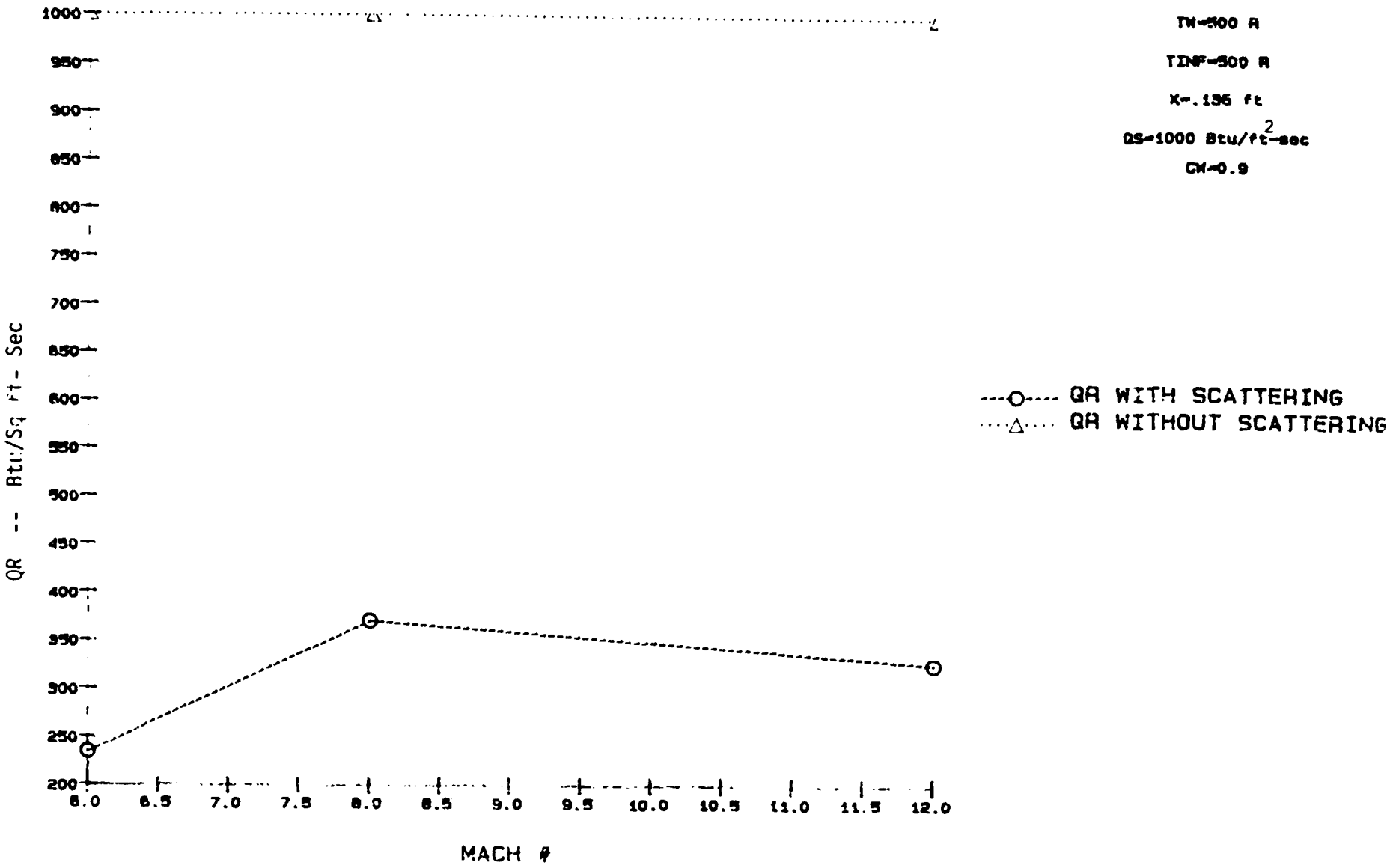

reduce the incident radiative flux by 75% for flow at Mach Number of 6. Similar reductions are seen at higher Mach Numbers also. Figure 17 shows a temperature profile in the boundary layer with the injection of absorbing and scattering particles. If the particles only absorb and do not scatter, the temperature in the boundary layer will be higher than the case where particles scatter radiation. The reason is that for the case of scattering particles part of the incident radiation is reflected out of the boundary layer instead of being absorbed resulting in lower temperatures in the boundary layer. The results show that for the case where there is no external incident thermal radiation the radiative flux is a very small fraction of the total heat flux. In this case, the injection of mass does not have any effect on the radiative heat transfer. However, even in such a case, there is a benefit that can be seen from Figure 18. This figure shows that mass injection in this case reduces the convective and thus the total heat flux. This happens because the injection of mass reduces the temperature gradient of the wall, thereby reducing the convective heat flux.

Fig: 17 TEMPERATURE PROFILE IN THE BOUNDARY LAYER WITH AND WITHOUT SCATTERING

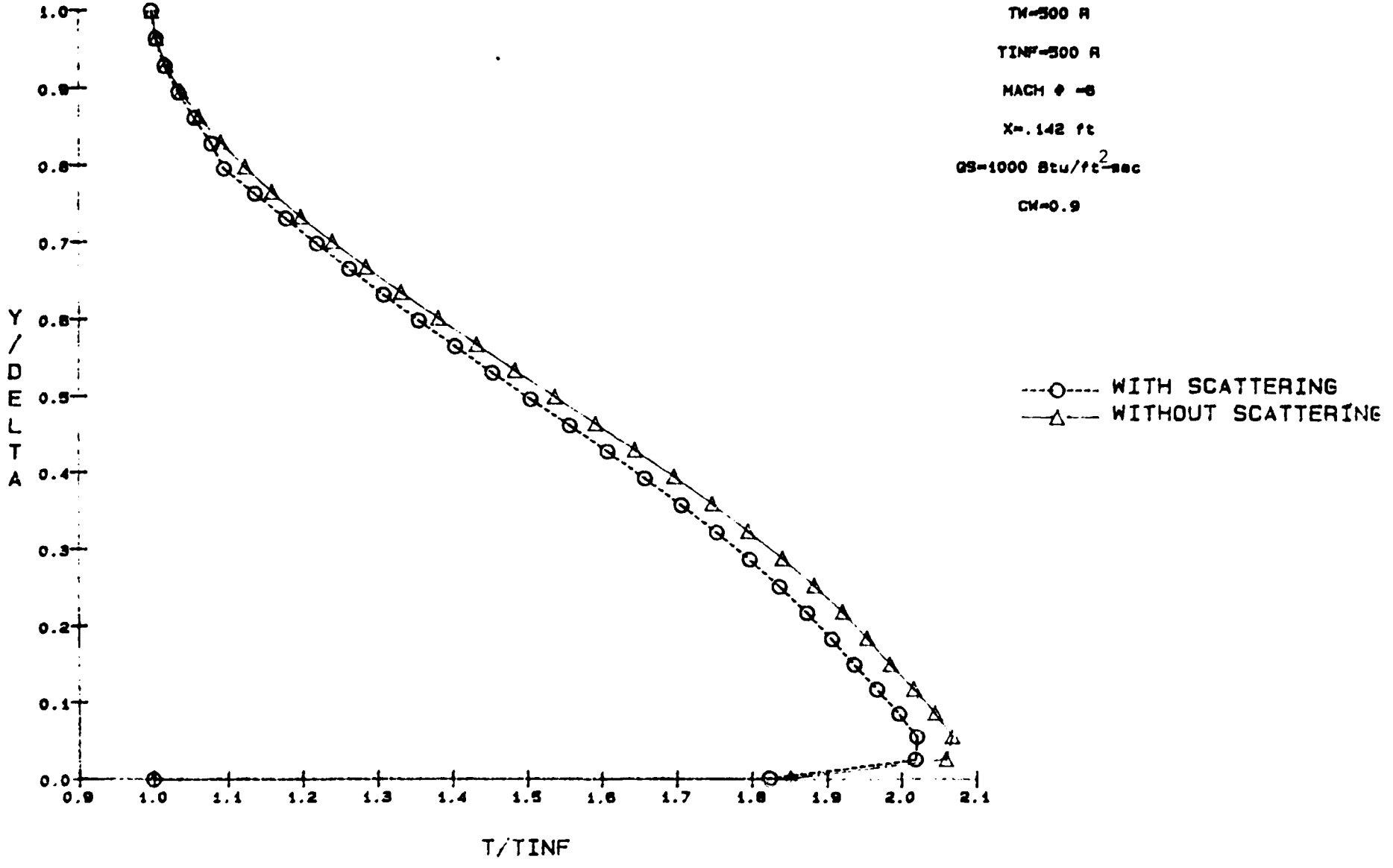

Fig: 18 RADIATIVE AND TOTAL HEAT FLUX AS A FUNCTION OF MACH #

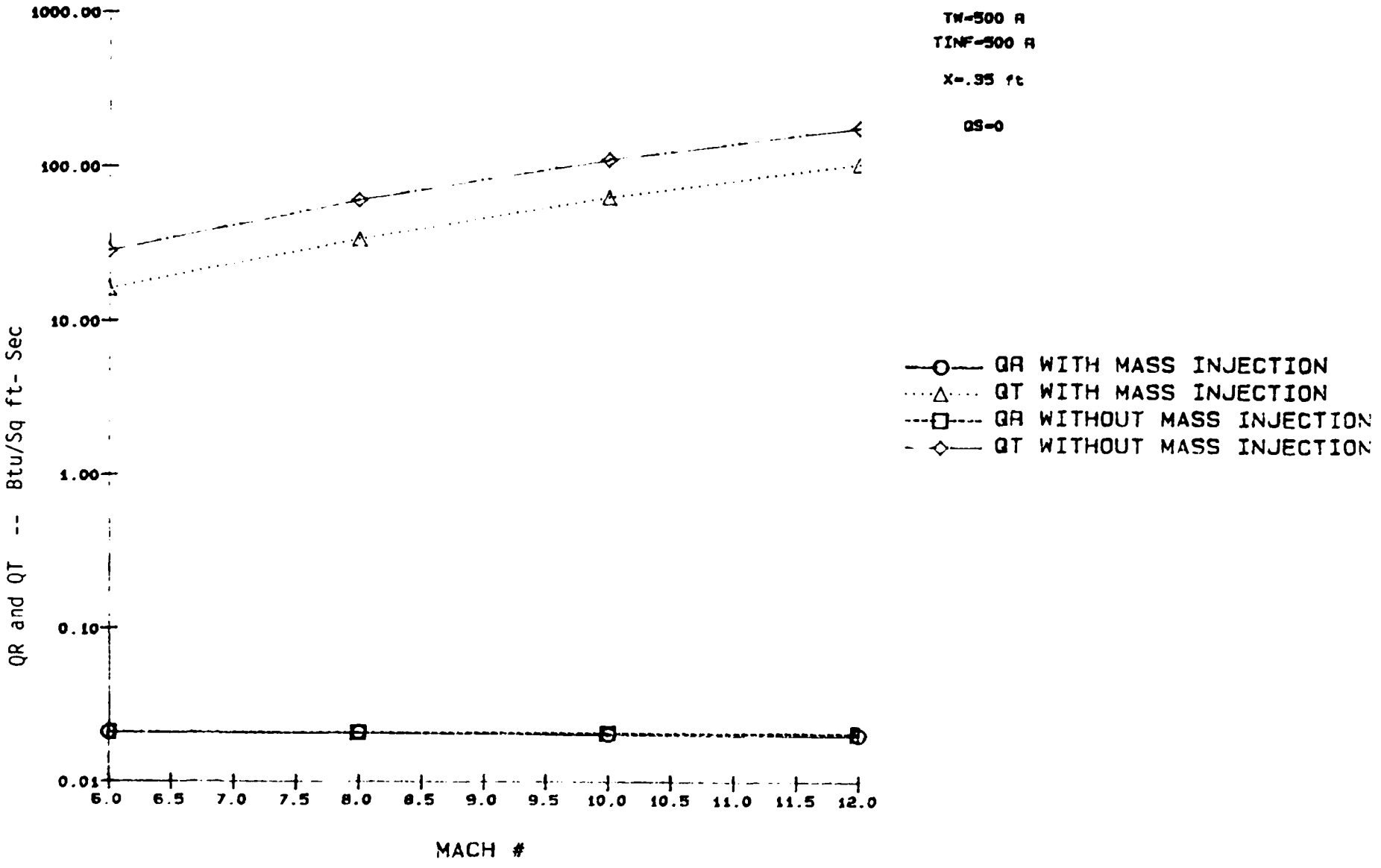

REFERENCES

1. D. Y. Goswami and R. I. Vachon, Radiative Heat-Transfer Analysis Using an Effective Absorptivity for Absorption, Emission and Scattering, Int. J. Heat Mass Transfer 20, pp 1233-1239, 1977.

2. Patankar, S. V. and Spalding, D. B., "Heat and Mass Transfer in Boundary Layers--A General Calculation Procedure," International Textbook Company, London, 1970.

3. Goswami, D. Y., et. al., "Mass Injection of Radiative and Convective Heat Transfer in High-Speed Turbulent Flow," Indian Journal of Technology, Vol. 14, pp 585-590, December 1976.

4. Lee, H. and Buckius, R. O., "Scaling Anisotropic Scattering in Radiation Heat Transfer for a Planar Medium," ASME Journal of Heat Transfer, Vol. 104, pp 68-75, 1982.

5. Lee, H. and Buckius, R. O., "Reducing Scattering to Nonscattering Problems in Radiation Heat Transfer," Int. J. Heat Mass Transfer, Vol. 26, No. 7, pp 1055-1062, 1983.

6. Lee, H. and Buckius, R. O., "Combined Mode Heat Transfer Analysis Utilizing Radiation Scaling," ASME Journal of Heat Transfer, Vol. 108, pp 626-632, August 1986.

7. Sparrow, E. M. and Cess, R. D., Radiation Heat Transfer, Brooks/Cole, Belmont, CA, 1966.

8. Van DeHulst, H. C., Light Scattering by Small Particles, John Wiley and Sons, New York, 1957.

9. Love, T. J. and Beattie, J. F., "Experimental Determination of Thermal Radiation Scattering by Small Particles," Report ARL 65-110, Office of Aerospace Research, U. S. Air Force, June 1965.

10. Chu, C. M., et. al., "Tables of Angular Distribution Coefficients for Light Scattering by Spheres," University of Michigan Press, Ann Arbor, MI, 1957.

11. Chromey, F. C., "Evaluation of Mie Equations for Coloured Spheres," Journal of the Optical Society of America, Vol. 50, No. 7, July 1960.

12. Gubareff, G. G., Janssen, J. E. and Torborg, R. H., Thermal Radiation Properties Survey, 2nd Ed., Honeywell Research Center, Minneapolis, Minnesota, 1960.

13. Touloukian, Y. S. and DeWitt, D. P., Thermal Radiative Properties, Metallic Elements and Alloys, Vol. VII, Plenum Press, New York, 1970.

14. Blau Jr., H. H. and Francis, H. A., "Surface Properties of Metals," NASA SP-55, pp 159-163, 1965.

15. Neuer, G. and Worner, B., "Influence of Surface Properties on the Total Emittance of Steel," Proceedings of the 7th Symposium on Thermophysical Properties, ASME, NY, pp 250-255, May 1977.

16. Keegan, H. J., Schleter, J. C. and Weidner, V. R., "Diffuse Spectral Reflectance of Metal Surfaces," NASA SP-55, pp 165-177, 1965.

17. Peletskij, V. E., Belskaya, E. A., Shur, B. A. and Listratov, I. V., "The Investigation of Electrical Resistivity and Total Hemispherical Emissivity of Titanium," Proceedings of the 7th Symposium on Thermophysical Properties, ASME, NY pp 231-235, May 1977.

18. Ramanathan, K. G., "Temperature Variation of Total Hemispherical Emissivities of Metals in the Range 150-1000 K," Proceedings of the 7th Symposium on Thermophysical Properties, ASME, NY, pp 272-278, May 1977.

19. Makino, T., Kawasaki, H. and Kunitomo, T., "Study of Radiative Properties of Heat Resisting Metals and Alloys (1st Rep., Optical Constants and Emissivities of Nickel, Cobalt and Chronium), Bull. of JSME, Vol. 25, No. 203, pp 804-822, 1982.

20. DeWitt, D. P., Taylor, R. E. and Riddle, T. K., "High Temperature Computer Controlled Emissometer for Spectral and Total Measurements on Conducting and Non-Conducting Materials," Proceedings of the 7th Symposium on Thermophysical Properties, ASME, New York, pp 256-264, 1977.

21. DeWitt, D. P., Taylor, R. E. and Johnson, P. E., "Spectral Emissivity of Ceramics at High Temperatures: Silicon Carbide and Silicon Nitride," ASME Paper 79-HT-24, 1979.

22. Wilson, R. Gale, "Hemispherical Spectral Emittance of Ablation Chars, Carbon and Zirconia (to 3700'K)," NASA Sp-55, pp 259-275, 1965.

23. Douglas, N. J., "Directional Solar Absoprtance Measurements," NASA SP-55, pp 293-301, 1965.

24. Khrustalev, B. A. and Rakov, A. M., "Methods of Determining the Integral and Spectral Radiative Properties of Materials at High Temperatures," Heat Transfer-Soviet Research, Vol. 1, No. 4, July 1969, pp 163-178.

25. Khrustalev, B. A. and Rakov, A. M., "Radiative Properties of Tantalum, Molybdenum, Nobium, Graphite and Nobium Carbide at High Temperatures," Heat Transfer-Soviet Research, Vol. 1, No. 4, 1969, pp 187-206.

26. Makino, T., Kunitomo, T., Sakai, I. and Kinoshita, H., "Thermal Radiation Properties of Ceramic Materials," Heat Transfer Japanese Reearch, Vol. 13, No. 4, pp 33-50, October 1984.

27. Makino, T., Kinoshita, H., Kobayashi, Y. and Kunitomo, T., "Thermal Radiation Properties of Refractory Metals and Electrically Conductive Ceramics at High Temperatures," Proceedings of the International Symposium on Heat Transfer, Beijing, Vol. 3, pp 116-123, October 1985.

28. Makino, T., "Thermal Radiation Properties of Metallis and Ceramic Materials at High Temperatures," Ph.D. Thesis, Kyoto University, September 1986.

29. Shafey, H. M. and Kunitomo, T., "Theoretical Study on Radiative Properties of an Optically Thick Painted Layer Containing Spherical Pigment," Bull. of JSME, Vol. 23, No. 182, pp 1366-1373, August 1980.

30. Shafey, H. M. and Kunitomo, T., "Theoretical Study on Radiative Properties of Doubly Painted Layer," Bull. of JSME, Vol. 25, No. 200, pp 213-216, February 1982.

31. Kunitomo, T. and Tsuboi, Y. and Shafey, H. M., "Dependent Scattering and Dependent Absorption of Light in a Fine Particle Dispersed Medium," Bull. of JSME, Vol. 28, No. 239, pp 854-859, May 1985.

32. Johnson and Beer, J. M., "The Zone Method Analysis of Radiant Heat Transfer: A Model for Luminous Radiation," Journal of the Institute of Fuel, September 1973, pp 301-309.

33. Markstein, G. H., "Radiative Properties of Plastic Fires," Proceedings of the 17th International Combustion Symposium, University of Leeds, England, August 1978. Published by Combustion Institute, Pittsburg, PA, 1979, pp 1053-1062.

34. Nagy, A. R. and Lenoir, J. M., "Absorption and Scattering of Thermal Radiation by a Cloud of Small Particles," AICh.E Journal, Vol. 18, No. 1, pp 155-160, Janury 1972.

35. Sanders, C. F. and Lenoir, J. M., "Radiative Transfer Through a Cloud of Absorbing-Scattering Particles," AICh.E Journal, Vol. 18, No. 1, pp 155-160, January 1972.

36. Love, T. J. and Beattie, J. F., "Experimental Determination of Thermal Radiation Scattering by Small Particles," Report ARL 65-110, Office of Aerospace Research, U. S. Air Force, June 1965.

APPENDIX A

RADIATIVE PROPERTIES OF METALS, ALLOYS, CERAMICS, ABLATION CHARS, SOOT CLOUDS AND PARTICLES, COMPILED FROM PUBLISHED LITERATURE

NOTE: Figure captions are taken from original papers. Reference numbers and equation numbers in figures refer to those in the original papers.

SPECTRAL EMITTANCE OF STAINLESS STEEL, PLATINUM, INCONEL
(Data from Ref. 14)

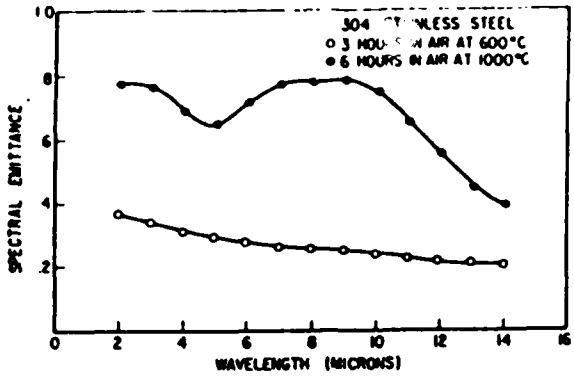

FIGURE 1.—*Spectral emittance of oxidized stainless steel.*

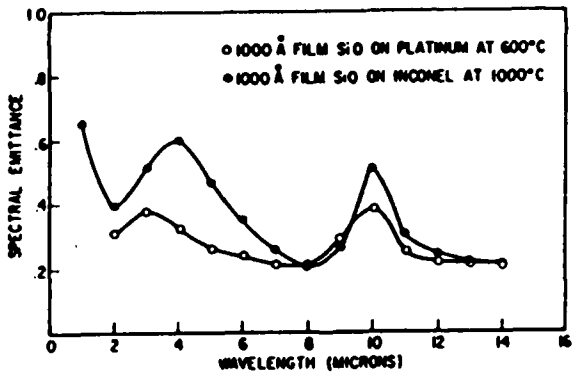

FIGURE 2.—*Spectral emittance of silicon monoxide coated platinum and Inconel.*

REFLECTANCE OF BERYLLIUM, STEEL, ALUMINUM AND PLATINUM
(Data from Ref. 15)

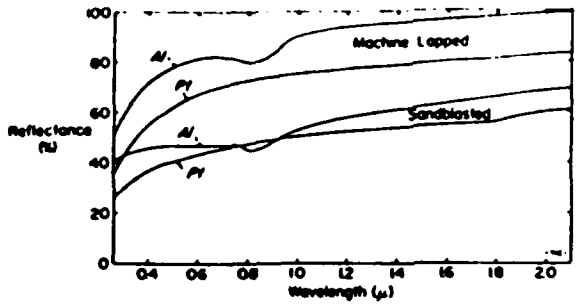

FIGURE 1.—*Diffuse spectral reflectances (0.26 to 2.1 μ) of machine-lapped and sandblasted samples of aluminum and of platinum. Each curve represents determinations at four orientations. There was no appreciable effect of orientation.*

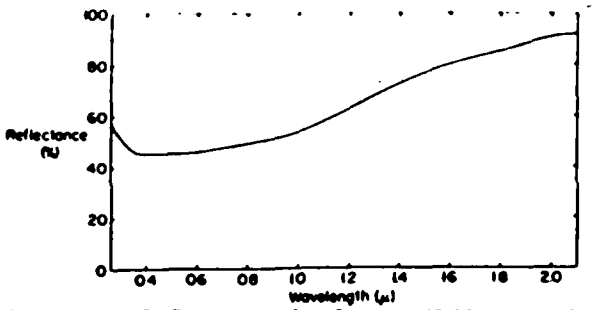

FIGURE 2.—*Diffuse spectral reflectance (0.26 to 2.1 μ) of surface of beryllium sample 1, hand-lapped to about 4 microinches. The curve represents determinations at eight orientations of the sample.*

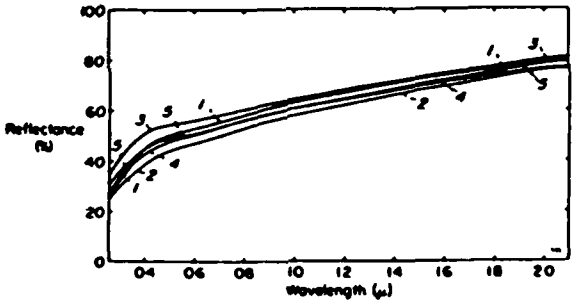

FIGURE 5.—*Diffuse spectral reflectances (0.26 to 2.1 μ) of steel gage blocks with commercial finishes. The variation in reflectance is due to differences in the steels used in the manufacture of the blocks and to oxide surface films.*

1. *Webber 5 min M-4*
2. *Webber 30 min NBS-2.*
3. *NPL 9 sec no. 5*
4. *Van Keuren 0.250 in. 222.*
5. *Pratt and Whitney 0.500 in. Triangle.*

TOTAL HEMISPHERICAL EMISSIVITY OF COPPER, SILVER AND ALUMINUM
(Data from Ref. 18)

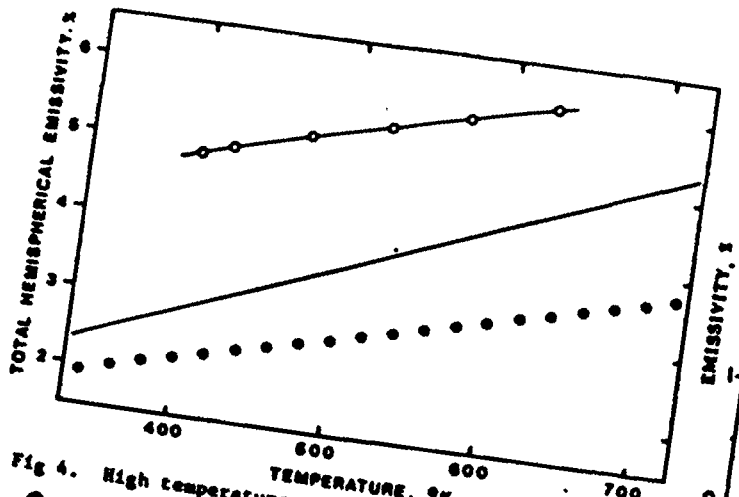

Fig 4. High temperature ε_h vs T curves of aluminum: ● Electropolished Al (17); ——, Eq (6); O, Best (14).

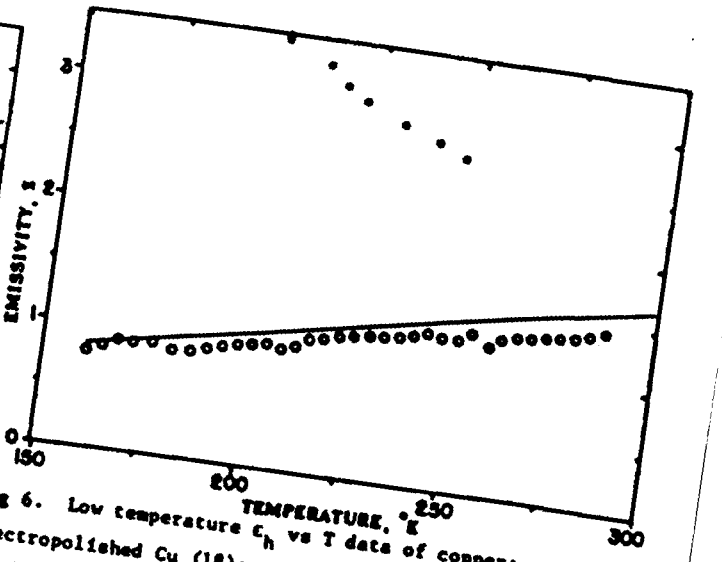

Fig 6. Low temperature ε_h vs T data of copper: O electropolished Cu (18); ——, Eq (6); —●—, Gaumer et al (19).

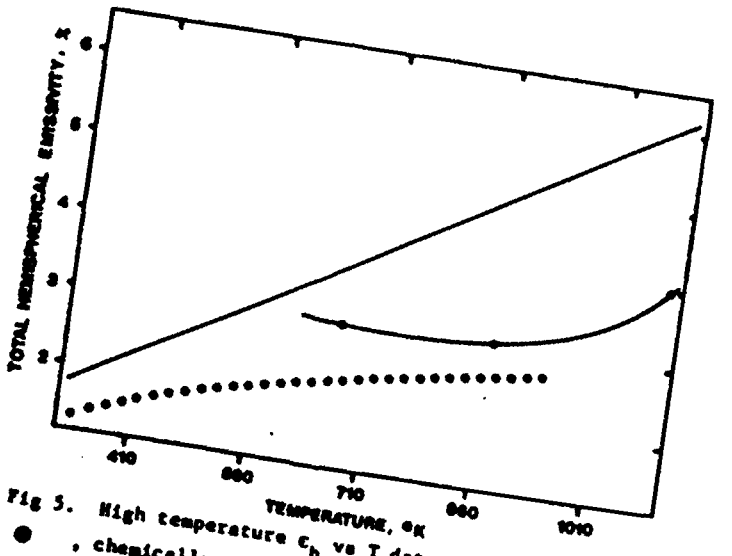

Fig 5. High temperature ε_h vs T data for silver: ●, chemically polished Ag (17); ——, Eq (6); —O—, Butler et al (20).

SPECETRAL AND TOTAL EMISSIVITY OF NICKEL, COBALT, CHROMIUM
(Data from Ref. 19)

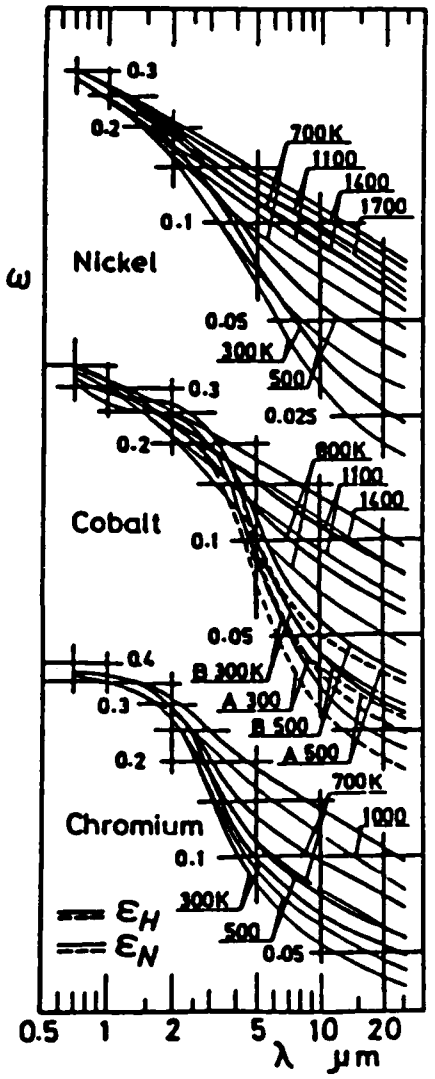

Figure 1-8 Spectra of emissivities of nickel, cobalt and chromium (Calc.) [57]

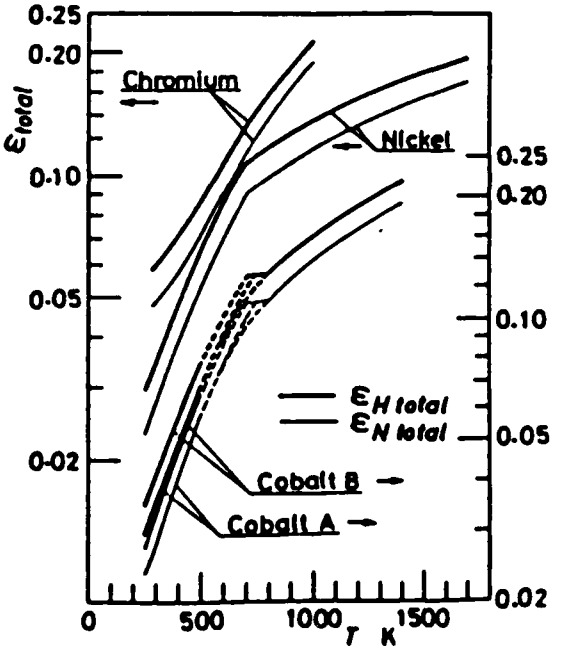

Figure 1-9 Total emissivities of nickel, cobalt and chromium (Calc.) [57]

SPECTRAL EMISSIVITY OF SILICON CARBIDE AND SILICON NITRIDE
(Data from Ref. 20, 21)

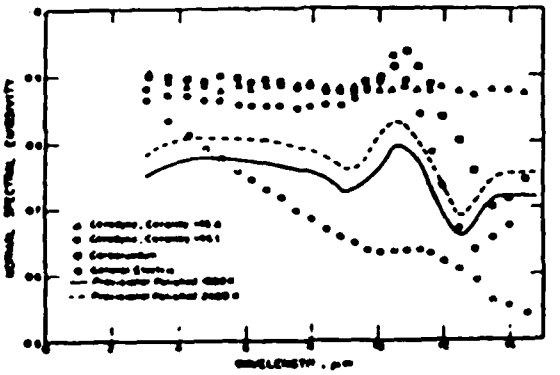

Fig. 3 Normal spectral emissivity of silicon carbide at 1900K

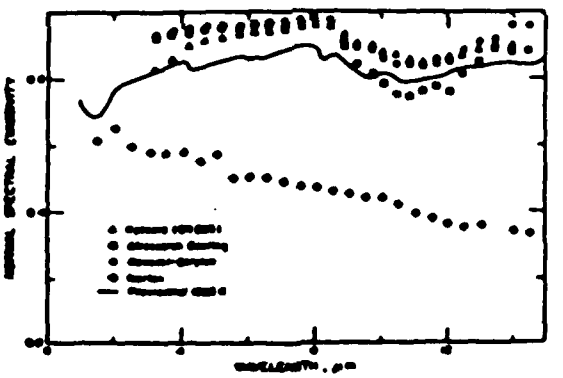

Fig. 5 Normal spectral emissivity of silicon nitride at 1700K

EMITTANCE OF OXIDIZED CARBON, GRAPHITE AND ZIRCONIA
(Data from Ref. 22)

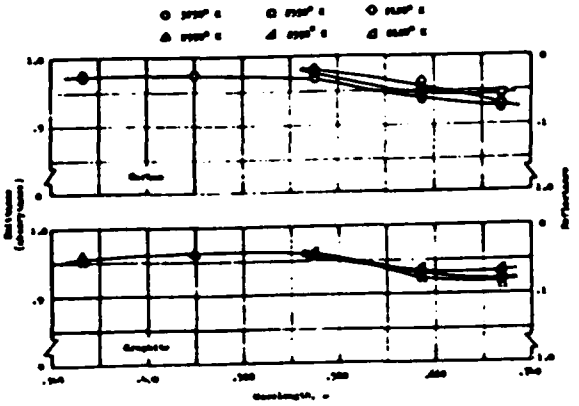

FIGURE 6.—*Emittance and reflectance of oxidized carbon and graphite plotted against wavelength.*

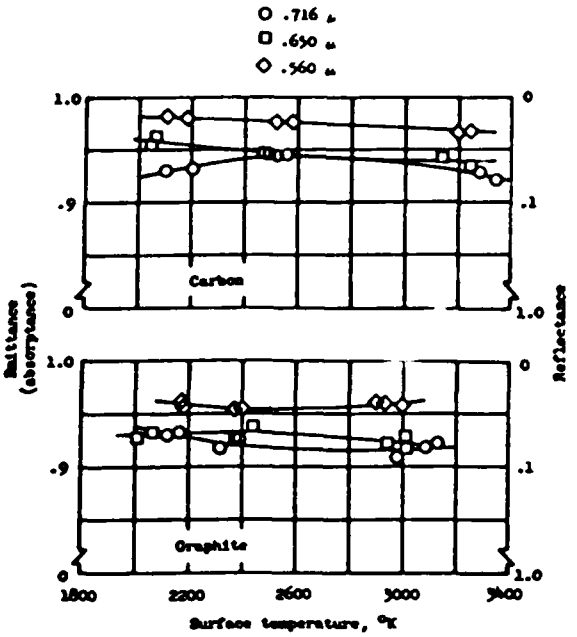

FIGURE 7.—*Emittance and reflectance of oxidized carbon and graphite plotted against temperature.*

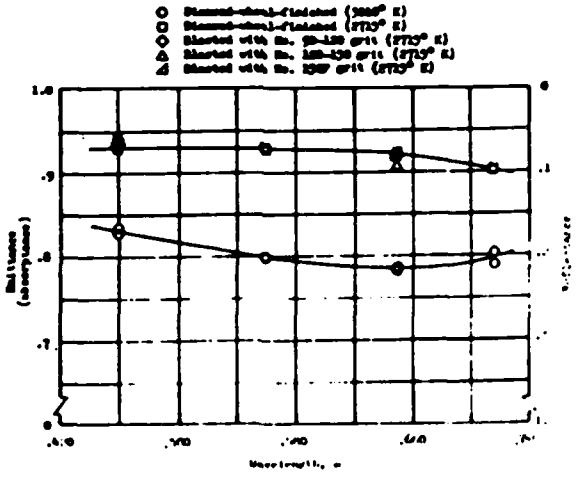

FIGURE 9.—*Emittance and reflectance of zirconia plotted against wavelength.*

SPECTRAL AND TOTAL EMITTANCE OF PHENOLIC NYLON CHAR
(Data from Ref. 22)

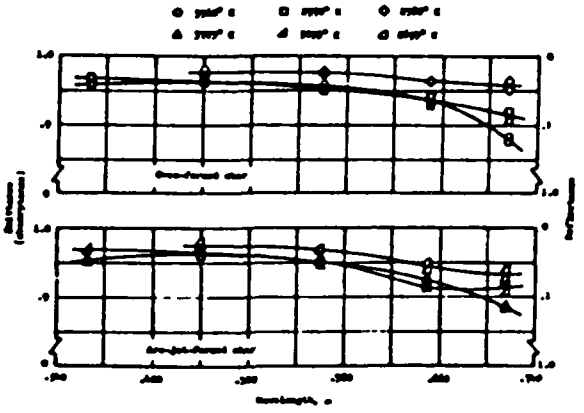

FIGURE 11.—*Emittance and reflectance of phenolic-nylon char plotted against wavelength.*

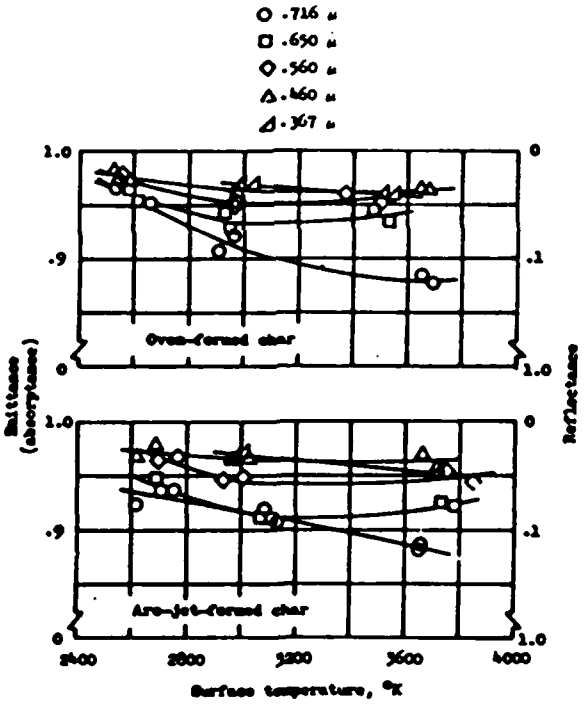

FIGURE 12.—*Emittance and reflectance of phenolic-nylon char plotted against temperature.*

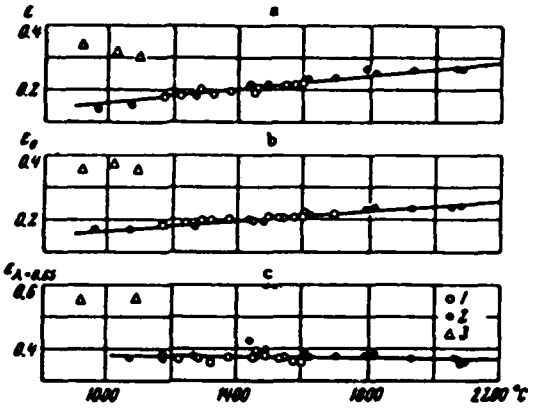

Fig. 1. The emissivities of molybdenum as a function of temperature. a) Total hemispherical emissivity; b) total normal emissivity; c) spectral emissivity for $\lambda = 0.65\,\mu$; 1) experiments in vacuum; 2) experiments in argon; 3) preheating.

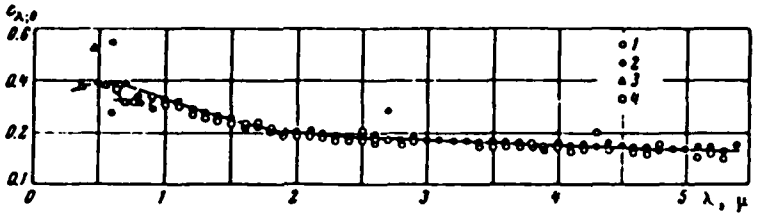

Fig. 2. The spectral emissivity of molybdenum as a function of the wavelength. 1) Measured by infrared spectrometer at t = 1681°C; measured by infrared spectrometer at t = 1825°C; 3) measured by the photographic method; 4) measured by the optical pyrometer.

Fig. 3. Integral emissivity of a niobium specimen (tubes with $d_{out} = 6.29$. $d_{in} = 5.29$) for studies in vacuum and argon. 1) Studies in vacuum; 2) studies in argon (without correction for natural convection); 3) studies in argon (with correction for natural convection).

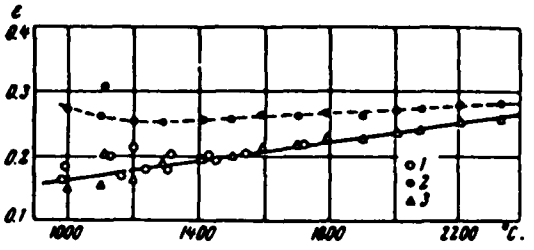

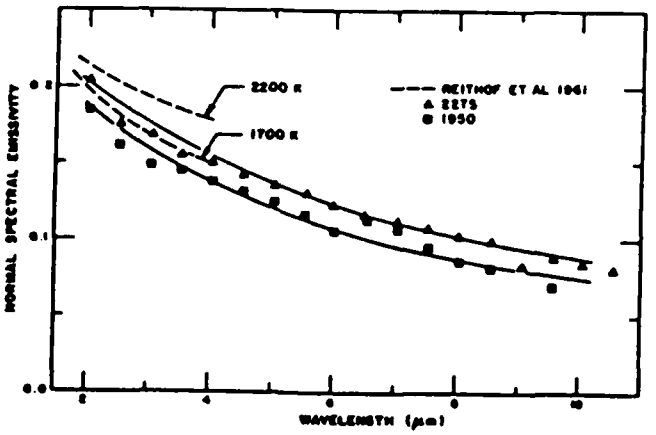

(Data from Ref. 21)

Fig. 6 Spectral Emissivity of Tantalum compared to Literature Values (15).

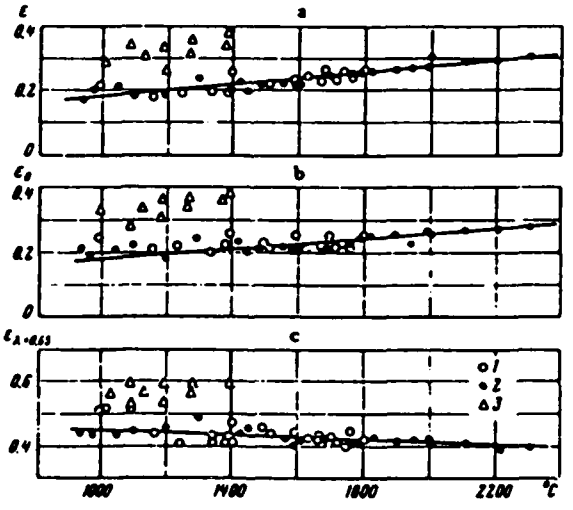

(Data from Ref. 24)

Fig. 7. The emissivities of tantalum as a function of temperature. a) Total hemispherical emissivity; b) total normal emissivity; c) spectral emissivity for $\lambda = 0.65$; 1) experiments under vacuum; 2) experiments in argon; 3) initial heating.

RADIATIVE PROPERTIES OF VARIOUS CERAMICS
(Data from Ref. 26, 27)

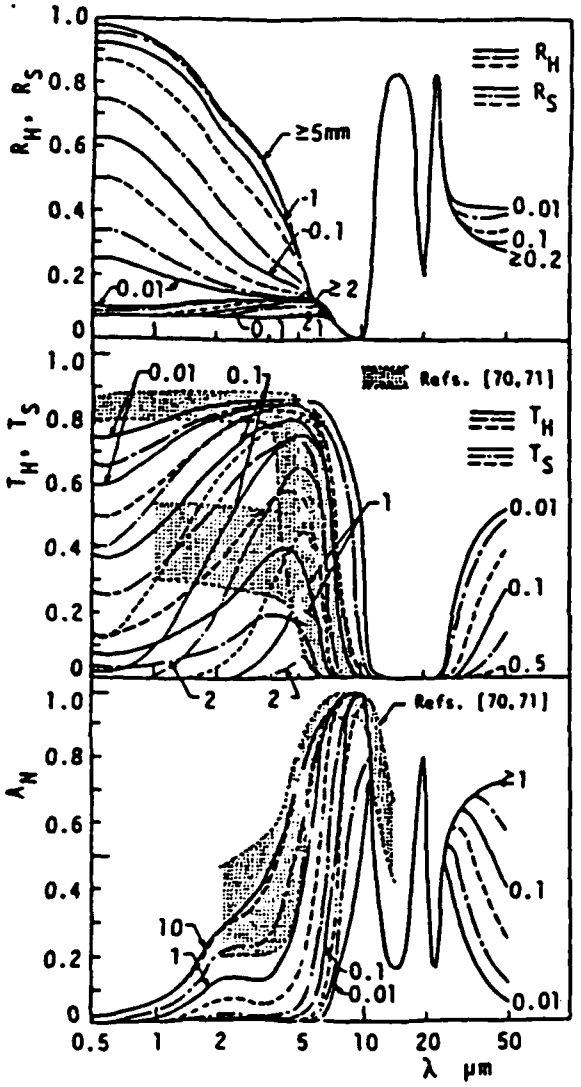

Figure 2-9 Spectra of reflectances, transmittances and an absorptance of alumina ceramic layers (Calc.) [201]

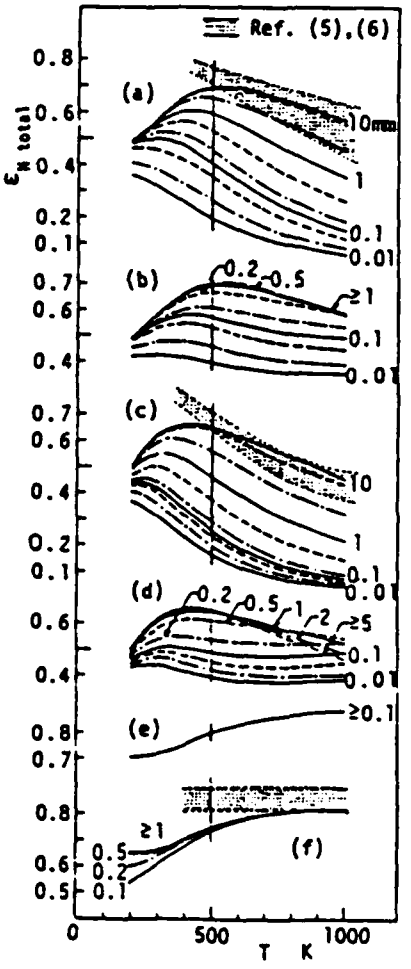

Figure 2-10 Total emittances of ceramic layers: a. Aluminum, b. Aluminum-Hastelloy X, c. Zirconium, d. Zirconium-Hastelloy X, e. Silicon nitride, f. Silicon carbide (Calc.) [92]

RADIATIVE PROPERTIES OF VARIOUS CERAMICS
(Data from Ref. 27, 28)

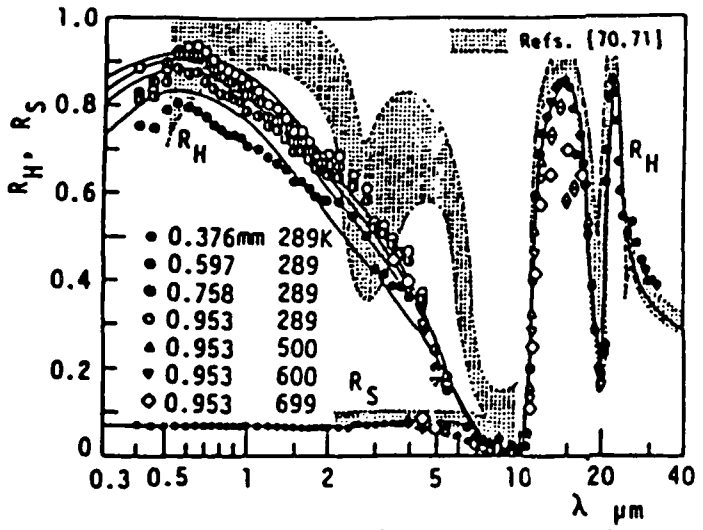

Figure 2-4 Reflectance spectra of white ceramic layers ---aluminum [92]

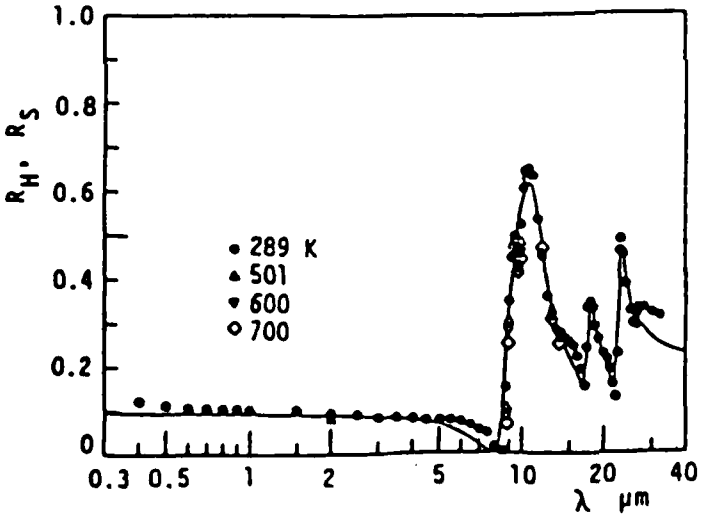

Figure 2-5 Reflectance spectra of a black ceramic ceramic ---silicon nitride [92]

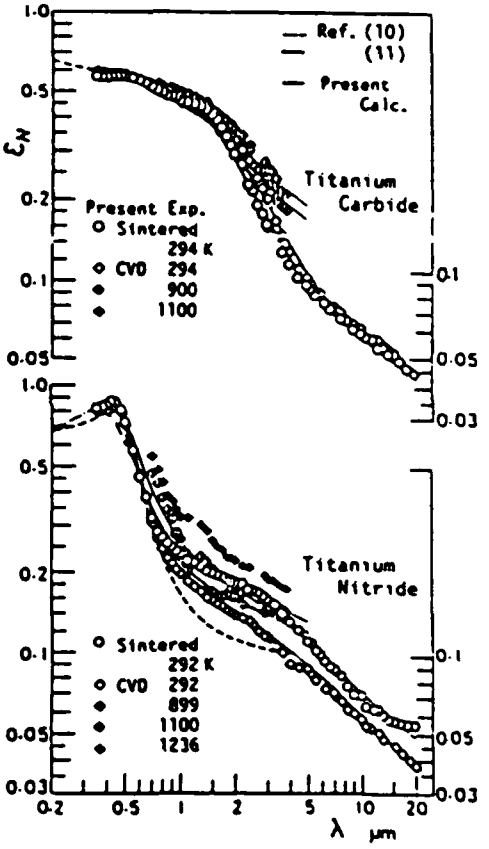

Figure 2-6 Emissivity spectra of electricall conductive ceramics [104]

ABSORPTION COEFFICIENT AND EMISSIVITY OF SOOT CLOUD
(Data from Ref. 32)

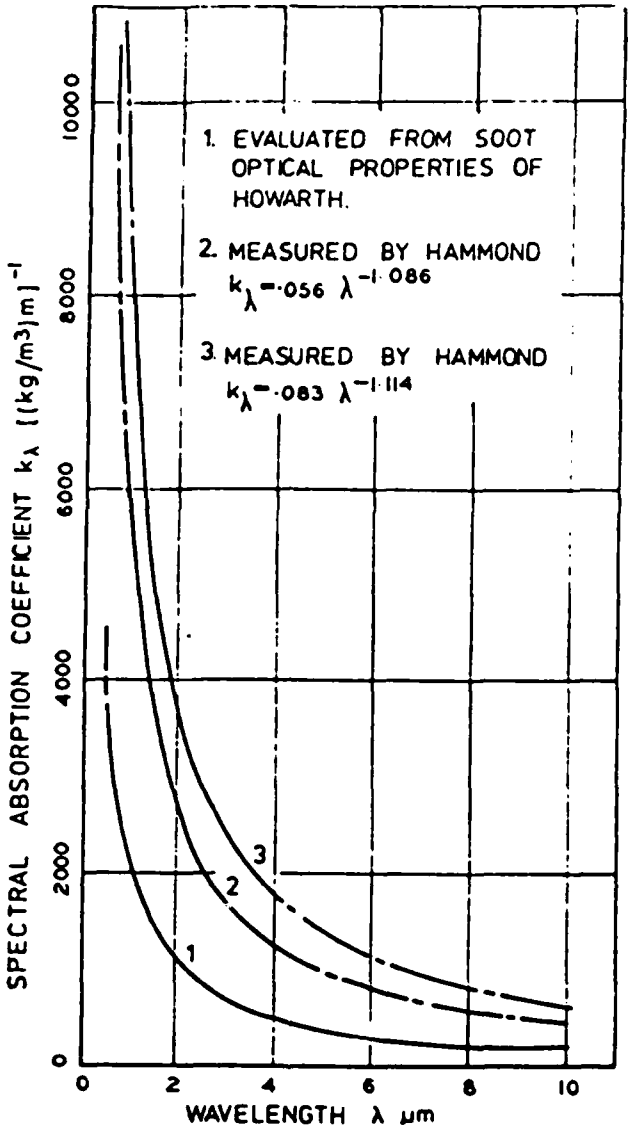

FIG. 3 Spectral absorption coefficient of a cloud of small soot particles.

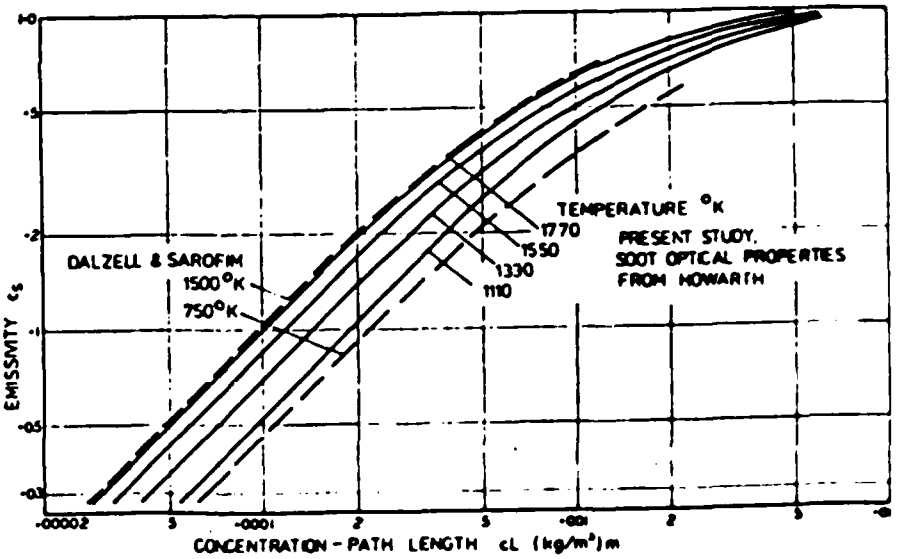

FIG. 4 (Right) Emissivity of a cloud of soot particles.

NORMAL TRANSMISSIVITY OF ALUMINUM OXIDE
PARTICLES SUSPENDED IN CLEAR SOLVENTS
(Data from Ref. 34)

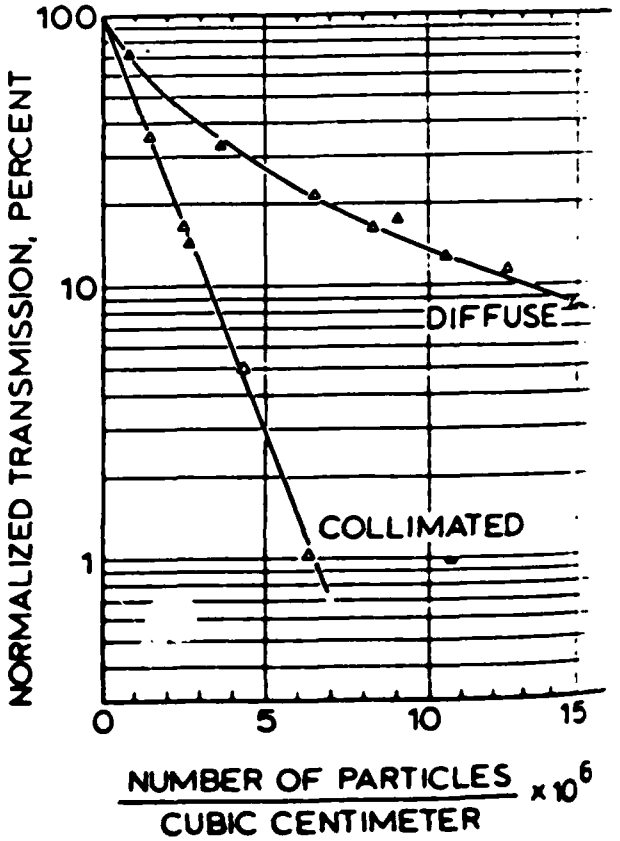

Fig. 3. Transmissivity of aluminum oxide particles in carbon tetrachloride, d = 6.28μ, λ_0 = 4.5μ.

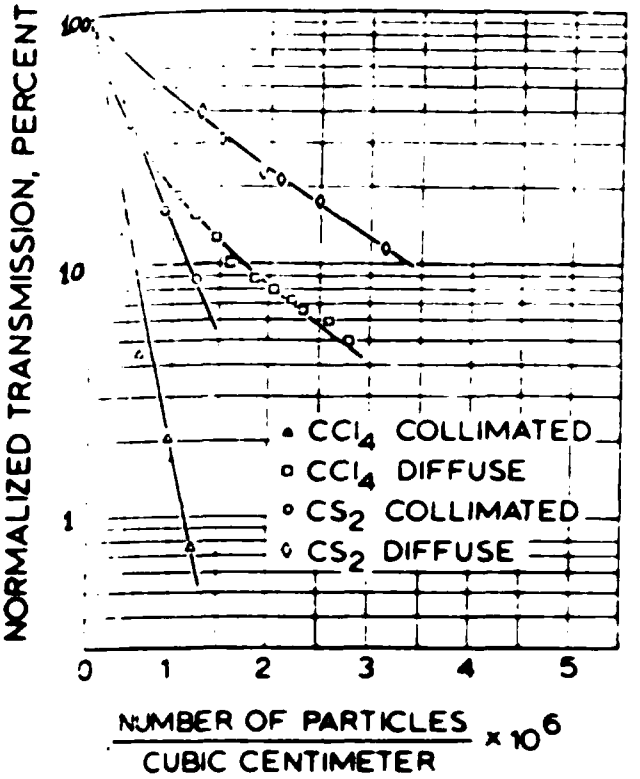

Transmissivity of aluminum oxide particles, d = 12.2μ, λ_0 = 4.5μ.

ABSORPTION AND SCATTERING PROPERTIES OF
ALUMINUM OXIDE PARTICLES
(Data from Ref. 34)

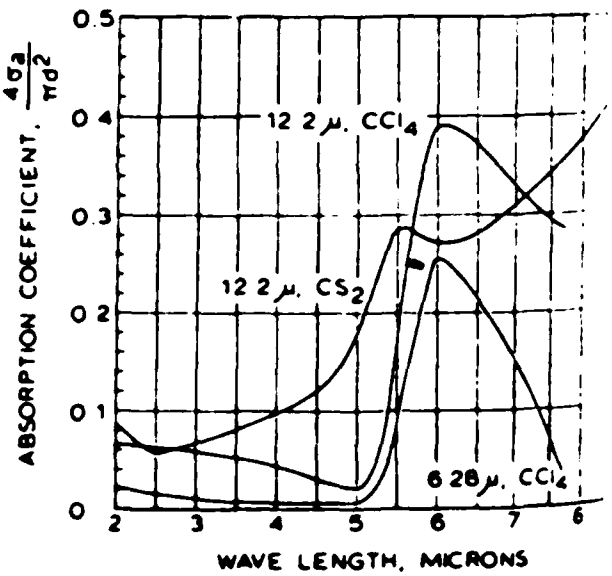

Fig. 8. Absorption coefficient of aluminum oxide particles

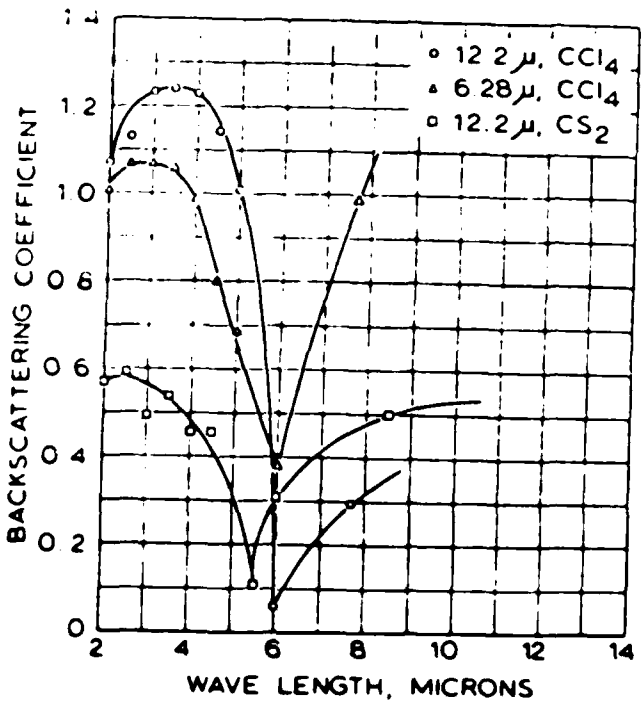

Fig. 6. Backscattering coefficient for various wavelengths.

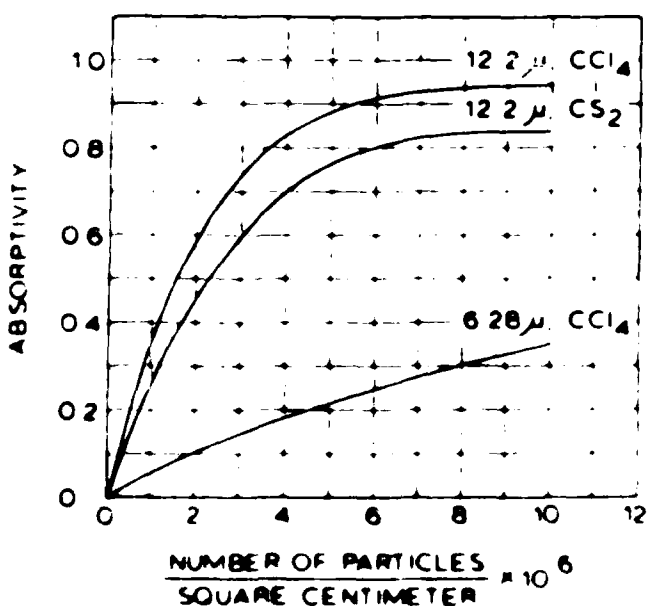

Fig. 12 Absorptivity of various particle clouds for a wavelength of 6.8μ

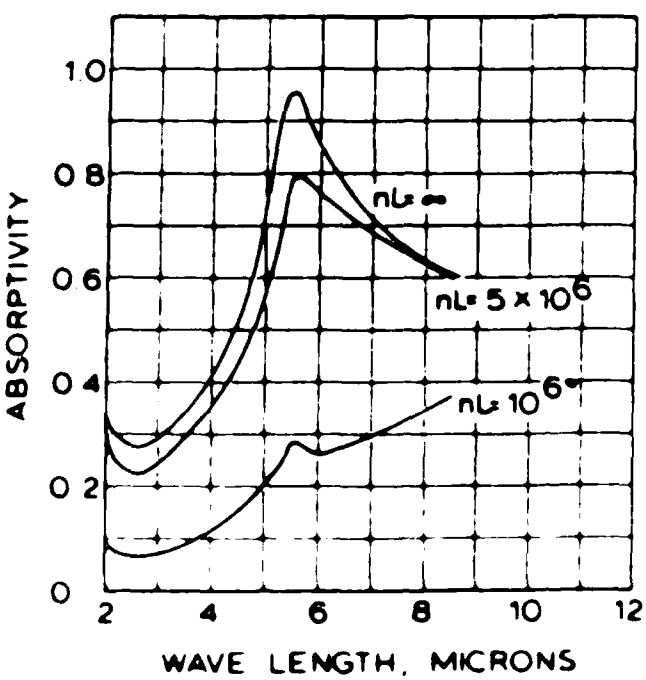

Fig. 11 Absorptivity of a cloud of aluminum oxide particles with a diameter of 12.2μ in carbon dioxide

APPENDIX B

COMPUTER PROGRAM LISTING

```
C         MAIN PART OF THE PROGRAM
          COMMON/BLK2/N,NP1,NP2,NP3,NEQ,NPH,KEX,KIN,KASE,KRAD,PEI,AMI,AME,
         1  DPDX,XU,XD,XP,XL,DX,INTG,CSALFA,HGS,CINF(10),PREF(10),
         2  PR(10),P(10),U(050),F(10,050),R(050),RHO(050),OM(050),Y(050),
         3  DEN(050),AMU(050)
          COMMON/BLK3/KRP,MACH,KR,INDI(10),INDE(10),SUMR,AK,ALMG,BETA,TAUI
         1  ,TAUE,VINF,DELTA,TW,TINF,QS,YL,UMAX,UMIN,FR,YIP,YEM,TR,HW,
         2  HF(10),GAMA(10),AJI(10),AJE(10),SC(050),AU(050),BU(050),CU(050),
         3  A(10,050),B(10,050),C(10,050),TEMPE(050),TEMP(050),PO(050),
         4  AMACH(050),CP(050)
          COMMON/BLK4/NH,NNO,NNP,NO,NN,NO2,NN2,NE,IND(10),STO,AKS,RT,FT,
         1  AMT,DRAGC,STNO,TAUIW,QW,UGU,UGD
          COMMON/BLK5/KRI,PINF,DIFF(50),NOPT,NSKAT
          COMMON/GC/GCON(050),AMOL(050)
          CHARACTER*16 NAME
          TYPE*,'TYPE THE NAME OF THE OUTPUT FILE'
          ACCEPT201,NAME
201       FORMAT(A16)
          OPEN(UNIT=1,FILE=NAME,STATUS='NEW')
          N = 30
          NOPT = 0
   10     CONTINUE
          X = 0.0
          INTG = 0
          CALL CONST
          GO TO 20
   15     N = N+1
          INTG = 0
          XU = 0.03

          KR = KRI
   20     CALL BEGIN
          CALL EXTRA
          AMI=0.
          AME=0.
          GO TO 30
   25     CALL READY
   30     CONTINUE
          INTG=INTG+1
          IF(INTG.GT.50)KR=KRI
          CALL LENGT
          CALL ENTRN
C    CHOICE OF FORWARD STEP
          FRA=0.05
          DX=FRA*PEI/(R(1)*AMI-R(NP3)*AME)
          IF(DX.GT..5*Y(NP3))DX=.5*Y(NP3)
          XD=XU+DX
C         ASSUMES FREE STREAM VELOCITY = AX + BXX + C
C         CALCULATES CHANGE IN FREE STREAM VELOCITY
          A1= 0.0
```

```
      B1= 0.0
      C1= VINF
      UGU = UGD
      UGD = A1 * XD + B1*XD * XD + C1
      DPDX=(UGU+UGD)*(UGU-UGD)*.5*RHO(NP3)/(XD-XU)
      IF(KASE.EQ.2) GO TO 35
      IF(KIN.EQ.1)CALL MASS(XU,XD,AMI)
      IF(KEX.EQ.1)CALL MASS(XU,XD,AME)
      CALL WALL
35    CALL COEFF
      CALL OUTPUT
C   SETTING UP VELOCITIES AT A FREE BOUNDARY
      IF(KEX.EQ.2) U(NP3)=UGD
      IF(KIN.EQ.2) U(1)=SQRT(U(1)-2.*(XD-XU)*DPDX/RHO(1))
      CALL SOLVE(AU,BU,CU,U,NP3)
C   SETTING UP VELOCITIES AT A SYMMETRY LINE
      IF(KIN.NE.3) GO TO  40
      U(1)=U(2)
      IF(KRAD.EQ.0) U(1)=.75*U(2)+.25*U(3)
40    IF(KEX.EQ.3) U(NP3)=.75*U(NP2)+.25*U(NP1)
45    CONTINUE
      IF(NEQ.EQ.1) GO TO  90
      DO 75 J=1,NPH
      DO 50 I=2,NP2
      AU(I)=A(J,I)
      BU(I)=B(J,I)
50    CU(I)=C(J,I)
      DO 55 I=1,NP3
55    SC(I)=F(J,I)
      CALL SOLVE(AU,BU,CU,SC,NP3)
      DO 60 I=1,NP3
60    F(J,I)=SC(I)
      IF(KASE.EQ.2) GO TO 65
C   SETTING UP WALL VALUES OF F
      IF(KIN.EQ.1.AND.INDI(J).EQ.2)F(J,I)=((1.+BETA+GAMA(J))*F(J,2)-
     1  (1.+BETA-GAMA(J))*F(J,3))*.5/GAMA(J)
      IF(KEX.EQ.1.AND.INDE(J).EQ.2)F(J,NP3)=((1.+BETA+GAMA(J))*
     1  F(J,NP2)-(1.+BETA-GAMA(J))*F(J,NP1))*.5/GAMA(J)
C   SETTING UP SYMMETRY-LINE VALUES OF F
65    IF(KIN.NE.3) GO TO 70
      IF(KRAD.EQ.0)F(J,1)=.75*F(J,2)+.25*F(J,3)
70    IF(KEX.EQ.3)F(J,NP3)=.75*F(J,NP2)+.25*F(J,NP1)
75    CONTINUE
C     CALCULATION OF AUXILIARY PARAMETERS
      DO 80 I=2,NP2
      TEMP(I)=(F(NH,I)-U(I)*U(I)/2.0)/CP(I)
      IF(TEMP(I).LE.0.0) TEMP(I)=TINF
      TEMPE(I) = TEMP(I)
80    CONTINUE
      CALL DENSTY
      DO 85 I = 2,NP2
```

```
      PO(I)=RHO(I)*(53.3*TEMP(I)+0.5*U(I)*U(I)/32.2)/144.
   85 AMACH(I)=U(I)/SQRT(1.4*53.3*32.2*ABS(TEMP(I)))
   90 XP=XU
      XU=XD
      PEI=PEI+DX*(R(1)*AMI-R(NP3)*AME)
      IF(INTG.GT. 50 .AND. NOPT .EQ. 1) GO TO 95
      GO TO 105
   95 DO 100 I =3,NP1
      IF (ABS(DIFF(I)) .GT. 1.5) GO TO 15
  100 CONTINUE
C     THE TERMINATION CONDITION
  105 IF(XU.LT.XL) GO TO 25
      GO TO 10
  110 STOP
      END
```

```
      SUBROUTINE CONST
      REAL MACH
      COMMON/BLK2/N,NP1,NP2,NP3,NEQ,NPH,KEX,KIN,KASE,KRAD,PEI,AMI,AME,
     1 DPDX,XU,XD,XP,XL,DX,INTG,CSALFA,HGS,CINF(10),PREF(10),
     2 PR(10),P(10),U(050),F(10,50),R(050),RHO(050),OM(050),Y(050),
     3 DEN(050),AMU(050)
      COMMON/BLK3/KRP,MACH,KR,INDI(10),INDE(10),SUMR,AK,ALMG,BETA,TAUI
     1 ,TAUE,VINF,DELTA,TW,TINF,QS,YL,UMAX,UMIN,FR,YIP,YEM,TR,HW,
     2 HF(10),GAMA(10),AJI(10),AJE(10),SC(050),AU(050),BU(050),CU(050),
     3 A(10,050),B(10,050),C(10,050),TEMPE(050),TEMP(050),PO(050),
     4 AMACH(050),CP(050)
      COMMON/BLK4/NH,NNO,NNF,NO,NN,NO2,NN2,NE,IND(10),STO,AKS,RT,FT,
     1 AMT,DRAGC,STNO,TAUIW,QW,UGU,UGD
      COMMON/BLK5/KRI,PINF,DIFF(50),NOPT,NSKAT
      COMMON/CWALL/CW
      COMMON/SANJ/SIGMEX,SIGMAB,PDEN,SIZE
C     UNITS ***** TEMP(R) **** PINF(LBF/IN2) ***************
C     UNITS ***** DEN(LBM/FT3) ** AMU(LBM/FT-SEC0 ** CP(FT2/SEC2-R)
C     IF KR=1 INTEGRAL RADIATION ANALYSIS IS USED
C     IF KR=2 RADIATION EFFECTS ARE NEGLECTED
C     IF KR=3 OPTICALLY THIN ANALYSIS IS USED
      WRITE(6,*)'INPUT THE VALUE TINF,TW,PINF,MACH,XL,KRI,NSKAT,
     1 CW,QS,REFT,SIGMEX,SIGMAB,SIZE,PDEN'
      WRITE(1,*)'INPUT THE VALUE TINF,TW,PINF,MACH,XL,KRI,NSKAT,
     1 CW,QS,REFT,SIGMEX,SIGMAB,SIZE,PDEN'
```

```
      READ(5,*)TINF,TW,PINF,MACH,XL,KRI,NSKAT,CW,QS,REFT,SIGMEX,
     1  SIGMAB,SIZE,PDEN
      WRITE(1,*)TINF,TW,PINF,MACH,XL,KRI,NSKAT,CW,QS,REFT,SIGMEX,
     1  SIGMAB,SIZE,PDEN
      KR = KRI
      TR=537.0
      XU= 0.03
      DINF=PINF*144./((53.3)*TINF)
      VISC=(1.2267E-05)*(TINF/TR)**.76
      VINF = MACH*SQRT(1.4*53.3*32.2*TINF)
      UGD = VINF
      DELTA=0.37*XU/((VINF*DINF*XU/VISC)**.2)
      IND(1)= 1
      NH=1
      AK=.435
      ALMG=.09
      FR=.01
      PREF(1)=0.9
      PREF(2)=0.9
      PREF(3)=0.9
      PR(1)=0.7
      PR(2)=0.7
      PR(3)=0.7
      P(1)= 3.68*(PR(1)/PREF(1)-1.0)*((PR(1)/PREF(1))**(-.25))
      P(2)=5.0*(PR(2)/PREF(2)-1.0)*((PR(2)/PREF(2))**(-0.25))
      P(3)=5.0*(PR(3)/PREF(3)-1.0)*((PR(3)/PREF(3))**(-0.25))
      RETURN
      END
```

```
      SUBROUTINE BEGIN

      COMMON/BLK2/N,NP1,NP2,NP3,NEQ,NPH,KEX,KIN,KASE,KRAD,PEI,AMI,AME,
     1 DPDX,XU,XD,XP,XL,DX,INTG,CSALFA,HGS,CINF(10),PREF(10),
     2 PR(10),P(10),U(050),F(10,050),R(050),RHO(050),DM(050),Y(050),
     3 DEN(050),AMU(050)
      COMMON/BLK3/KRP,MACH,KR,INDI(10),INDE(10),SUMR,AK,ALMG,BETA,
     1  TAUI,TAUE,VINF,DELTA,TW,TINF,QS,YL,UMAX,UMIN,FR,YIP,YEM,TR,HW,
     2  HF(10),GAMA(10),AJI(10),AJE(10),SC(050),AU(050),BU(050),
     3  CU(050),A(10,050),B(10,050),C(10,050),TEMPE(050),TEMP(050),
```

```
     4  PO(050),AMACH(050),CP(050)
        COMMON/BLK4/NH,NNO,NNP,NO,NN,NO2,NN2,NE,IND(10),STO,AKS,RT,FT,
     1  AMT,DRAGC,STNO,TAUIW,QW,UGU,UGD
        COMMON/BLK5/KRI,PINF,DIFF(50),NOPT,NSKAT
        COMMON/CWALL/CW
        DIMENSION CINW(10)
C     PROBLEM SPECIFICATION
        KRAD = 0
        KIN = 1
        NEQ=4
        KEX = 2
        KASE=2
        IF(KIN.EQ.1.OR.KEX.EQ.1) KASE=1
        NPH=NEQ-1
        NP1=N+1
        NP2=N+2
        NP3=N+3
C     INITIAL VELOCITY PROFILE
        U(1)=0.0
        U(2)=0.0
        DO 10 I =3,NP1
        Y(I)=DELTA*((FLOAT(I-2))/FLOAT(N))
   10   U(I)=VINF*(Y(I)/DELTA)**.143
        Y(NP3) = DELTA
        U(NP3)=VINF
C     CALCULATION OF SLIP VELOCITIES AND DISTANCES
        BETA=.143
        GO TO (15,20,25) ,KIN
   15   U(2)=U(3)/(1.+2.*BETA)
        Y(2)=Y(3)*BETA/(2.+BETA)
        GO TO 35
   20   U11=U(1)*U(1)
        U13=U(1)*U(3)
        U33=U(3)*U(3)
        SQ=84.*U11-12.*U13+9.*U33
        U(2)=(16.*U11-4.*U13+U33)/(2.*(U(1)+U(3))+SQRT(SQ))
        Y(2)=Y(3)*(U(2)+U(3)-2.*U(1))*.5/(U(2)+U(3)+U(1))
        GO TO 35
   25   IF(KRAD.NE.0) GO TO 30
        U(2)=(4.*U(1)-U(3))/3.
        Y(2)=0.
        GO TO 35
   30   U(2)=U(1)
        Y(2)=Y(3)/3.
   35   GO TO (40,45,50) ,KEX
   40   U(NP2)=U(NP1)/(1.+2.*BETA)
        Y(NP2)=Y(NP3)-(Y(NP3)-Y(NP1))*BETA/(2.+BETA)
        GO TO 55
   45   U11=U(NP1)*U(NP1)
        U13=U(NP1)*U(NP3)
        U33=U(NP3)*U(NP3)
```

```
      SQ=84.*U33-12.*U13+9.*U11
      U(NP2)=(16.*U33-4.*U13+U11)/(2.*(U(NP1)+U(NP3))+SQRT(SQ))
      Y(NP2)=Y(NP3)-(Y(NP3)-Y(NP1))*(U(NP2)+U(NP1)-2.*U(NP3))*.5/
     1 (U(NP2)+U(NP1)+U(NP3))
      GO TO 55
   50 U(NP2)=(4.*U(NP3)-U(NP1))/3
      Y(NP2)=Y(NP3)
   55 CONTINUE
C  INITIAL PROFILES OF OTHER DEPENDENT VARIABLES
      CP1=5990.0
      CP2=5990.0
      F(2,1)=1.0-CW
      F(3,1)=CW
      F(2,NP3)=1.0
      F(3,NP3)=0.0
      TEMP(NP3)= TINF
      HCW = 0.0
      HCG = 0.0
      HGS=CP1*TINF
      HW= (CP1*F(2,1)+CP2*F(3,1))*TW
      HG=HGS+0.5*VINF*VINF
      F(NH,1)=HW
      F(NH,NP3) = HG
      DO 60 I=3,NP1
      F(NH,I)= HW+(HG-HW)*(Y(I)/DELTA)**.143
      F(3,I)=CW*(1.0-U(I)/VINF)
      F(2,I)=1.0-F(3,I)
   60 CONTINUE
C   CALCULATION OF CORRESPONDING SLIP VALUES
      DO 100 J=1,NPH
      GAMA(J)=.143
      GO TO (65,70,75),KIN
   65 F(J,2)=F(J,1)+(F(J,3)-F(J,1))*(1.+BETA-GAMA(J))/(1.+BETA+
     1 GAMA(J))
      GO TO 80
   70 G=(U(2)+U(3)-8.*U(1))/(5.*(U(2)+U(3))+8.*U(1))
      GF=(1.-PREF(J))/(1.+PREF(J))
      GF=(G+GF)/(1.+G*GF)
      F(J,2)=F(J,3)*GF+(1.-GF)*F(J,1)
      GO TO 80
   75 F(J,2)=F(J,1)
      IF(KRAD.EQ.0)F(J,2)=(4.*F(J,1)-F(J,3))/3.
   80 GO TO (85,90,95),KEX
   85 F(J,NP2)=F(J,NP3)+(F(J,NP1)-F(J,NP3))*(1.+BETA-GAMA(J))/(1.+
     1 BETA-GAMA(J))
      GO TO 100
   90 G=(U(NP2)+U(NP1)-8.*U(NP3))/(5.*(U(NP2)+U(NP1))+8.*U(NP3))
      GF=(1.-PREF(J))/(1.+PREF(J))
      GF=(G+GF)/(1.+G*GF)
      F(J,NP2)=F(J,NP1)*GF+(1.-GF)*F(J,NP3)
      GO TO 100
   95 F(J,NP2)=(4.*F(J,NP3)-F(J,NP1))/3.
  100 CONTINUE
      RETURN
      END
```

```
      SUBROUTINE READY
      COMMON/BLK2/N,NP1,NP2,NP3,NEQ,NPH,KEX,KIN,KASE,KRAD,PEI,AMI,AME,
     1  DPDX,XU,XD,XP,XL,DX,INTG,CSALFA,HGS,CINF(10),PREF(10),
     2  PR(10),P(10),U(050),F(10,050),R(050),RHO(050),OM(050),Y(050),
     3  DEN(050),AMU(050)
      COMMON/BLK3/KRP,MACH,KR,INDI(10),INDE(10),SUMR,AK,ALMG,BETA,TAUI
     1  ,TAUE,VINF,DELTA,TW,TINF,QS,YL,UMAX,UMIN,PR,YIP,YEM,  TR,HW,
     2  HF(10),GAMA(10),AJI(10),AJE(10),SC(050),AU(050),BU(050),CU(050),
     3  A(10,050),B(10,050),C(10,050),TEMPE(050),TEMP(050),PO(050),
     4  AMACH(050),CP(050)
      COMMON/BLK4/NH,NNO,NNP,NO,NN,NO2,NN2,NE,IND(10),STO,AKS,RT,FT,
     1  AMT,DRAGC,STNO,TAUIW,QW,UGU,UGD
      CALL RAD(XU,R(1),CSALFA)
C     Y NEAR THE I BOUNDARY
      GO TO (10,15,20) ,KIN
   10 Y(2)=(1.+BETA)*OM(3)*4./((3.*RHO(2)+RHO(3))*(U(2)+U(3)))
      GO TO 25
   15 Y(2)=12.*OM(3)/((3.*RHO(2)+RHO(3))*(U(2)+U(3)+4.*U(1)))
      GO TO 25
   20 Y(2)=.5*OM(3)/(RHO(1)*U(1))
   25 Y(3)=Y(2)+.25*OM(3)*(1./(RHO(3)*U(3))+2./(RHO(3)*U(3)+RHO(2)*
     1 U(2)))
C     Y  S FOR INTERMEDIATE GRID POINTS
      DO 30 I=4,NP1
   30 Y(I)=Y(I-1)+.5*(OM(I)-OM(I-1))*(1./(RHO(I)*U(I))+1./(RHO(I-1)*
     1 U(I-1)))
C Y NEAR THE E BOUNDARY
      Y(NP2)=Y(NP1)+.25*(OM(NP2)-OM(NP1))*(1./(RHO(NP1)*U(NP1))+2./
     1 (RHO(NP1)*U(NP1)+RHO(NP2)*U(NP2)))
      GO TO (35,40,45),KEX
   35 Y(NP3)=Y(NP2)+(1.+BETA)*(OM(NP2)-OM(NP1))*4./((RHO(NP1)+3.*
     1 RHO(NP2))*(U(NP1)+U(NP2)))
      GO TO 50
   40 Y(NP3)=Y(NP2)+12.*(OM(NP2)-OM(NP1))/((RHO(NP1)+3.*RHO(NP2))*(
     1 U(NP2)+U(NP1)+4.*U(NP3)))
      GO TO 50
   45 Y(NP3)=Y(NP2)+.5*(OM(NP2)-OM(NP1))/(RHO(NP3)*U(NP3))
   50 IF(CSALFA.EQ.0..OR.KRAD.EQ.0) GO TO 60
      DO 55 I=2,NP3
   55 Y(1)=2.*Y(I)*PEI/(R(1)+SQRT(R(1)*R(1)+2.*Y(I)*PEI*CSALFA))
      GO TO 70
   60 DO 65 I=2,NP3
   65 Y(I)=PEI*Y(I)/R(1)
   70 Y(2)=2.*Y(2)-Y(3)
      Y(NP2)=2.*Y(NP2)-Y(NP1)
C     CALCULATION OF THE RADII
      DO 75 I=2,NP3
      IF(KRAD.EQ.0) R(I)=R(1)
      IF(KRAD.NE.0) R(I)=R(1)+Y(I)*CSALFA
   75 CONTINUE
      RETURN
      END
```

```
      SUBROUTINE DENSTY
      COMMON/BLK2/N,NP1,NP2,NP3,NEQ,NPH,KEX,KIN,KASE,KRAD,PEI,AMI,AME,
     1  DPDX,XU,XD,XP,XL,DX,INTG,CSALFA,HGS,CINF(10),PREF(10),
     2  PR(10),P(10),U(050),F(10,050),R(050),RHO(050),OM(050),Y(050),
     3  DEN(050),AMU(050)
      COMMON/BLK3/KRP,MACH,KR,INDI(10),INDE(10),SUMR,AK,ALMG,BETA,TAUI
     1  ,TAUE,VINF,DELTA,TW,TINF,QS,YL,UMAX,UMIN,FR,YIP,YEM, TR,HW,
     2  HF(10),GAMA(10),AJI(10),AJE(10),SC(050),AU(050),BU(050),CU(050),
     3  A(10,050),B(10,050),C(10,050),TEMPE(050),TEMP(050),PO(050),
     4  AMACH(050),CP(050)
      COMMON/BLK4/NH,NNO,NNP,NO,NN,NO2,NN2,NE,IND(10),STO,AKS,RT,FT,
     1  AMT,DRAGC,STNO,TAUIW,QW,UGU,UGD
      DO 115 I=1,NP3
      RHO(I)=     DEN(I)*(TR/TEMP(I))
  115 CONTINUE
      RETURN
      END


      SUBROUTINE RAD(X,R1,CSALFA)
C       APPLICABLE TO PLANE FLOWS
      CSALFA = 1.0
      R1 = 1.0
      RETURN
      END
      FUNCTION VISCO(I)
      COMMON/BLK2/N,NP1,NP2,NP3,NEQ,NPH,KEX,KIN,KASE,KRAD,PEI,AMI,AME,
     1  DPDX,XU,XD,XP,XL,DX,INTG,CSALFA,HGS,CINF(10),PREF(10),
     2  PR(10),P(10),U(050),F(10,050),R(050),RHO(050),OM(050),Y(050),
     3  DEN(050),AMU(050)
      COMMON/BLK3/KRP,MACH,KR,INDI(10),INDE(10),SUMR,AK,ALMG,BETA,TAUI
     1  ,TAUE,VINF,DELTA,TW,TINF,QS,YL,UMAX,UMIN,FR,YIP,YEM, TR,HW,
     2  HF(10),GAMA(10),AJI(10),AJE(10),SC(050),AU(050),BU(050),CU(050),
     3  A(10,050),B(10,050),C(10,050),TEMPE(050),TEMP(050),PO(050),
     4  AMACH(050),CP(050)
      COMMON/BLK4/NH,NNO,NNP,NO,NN,NO2,NN2,NE,IND(10),STO,AKS,RT,FT,
     1  AMT,DRAGC,STNO,TAUIW,QW,UGU,UGD
      VISCO=AMU(I)*(TEMP(I)/TR)**.76
      RETURN
      END
```

```
      SUBROUTINE LENGT
      COMMON/BLK2/N,NP1,NP2,NP3,NEQ,NPH,KEX,KIN,KASE,KRAD,PEI,AMI,AME,
     1  DPDX,XU,XD,XF,XL,DX,INTG,CSALFA,HGS,CINF(10),PREF(10),
     2  PR(10),P(10),U(050),F(10,050),R(050),RHO(050),OM(050),Y(050),
     3  DEN(050),AMU(050)
      COMMON/BLK3/KRP,MACH,KR,INDI(10),INDE(10),SUMR,AK,ALMG,BETA,TAUI
     1  ,TAUE,VINF,DELTA,TW,TINF,PS,YL,UMAX,UMIN,FR,YIP,YEM,TR,HW,
     2  HF(10),GAMA(10),AJI(10),AJE(10),SC(050),AU(050),BU(050),CU(050),
     3  A(10,050),B(10,050),C(10,050),TEMPE(050),TEMP(050),PO(050),
     4  AMACH(050),CP(050)
      COMMON/BLK4/NH,NNO,NNP,NO,NN,NO2,NN2,NE,IND(10),STO,AKS,PT,PT,
     1  AMT,DRAGC,STNO,TAUIW,QW,UGU,UGD
C  SEARCH FOR MAXIMUM AND MINIMUM VELOCITITES
   10 UMAX=U(1)
      UMIN=U(1)
      DO 15 J=3,NP3
      IF(J.EQ.NP2) GO TO 15
      IF(U(J).GT.UMAX) UMAX=U(J)
      IF(U(J).LT.UMIN) UMIN=U(J)
   15 CONTINUE
      DIF=ABS(UMAX-UMIN)*FR
C     SEARCH FOR THE I BOUNDARY
      IF(KIN.NE.2) GO TO 35
      U21=ABS(.5*(U(2)+U(3))-U(1))
      IF(U21.LT.DIF) GO TO 20
      YIP=SQRT(DIF/U21)*(Y(2)+Y(3))*.5
      GO TO 40
   20 J=2
   25 J=J+1
      UJ1=U(J)-U(1)
      IF(ABS(UJ1).GE.DIF) GO TO 30
      GO TO 25
   30 A1=1.
      IF(UJ1.LT.0.) A1=-1.
      YIP=Y(J-1)+(Y(J)-Y(J-1))*(U(1)+A1*DIF-U(J-1))/(U(J)-U(J-1))
      GO TO 40
   35 YIP=0.
C  SEARCH NEAR THE E BOUNDARY
   40 IF(KEX.NE.2) GO TO 60
      U21=ABS(.5*(U(NP1)+U(NP2))-U(NP3))
      IF(U21.LT.DIF) GO TO 45
      YEM=SQRT(DIF/U21)*(.5*(Y(NP1)+Y(NP2))-Y(NP3))+Y(NP3)
      GO TO 65
   45 J=NP2
   50 J=J-1
      UJ1=U(J)-U(NP3)
      IF(ABS(UJ1).GE.DIF) GO TO 55
      GO TO 50
   55 A1=1.
      IF(UJ1.LT.0.)A1=-1.
      YEM=Y(J+1)+(Y(J)-Y(J+1))*(U(NP3)+A1*DIF-U(J+1))/(U(J)-U(J+1))
      GO TO 65
   60 YEM=Y(NP3)
   65 YL=YEM-YIP
      RETURN
      END
```

```
      SUBROUTINE MASS(XU,XD,AM)
C     APPLICABLE TO POROUS WALL
      AM = 0.0
      RETURN
      END




      SUBROUTINE ENTRN
      COMMON/BLK2/N,NP1,NP2,NP3,NEQ,NPH,KEX,KIN,KASE,KRAD,PEI,AMI,AME,
     1 DPDX,XU,XD,XP,XL,DX,INTG,CSALFA,HGS,CINF(10),PREF(10),
     2 PR(10),P(10),U(050),F(10,050),R(050),RHO(050),OM(050),Y(050),
     3 DEN(050),AMU(050)
      COMMON/BLK3/KRP,MACH,KR,INDI(10),INDE(10),SUMR,AK,ALMG,BETA,TAUI
     1 ,TAUE,VINF,DELTA,TW,TINF,QS,YL,UMAX,UMIN,FR,YIP,YEM, TR,HW,
     2 HF(10),GAMA(10),AJI(10),AJE(10),SC(050),AU(050),BU(050),CU(050),
     3 A(10,050),B(10,050),C(10,050),TEMPE(050),TEMP(050),PO(050),
     4 AMACH(050),CP(050)
      COMMON/BLK4/NH,NNO,NNP,NO,NN,NO2,NN2,NE,IND(10),STO,AKS,RT,FT,
     1 AMT,DRAGC,STNO,TAUIW,QW,UGU,UGD
C     THIS SUBROUTINE USES THE MIXING-LENGT HYPOTHESIS.
      GO TO (70,75,80),KIN
   70 GO TO  85
   75 AMI=8.*RHO(1)*((ALMG*YL)/(Y(2)+Y(3)))**2*ABS(U(2)+U(3)-2.*U(1))
      GO TO 85
   80 AMI=0.
   85 GO TO (90,95,100),KEX
   90 RETURN
   95 AME=-8.*RHO(NP3)*((ALMG*YL)/(Y(NP1)+Y(NP2)-2.*Y(NP3)))**2*ABS(
     1 U(NP1)+U(NP2)-2.*U(NP3))
      RETURN
  100 AME=0.
      RETURN
      END




      SUBROUTINE WALL
      COMMON/BLK2/N,NP1,NP2,NP3,NEQ,NPH,KEX,KIN,KASE,KRAD,PEI,AMI,AME,
     1 DPDX,XU,XD,XP,XL,DX,INTG,CSALFA,HGS,CINF(10),PREF(10),
     2 PR(10),P(10),U(050),F(10,050),R(050),RHO(050),OM(050),Y(050),
     3 DEN(050),AMU(050)
```

```
      COMMON/BLK3/KRP,MACH,KR,INDI(10),INDE(10),SUMR,AK,ALMG,BETA,TAUI
     1  ,TAUE,VINF,DELTA,TW,TINF,QS,YL,UMAX,UMIN,FR,YIP,REM, TR,HW,
     2  HF(10),GAMA(10),AJI(10),AJE(10),SC(050),AU(050),BU(050),CU(050),
     3  A(10,050),B(10,050),C(10,050),TEMPE(050),TEMP(050),PO(050),
     4  AMACH(050),CP(050)
      COMMON/BLK4/NH,NNO,NNP,NO,NN,NO2,NN2,NE,IND(10),STO,AKS,RT,FT,
     1  AMT,DRAGC,STNO,TAUIW,QW,UGU,UGD
C  CALCULATION OF BETA FOR THE I  BOUNDARY
      IF(KEX.NE.1) GO TO 25
   10 YI=Y(NP3)-.5*(Y(NP1)+Y(NP2))
      UI=.5*(U(NP2)+U(NP1))
      RH=.25*(3.*RHO(NP2)+RHO(NP1))
      RE=RH*UI*YI/VISCO(NP3)
      FP=DPDX*YI/(RH*UI*UI)
      AM=AME/(RH*UI)
      CALL WF1(RE,FP,AM,S)
      BETA=SQRT(ABS(S+FP+AM))/AK
      TAUE=S*RH*UI*UI
      IF(NEQ.EQ.1) GO TO 20
C  CALCULATION OF GAMA  S FOR THE E BOUNDARY
      DO 15 J=1,NPH
      CALL WF2(RE,FP,AM,PR(J),PREF(J),P(J),SF)
      GAMA(J)=(SF+AM)*PREF(J)/(AK*AK*BETA)
      IF(INDE(J).EQ.1)AJE(J)=SF*RH*UI*(F(J,NP2)+F(J,NP1)-2.*F(J,NP3))*
     1  .5
   15 CONTINUE
   20 IF(KIN.NE.1)RETURN
C   CALCULATION OF BETA FOR THE I BOUNDARY
   25 YI=.5*(Y(2)+Y(3))
      UI=.5*(U(2)+U(3))
      RH=.25*(3.*RHO(2)+RHO(3))
      RE=RH*UI*YI/VISCO(1)
      FP=DPDX*YI/(RH*UI*UI)
      AM=AMI/(RH*UI)
      CALL WF1(RE,FP,AM,S)
      BETA=SQRT(ABS(S+FP+AM))/AK
      TAUI=S*RH*UI*UI
      TAUIW = TAUI/32.2
      DRAGC = (TAUI/(RHO(NP3)*U(NP3)*U(NP3)))*2.
      IF(NEQ.EQ.1) RETURN
C  CALCULATION OF GAMA S FOR THE I BOUNDARY
      DO 35 J=1,NPH
   30 CALL WF2(RE,FP,AM,PR(J),PREF(J),P(J),SF)
      HI= .5*(F(NH,2)+F(NH,3))
      PHI = (UI*UI/(2.0*(HI-F(NH,2))))*((1.0-PREF(NH))*SF*PREF(NH)/
     1  (AK*AK*BETA)-2.0*BETA*(1.0-PREF(NH)))
      IF(J.EQ.1) STNO=SF*(RH*UI/(RHO(NP3)*U(NP3)))
      GAMA(J)=(SF+AM)*PREF(J)/(AK*AK*BETA)-PHI
      IF(INDI(J).EQ.1)AJI(J)=SF*RH*UI*(2.*F(J,1)-F(J,2)-F(J,3))*.5
   35 CONTINUE
      TAO = 0.015
      TA = TAO*(0.5*(TEMP(3)+TW)/TR)**0.76
      QW = TA*(TEMP(3)-TW)/(Y(3)*3600.)
      RETURN
      END
```

```
      SUBROUTINE WF(R,F,AM,S
      COMMON/BLK3/KRF,MACH,KR,INDI(10),INDE(10),SUMR,AK,ALMG,BETA,TAUI
     1  ,TAUE,VINF,DELTA,TW,TINF,QS,YL,UMAX,UMIN,FR,YIF,YEM,TR,HW,
     2  HF(10),GAMA(10),AJI(10),AJE(10),SC(050),AU(050),BU(050),CU(050),
     3  A(10,050),B(10,050),C(10,050),TEMPE(050),TEMP(050),PO(050),
     4  AMACH(050),CF(050)
      COMMON/BLK4/NH,NNO,NNF,NO,NN,NO2,N2,NE,IND(10),STO,AKS,RT,FT,
     1  AMT,DRAGC,STNO,TAUIW,QW,UGU,UGD
10    AKS=AK*AK
      RT=R*AKS
      ST=1./RT-.1561*RT**(-.4)+.0872*RT**(-.8)+.0371*RT**(-1.6)
      STO=ST
      IF(F.EQ.0.) GO TO 15
      FT=F/AKS
      FM=1.-4.*FT*RT/(.585+RT**2.5)**.4
      IF(FM.LT.0.)FM=0.
      ST=ST*FM**1.6
      GO TO 20
15    IF(AM.EQ.0.) GO TO 20
      AMT=AM/AKS
      AMM=1.-AMT/(7.74*RT**(-1.17)+.956*RT**(-.25))
      ST=ST*AMM**4
20    S=ST*AKS
      RETURN
      END
```

```
      SUBROUTINE WF2(R,F,AM, FR,PRT,P,S)
      COMMON/BLK3/KRF,MACH,KR,INDI(10),INDE(10),SUMR,AK,ALMG,BETA,TAUI
     1  ,TAUE,VINF,DELTA,TW,TINF,QS,YL,UMAX,UMIN,FR,YIF,YEM,TR,HW,
     2  HF(10),GAMA(10),AJI(10),AJE(10),SC(050),AU(050),BU(050),CU(050),
     3  A(10,050),B(10,050),C(10,050),TEMPE(050),TEMP(050),PO(050),
     4  AMACH(050),CF(050)
      COMMON/BLK4/NH,NNO,NNF,NO,NN,NO2,N2,NE,IND(10),STO,AKS,RT,FT,
     1  AMT,DRAGC,STNO,TAUIW,QW,UGU,UGD
      ST1=STO/(1.0+P*SQRT(STO))
      IF(F.EQ.0.0)GO TO 10
      SSEP=1.725*RT**(-.3333)*(P+6.8)**(-1.165)
      FD=.25*FT*RT/(1.+.0625*RT)
      ST1=ST1*(1.0-FD)+FD*SSEP
10    ST=ST1*PRT
      S=ST*AKS
      RETURN
      END
```

```
      SUBROUTINE OUTPUT
      REAL MACH
      COMMON/BLK1/N,NP1,NP2,NP3,NEQ,NEH,KEX,KIN,KASE,KRAD,EEI,AMI,AME,
     [illegible],XD,XE,XI,DX,INTG,ESALFA,HGS,CINF(10),FREF(10),
     [illegible],E(10),U(050),F(10,050),R(050),RHO(050),OM(050),Y(050),
     1 DEN(050),AMU(050)
      COMMON/BLK3/AKI,MACH,KR,INDI(10),INDE(10),SUMR,AK,ALMG,BETA,TAUI
     1 ,TAUE,VINF,DELTA,TW,TINF,QS,YI,UMAX,UMIN,PR,YIP,YEM,TR,HW,
      BE(10),GAMA(10),AJI(10),AJE(10),SC(050),AU(050),BU(050),CU(050),
     3 A(10,050),B(10,050),C(10,050),TEMPP(050),TEMP(050),PO(050),
     4 AMACH(050),CP(050)
      COMMON/BLK4/NH,NNO,NNP,NO,NN,NO2,NN2,NE,IND(10),STO,AKS,RT,FT,
     1 AMT,DRAGC,STNO,TAUIW,QW,UGU,UGP
      COMMON/BLK5/KRI,PINF,DIFF(050),NOPT,NSKAT
      DIMENSION YDL(050),TDL(050)
      IF(INTG.NE.1) GO TO 20
      WRITE(6,15)TINF,TW,MACH,KRAD,KIN,NEQ,KEX,N,HGS,HW,PR(1),
     1 VINF,DELTA,PINF,KRI
      WRITE(1,15)TINF,TW,MACH,KRAD,KIN,NEQ,KEX,N,HGS,HW,PR(1),
     1 VINF,DELTA,PINF,KRI
   15 FORMAT(///1X,7HTINF = F6.1/1X,5HTW = F6.1/1X,
     1 10HMACH NO = F4.1/1X,7HKRAD = I2/1X,6HKIN = I2/1X
     2 ,6HNEQ = I2/1X,6HKEX = I2/1X,4HN = I3/1X,6HHGS = E13.4/1
     3 X,5HHW = E13.4/1X,13HPRANDTL NO = F4.1/1X,7HVINF = E13.4/1X,
     4 8HDELTA = E13.4,/1X,'PINF = ',E13.4,/1X,'KR = 'I2)
   20 CONTINUE
C      IF(KR.NE.2) GO TO 25
      IF(FLOAT(INTG-1)/50..NE.FLOAT((INTG-1)/50)) RETURN
   25 CONTINUE
      VISC=(1.2267E-05)*(TINF/TR)**.76
      DINF=PINF*144./(53.3*TINF)
      RENX=VINF*DINF*XU/VISC
      DO 30 I=2,NP2
      YDL(I)=Y(I)/Y(NP3)
   30 TDL(I)=TEMP(I)/TINF
      IF(KR.EQ.2) SUMR=0.0
C      IF(KR.EQ.1) CALL RADWAL
      WRITE(6,35)XU,RENX,AME,SUMR
      WRITE(1,35)XU,RENX,AME,SUMR
   35 FORMAT(7H1  XU = 2PE11.2,4H  FT,10X,9H  RE,X = 1PE9.2,
     1 4X,' AME = ',2PE13.4,5X,' QR = ',2PE13.4, 'BTU/(SQ-FT SEC) ')
      WRITE(6,40)DRAGC,STNO,TAUIW,QW
      WRITE(1,40)DRAGC,STNO,TAUIW,QW
   40 FORMAT(10H   DRAGC = 2PE13.4,10H    STNO = 2PE13.4,11H   TAUIW =
     1 2PE13.4,9HLBF/SQ-FT,8H   QW = 2PE13.4,15HBTU/(SQ-FT SEC))
      QT=-SUMR+QW
      QRQW=-SUMR/QW
      WRITE(6,*)'THE VALUE'
      WRITE(1,*)'THE VALUE'
      WRITE(6,59)QT,QRQW
      WRITE(1,59)QT,QRQW
   59 FORMAT(7H  QT = 2PE13.4,15HBTU/(SQ-FT,SEC),
     1        10H   QRQW = 2PE13.4)
      IF(NOPT.EQ.1) GO TO 45
      GO TO 75
```

```
   45    DO 50 I=2,NP2
   50    DIFF(I)=((TEMP(I+1)-TEMP(I))/TEMP(I))*100.0
         WRITE(6,55)
         WRITE(1,55)
   55    FORMAT(1HO,8X,1HY,11X,1HU,11X,1HH,11X,1HT,11X,2HPO,10X,1HM,
        1  10X,3HRHO,8X,4HDIFF/)
         WRITE(6,60)
         WRITE(1,60)
   60    FORMAT(6X,4H(FT),7X,8H(FT/SEC),4X,10H(FT2/SEC2),4X,7H(DEG-R),4X,
        1  9H(LBF/IN2),14X,9H(LBM/FT3),6X,9H(PERCENT)/)
         WRITE(6,65)Y(NP3),U(NP3),F(1,NP3)
         WRITE(1,65)Y(NP3),U(NP3),F(1,NP3)
   65    FORMAT(1H  1P8E12.3)
         DO 70 J1=2,NP2
         J2=NP2-J1+2
         WRITE(6,65)Y(J2),U(J2),F(1,J2),TEMP(J2),
        1  PO(J2),AMACH(J2),RHO(J2),F(2,J2),F(3,J2)
         WRITE(1,65)Y(J2),U(J2),F(1,J2),TEMP(J2),
        1  PO(J2),AMACH(J2),RHO(J2),F(2,J2),F(3,J2)
   70    CONTINUE
         WRITE(6,65)Y(1),U(1),F(1,1)
         WRITE(1,65)Y(1),U(1),F(1,1)
         GO TO 100
   75    WRITE(6,80)
         WRITE(1,80)
   80    FORMAT(1HO,8X,1HY,11X,1HU,11X,1HH,11X,1HT,11X,2HPO,10X,1HM,
        1  10X,3HRHO,10X,7HY/DELTA,10X,6HT/TINF/)
         WRITE(6,85)
         WRITE(1,85)
   85    FORMAT(6X,4H(FT),7X,8H(FT/SEC),4X,10H(FT2/SEC2),4X,7H(DEG-R),4X,
        1  9H(LBF/IN2),14X,9H(LBM/FT3)/)
         WRITE(6,90)Y(NP3),U(NP3),F(1,NP3)
         WRITE(1,90)Y(NP3),U(NP3),F(1,NP3)
   90    FORMAT(1H  1P9E12.3)
         DO 95 J1=2,NP2
         J2=NP2-J1+2
         WRITE(6,90)Y(J2),U(J2),F(1,J2),TEMP(J2)
        1 ,PO(J2),AMACH(J2),RHO(J2),YDL(J2),TDL(J2)
         WRITE(1,90)Y(J2),U(J2),F(1,J2),TEMP(J2)
        1 ,PO(J2),AMACH(J2),RHO(J2),YDL(J2),TDL(J2)
   95    CONTINUE
         WRITE(6,90)Y(1),U(1),F(1,1)
         WRITE(1,90)Y(1),U(1),F(1,1)
  100    CONTINUE
         IF(KR.EQ.1) WRITE(6,105)
         IF(KR.EQ.1) WRITE(1,105)
  105    FORMAT(6X,'RADIATION EFFECTS INCLUDED - INTEGRAL')
         IF(KR.EQ.2) WRITE(6,110)
         IF(KR.EQ.2) WRITE(1,110)
  110    FORMAT(6X,12HNO RADIATION)
         IF(KR.EQ.3) WRITE(6,115)
         IF(KR.EQ.3) WRITE(1,115)
  115    FORMAT(6X,'RADIATION EFFECTS INCLUDED -OPTICALLY THIN')
         RETURN
         END
```

```
      SUBROUTINE COEFF
      COMMON/BLK2/N,NP1,NP2,NP3,NEQ,NPH,KEX,KIN,KASE,KRAD,PEI,AMI,AME,
     1  DPDX,XU,XD,XP,XL,DX,INTG,CSALFA,HGS,CINF(10),PREF(10),
     2  PR(10),P(10),U(050),F(10,050),R(050),RHO(050),OM(050),Y(050),
     3  DEN(050),AMU(050)

      COMMON/BLK3/KRF,MACH,KR,IND1(10),INDE(10),SUMR,AK,ALMG,BETA,TAUI
     1  ,TAUE,VINF,DELTA,TW,TINF,QS,YL,UMAX,UMIN,FR,YIP,YEM,TR,HW,
     2  HF(10),GAMA(10),AJI(10),AJE(10),SC(050),AU(050),BU(050),CU(050),
     3  A(10,050),B(10,050),C(10,050),TEMPE(050),TEMP(050),PO(050),
     4  AMACH(050),CP(050)
      COMMON/BLK4/NH,NNO,NNP,NO,NN,NO2,NN2,NE,IND(10),STO,AKS,RT,FT,
     1  AMT,DRAGC,STNO,TAUIW,QW,UGU,UGD
      DIMENSION G1(200),G2(200),G3(200),D(10,200),S1(200),S2(200),
     1  S3(200)
      IF(KR.EQ.1) CALL RADPRM
C     CALCULATION OF SMALL C S
      DO 10 I=2,NP1
      RA=.5*(R(I+1)+R(I))
      RH=.5*(RHO(I+1)+RHO(I))
      UM=.5*(U(I+1)+U(I))
      CALL VEFF(I,I+1,EMU)
   10 SC(I)=RA*RA*RH*UM*EMU/(PEI*PEI)
C     THE CONVESSION TERM
      SA=R(1)*AMI/PEI
      SB=(R(NP3)*AME-R(1)*AMI)/PEI
      DX=XD-XU
      DO 25 I=3,NP1
      OMD=OM(I+1)-OM(I-1)
      P2=.25/DX
      P3=P2/OMD
      P1=(OM(I+1)-OM(I))*P3
      P3=(OM(I)-OM(I-1))*P3
      P2=3.*P2
      Q=SA/OMD
      R2=-SB*.25
      R3=R2/OMD
      P1=-(OM(I+1)+3.*OM(I))*R3
      R3=(OM(I-1)+3.*OM(I))*R3
      G1(I)=P1+Q+R1
      G2(I)=P2+R2
      G3(I)=P3-Q+R3
      CU(I)=-P1*U(I+1)-P2*U(I)-P3*U(I-1)
C     THE DIFFUSION TERM
      AU(I)=2./OMD
      BU(I)=SC(I-1)*AU(I)/(OM(I)-OM(I-1))
      AU(I)=SC(I)*AU(I)/(OM(I+1)-OM(I))
      IF(NEQ.EQ.1) GO TO 20
      DO 15 J=1,NPH
      C(J,I)=-P1*F(J,I+1)-P2*F(J,I)-P3*F(J,I-1)
      CALL SOURCE(J,I,CS,D(J,I))
      C(J,I)=-C(J,I)+CS-F(J,I)*D(J,I)
      A(J,I)=AU(I)/PREF(J)
      B(J,I)=BU(I)/PREF(J)
   15 CONTINUE
```

```
C       SOURCE TERM FOR VELOCITY EQUATION
   20   S1(I)=DPDX*DX
        S2(I)=P2*S1(I)/(RHO(I)*U(I))
        S3(I)=P3*S1(I)/(RHO(I-1)*U(I-1))
        S1(I)=P1*S1(I)/(RHO(I+1)*U(I+1))
        CU(I)=-CU(I)-2.*(S1(I)+S2(I)+S3(I))
        S1(I)=S1(I)/U(I+1)
        S2(I)=S2(I)/U(I)
        S3(I)=S3(I)/U(I-1)
   25   CONTINUE
C       COEFFICIENTS IN THE FINAL FORM
        DO 30 I=3,NP1
        RL=1./(G2(I)+AU(I)+BU(I)-S2(I))
        AU(I)=(AU(I)+S1(I)-G1(I))*RL
        BU(I)=(BU(I)+S3(I)-G3(I))*RL
   30   CU(I)=CU(I)*RL
        IF(NEQ.EQ.1) GO TO 40
        DO 35 J=1,NPH
        DO 35 I=3,NP1
        RL=1./(G2(I)+A(J,I)+B(J,I)-D(J,I))
        A(J,I)=(A(J,I)-G1(I))*RL
        B(J,I)=(B(J,I)-G3(I))*RL
        C(J,I)=C(J,I)*RL
   35   CONTINUE
   40   CALL SLIP
        RETURN
        END
```

```
        SUBROUTINE VEFF(I,IP1,EMU)
        COMMON/BLK2/N,NP1,NP2,NP3,NEQ,NPH,KEX,KIN,KASE,KRAD,FEI,AMI,AME,
     1  DPDX,XU,XD,XP,XL,DX,INTG,CSALFA,HGS,CINF(10),PREF(10),
     2  PR(10),P(10),U(050),F(10,050),R(050),RHO(050),OM(050),Y(050),
     3  DEN(050),AMU(050)
        COMMON/BLK3/KRP,MACH,KR,INDI(10),INDE(10),SUMR,AK,ALMG,BETA,TAUI
     1  ,TAUE,VINF,DELTA,TW,TINF,QS,YL,UMAX,UMIN,FR,YIP,YEM,TR,HW,
     2  HF(10),GAMA(10),AJI(10),AJE(10),SC(050),AU(050),BU(050),CU(050),
     3  A(10,050),B(10,050),C(10,050),TEMPE(050),TEMP(050),PO(050),
     4  AMACH(050),CP(050)
        COMMON/BLK4/NH,NNO,NNP,NO,NN,NO2,NN2,NE,IND(10),STO,AKS,RT,FT,
     1  AMT,DRAGC,STNO,TAUIW,QW,UGU,UGD
C       THIS SUBROUTINE USES THE MIXING-LENGT HYPOTHESIS
        AL=ALMG*YL
        YM=(Y(I)+Y(IP1))*.5
        IF(YM.LT.AL/AK)AL=AK*YM
   10   EMU=.5*(RHO(I)+RHO(IP1))*AL*AL*ABS((U(I)-U(IP1))/(Y(I)-Y(IP1)))
        RETURN
        END
```

```
      SUBROUTINE SOURCE(J,I,CS,DS)
C     FOR CONSERVATION OF STAGNATION ENTHALPY
C     CAUTION USE CONSISTENT UNITS
C     THE DOT PRODUCT OF F WITH J IS NEGLECTED
      COMMON BLK1/LS1,IS,AS,BS,TEMPA(050),RHOA(050),YA(050),FR2(050),
     1 FR3(050),TAU2(050),TAU3(050),ZK2(050),ZK3(050)
      COMMON/BLK2/N,NP1,NP2,NP3,NEQ,NFH,NEX,NIN,NASE,NRAD,PEI,AMI,AMF,
     1 DELX,XU,XD,XF,XL,DX,INTG, CSALFA,HGS,CINF(10),PREF(10),
     2 FR(10),F(10),U(050),F(10,050),R(050),RHO(050),OM(050),Y(050),
     3 DEN(050),AMU(050)
      COMMON/BLK3/RP,MACH,NR,INDI(10),INDE(10),SUMR,AR,ALMG,BETA,TAUI
     1 ,TAUE,VINF,DELTA,TW,TINF,QS,YL,UMAX,UMIN,FR,YIF,YEM,   TF,HW,
     2 HF(10),GAMA(10),AJI(10),AJE(10),SC(050),AU(050),BU(050),CU(050),
     3 A(10,050),B(10,050),C(10,050),TEMPE(050),TEMP(050),PO(050),
     4 AMACH(050),CP(050)
      COMMON/BLK4/NH,NNO,NNF,NO,NN,NO2,NN2,NE,IND(10),STO,AKS,RT,FT,
     1 AMT,DRAGC,STNO,TAUIW,DW,UGU,UGD
      DIMENSION RCS(200)
      REN=0.075
      IF (J.NE.1)GO TO 20
      CS=SC(I)*(U(I+1)*U(I+1)-U(I)*U(I))/(OM(I+1)-OM(I))
      CS=CS-SC(I-1)*(U(I)*U(I)-U(I-1)*U(I-1))/(OM(I)-OM(I-1))
      CS=(1.-1./PREF(J))*CS/(OM(I+1)-OM(I-1))
      IF (NR.EQ.3) GO TO 15
      AS=0.0
      BS=0.0
      IF(NR.EQ.1) CALL RADCOM(I)
      CS=AS+CS
      DS=BS
      GO TO 25
   15 CONTINUE
      ZK=115.*(RHO(I)/REN)*(TEMP(I)/(10.**4.))**5.
      RCS(I)=2.*1.714E-9*ZK*(QS+TEMP(1)**4.+TEMP(NP3)**4.-2*(TEMP(I)
     1 **4.))
      CS=.2162*32.2*RCS(I)/(RHO(I)*U(I))+CS
      DS=(2.*1.714E-9*(0.0575*(TEMP(I)/(10.**4.))**4.*(TEMP(1)**4.+
     1 TEMP(NP3)**4.-2.*(TEMP(I)**4.))/REN-8.*(ZK/RHO(I))*TEMP(I)**3.)/
     2   (CP(I)*U(I)))*.2162*32.2
      IF(I.EQ.NP1) GO TO 30
      GO TO 25
   20 CONTINUE
      CS=0.0
      DS=0.0
   25 CONTINUE
      RETURN
   30 CONTINUE
      ZK1=115.*(RHO(1)/REN)*(TEMP(1)/(10.**4.))**5.
      ZKNP3=115.*(RHO(NP3)/REN)*(TEMP(NP3)/(10.**4.))**5.
      RC1=2.*1.714E-9*ZK1*(TEMP(NP3)**4.-TEMP(1)**4.)
      RCNP3=2.*1.714E-9*ZKNP3*(TEMP(1)**4.-TEMP(NP3)**4.)
      SUMR=0.0
      DO 35 J=4,NP1
      SUMR=(RCS(I)+RCS(I-1))*(Y(I)-Y(I-1))*.5+SUMR
   35 CONTINUE
      SUMR=SUMR+(RCS(3)+RC1)*(Y(3)-Y(1))*.5+(RCNP3+RCS(NP1))*(Y(NP3)-
     1 Y(NP1))*.5
      SUMR=(QS+.5*SUMR+1.714E-9*TEMP(1)**4.)/3600.
      RETURN
      END
```

```
      SUBROUTINE SLIP
      COMMON/BLK2/N,NP1,NP2,NP3,NEQ,NEM,KEX,KIN,KASE,KRAD,PET,AME,AMI,
     1  DPDX,XU,XD,XF,XL,DX,INTG,CSALFA,HGS,CINF(10),PREF(10),
     2  PR(10),P(10),U(050),F(10,050),R(050),RHO(050),OM(050),Y(050),
     3  DEN(050),AMU(050)
      COMMON/BLK3/AKF,MACH,AK,INDI(10),INDE(10),SUMR,AK,ALMG,BETA,TAUI
     1  ,TAUE,VINF,DELTA,TW,TINF,QS,YL,UMAX,UMIN,FF,YIF,YEM,   TR,HW,
     2  HF(10),GAMA(10),AJI(10),AJE(10),SC(050),AU(050),BU(050),CU(050),
     3  A(10,050),B(10,050),C(10,050),TEMPE(050),TEMP(050),RO(050),
     4  AMACH(050),CF(050)
      COMMON/BLK4/NH,NNO,NNF,NO,NN,NO2,NN2,NE,IND(10),STO,ANS,RT,FT,
     1  AMT,DRAGC,STNO,TAUIW,QW,UGU,UGP
C     SLIP COEFFICIENTS NEAR THE I BOUNDARY FOR VELOCITY EQUATION EQUATION
      CU(2)=0.
      CU(NP2)=0.
      GO TO (10,15,20),KIN
   10 BU(2)=0.
      AU(2)=1./(1.+2.*BETA)
      GO TO 30
   15 SQ=84.*U(1)*U(1)-12.*U(1)*U(3)+9.*U(3)*U(3)
      BU(2)=8.*(2.*U(1)+U(3))/(2.*U(1)+7.*U(3)+SQRT(SQ))
      AU(2)=1.-BU(2)
      GO TO 30
   20 BU(2)=0.
      CALL VEFF(2,3,EMU)
      AK1=1./DX-DPDX/(RHO(1)*U(1)*U(1))
      AK2=-U(1)*AK1+DPDX/(RHO(1)*U(1))
      AJ=RHO(1)*U(1)*.25*(Y(2)+Y(3))**2/EMU
      IF(KRAD.EQ.0) GO TO 25
      AU(2)=2./(2.+AJ*AK1)
      CU(2)=-.5*AJ*AK2*AU(2)
      GO TO 30
   25 CU(2)=1./(2.+3.*AJ*AK1)
      AU(2)=CU(2)*(2.-AJ*AK1)
      CU(2)=-CU(2)*4.*AJ*AK2
C     SLIP COEFFICIENTS NEAR THE E BOUNDARY FOR VELOCITY EQUATION
   30 GO TO (35,40,45),KEX
   35 AU(NP2)=0.
      BU(NP2)=1./(1.+2.*BETA)
      GO TO 50
   40 SQ=84.*U(NP3)*U(NP3)-12.*U(NP3)*U(NP1)+9.*U(NP1)*U(NP1)
      AU(NP2)=8.*(2.*U(NP3)+U(NP1))/(2.*U(NP3)+7.*U(NP1)+SQRT(SQ))
      BU(NP2)=1.-AU(NP2)
      GO TO 50
   45 AU(NP2)=0.
      CALL VEFF(NP1,NP2,EMU)
      BK1=1./DX-DPDX/(RHO(NP3)*U(NP3)*U(NP3))
      BK2=-U(NP3)*BK1+DPDX/(RHO(NP3)*U(NP3))
      BJ=RHO(NP3)*U(NP3)*.25*(2.*Y(NP3)-Y(NP1)-Y(NP2))**2/EMU
      CU(NP2)=1./(2.+3.*BJ*BK1)
      BU(NP2)=CU(NP2)*(2.-BJ*BK1)
      CU(NP2)=-CU(NP2)*4.*BJ*BK2
   50 IF(NEQ.EQ.1)RETURN
```

```
C       SLIP COEFFICIENTS NEAR THE I BOUNDARY FOR OTHER EQUATIONS
        DO 105 J=1,NPH
        C(J,2)=0.
        C(J,NP2)=0.
        GO TO (55,65,70),KIN
   55   CALL FBC(XD,J,INDI(J),QI)
        IF(INDI(J).EQ.1) GO TO 60
        AJI(J)=QI
        A(J,2)=1.
        B(J,2)=0.
        C(J,2)=8.*(1.+2.*BETA)*PREF(J)*AJI(J)/(AK*AK*BETA*(1.+BETA)*(1.+
     1  BETA)*(3.*RHO(2)+RHO(3))*U(3))
        GO TO 80
   60   F(J,1)=QI
        A(J,2)=(1.+BETA-GAMA(J))/(1.+BETA+GAMA(J))
        B(J,2)=1.-A(J,2)
        GO TO 80
   65   A(J,2)=(U(2)+U(3)-8.*U(1))/(5.*(U(2)+U(3))+8.*U(1))
        GF=(1.-PREF(J))/(1.+PREF(J))
        A(J,2)=(A(J,2)+GF)/(1.+A(J,2)*GF)
        B(J,2)=1.-A(J,2)
        GO TO 80
   70   B(J,2)=0.
        CALL SOURCE(J,1,CS,DS)
        AK1=1./DX-DS
        AK2=-AK1*F(J,1)-CS
        AJF=AJ*PREF(J)
        IF(KRAD.EQ.0) GO TO 75
        A(J,2)=2./(2.+AJF*AK1)
        C(J,2)=-.5*AJF*AK2*A(J,2)
        GO TO 80
   75   C(J,2)=1./(2.+3.*AJF*AK1)
        A(J,2)=C(J,2)*(2.-AJF*AK1)
        C(J,2)=-C(J,2)*4.*AJF*AK2
C       SLIP COEFFICIENTS NEAR THE E BOUNDARY FOR OTHER EQUATIONS
   80   GO TO (85,95,100),KEX
   85   CALL FBC(XD,J,INDE(J),QE)
        IF(INDE(J).EQ.1) GO TO 90
        AJE(J)=QE
        B(J,NP2)=1.
        A(J,NP2)=0.
        C(J,NP2)=-8.*(1.+2.*BETA)*PREF(J)*AJE(J)/(AK*AK*BETA*(1.+BETA)*
     1  (1.+BETA)*(RHO(NP1)+3.*RHO(NP2))*U(NP1))
        GO TO 105
   90   F(J,NP3)=QE
        B(J,NP2)=(1.+BETA-GAMA(J))/(1.+BETA+GAMA(J))
        A(J,NP2)=1.-B(J,NP2)
        GO TO 105
   95   B(J,NP2)=(U(NP2)+U(NP1)-8.*U(NP3))/(5.*(U(NP2)+U(NP1))+8.*
     1  U(NP3))
        GF=(1.-PREF(J))/(1.+PREF(J))
        B(J,NP2)=(B(J,NP2)+GF)/(1.+B(J,NP2)*GF)
        A(J,NP2)=1.-B(J,NP2)
```

```
      GO TO 105
  100 A(J,NP2)=0.
      CALL SOURCE(J,NP3,CS,DS)
      BK1=1./DX-DS
      BK2=-BK1*F(J,NP3)-CS
      BJF=BJ*PREF(J)
      C(J,NP2)=1./(2.+3.*BJF*BK1)
      B(J,NP2)=C(J,NP2)*(2.-BJF*BK1)
      C(J,NP2)=-C(J,NP2)*4.*BJF*BK2
  105 CONTINUE
      RETURN
      END
```

```
      SUBROUTINE FBC(X,J,IND,AJFS)
      COMMON/BLK3/KRP,MACH,KR,INDI(10),INDE(10),SUMR,AK,ALMG,BETA,TAUI
     1 ,TAUE,VINF,DELTA,TW,TINF,QS,YL,UMAX,UMIN,FR,YIP,YEM,TR,HW,
     2 HF(10),GAMA(10),AJI(10),AJE(10),SC(050),AU(050),BU(050),CU(050),
     3 A(10,050),B(10,050),C(10,050),TEMPE(050),TEMP(050),PO(050),
     4 AMACH(050),CP(050)
      IND=1
C     H MUST HAVE UNITS FT.FT/SEC.SEC
      IF (J.EQ.1) GO TO 105
      GO TO 110
  105 AJFS = HW
  110 IF(J.EQ.2) GO TO 115
      GO TO 120
  115 AJFS=1.0-CW
  120 IF(J.EQ.3)GO TO 125
      GO TO 130
  125 AJFS=CW
  130 RETURN
      END
```

```
      SUBROUTINE EXPNI(RES,N,X,IER)
C     THIS SUBROUTINE EVALUATES THE EXPONENTIAL INTEGRAL FUNCTIONS IN
C     THE RADIATION SOURCE TERMS
C     TEST OF RANGE
      IER=0
      IF(ABS(X).LE..00001) GO TO 10
      GO TO 25
   10 IF(X)15,20,20
   15 X=-.00001
      GO TO 25
   20 X=.00001
   25 IF(X-4.) 30,55,35
   30 IF(X+4.) 65,55,50
C     ARGUMENT IS GREATER THAN 4
   35 ARG=4./X
      RES=EXP(-X)*((((((((.00094427614*ARG-.0049362007)*ARG+
     1 .011723273)*ARG-.017555779)*ARG+.020412099)*ARG-.022951979)*ARG+
     2 .031208561)*ARG-.062498588)*ARG+.24999999)*ARG
   40 IF(N.EQ.1) RETURN
      NM1=N-1
      EXPX=EXP(-X)
      XN1=1.
      DO 45 N1=1,NM1
      RES=(EXPX-X*RES)/XN1
   45 XN1=XN1+1.
      RETURN
C     ARGUMENT IS ABSOLUTELY LESS OR EQUAL 4
   50 IF(X)55,60,55
   55 RES=-ALOG(ABS(X))-((((((((((((.10317602E-11*X-.15798675E-10)*X+
     1 .16826592E-9)*X-.21915699E-8)*X+.27635830E-7)*X-.30726221E-6)*X+
     2 .30996040E-5)*X-.28337590E-4)*X+.23148392E-3)*X-.0016666906)*X+
     3 .010416662)*X-.055555520)*X+.25)*X-1.0)*X-.57721566
      GO TO 40
   60 RES=1.E37
      GO TO 40
C    ARGUMENT IS LESS THAN -4
   65  IER=1
      RETURN
      END
```

```
      SUBROUTINE SOLVE(A,B,C,F,NP3)
C     THIS SOLVES EQUATIONS OF THE FORM
C     F(I)=A(I)*F(I+1)+B(I)*F(I-1)+C(I)
C     FOR I=2,NP2
      DIMENSION A(NP3),B(NP3),C(NP3),F(NP3)
      NP2=NP3-1
      B(2) = B(2)*F(1) + C(2)
      DO 10 I=3,NP2
      T = 1./(1.-B(I)*A(I-1))
      A(I)= A(I)*T
   10 B(I)= (B(I)*B(I-1) + C(I))*T
      DO 15 I=2,NP2
      J=NP2-I+2
   15 F(J)=A(J)*F(J+1)+B(J)
      RETURN
      END
```

```
      REAL FUNCTION EBLT(K,WV)
      REAL WV(K)
C     THIS FUNCTION SUBPROGRAM CALCULATES PLANCKS RADIATION FUNCTION
      COMMON/BLK1/LST,TS,AS,BS,TEMPA(050),RHOA(050),YA(050),EB2(050),
     1 EB3(050),TAU2(050),TAU3(050),ZK2(050),ZK3(050)
      COMMON/BLK3/KRP,MACH,KR,INDI(10),INDE(10),SUMR,AK,ALMG,BETA,TAUI
     1 ,TAUE,VINF,DELTA,TW,TINF,QS,YL,UMAX,UMIN,FR,YIP,YEM,TR,HW,
     2 HF(10),GAMA(10),AJI(10),AJE(10),SC(050),AU(050),BU(050),
     3 CU(050),A(10,050),B(10,050),C(10,50),TEMPE(050),TEMP(050),
     4 PO(050),AMACH(050),CP(050)
      C1=1.187E 08
      C2=25896.0
      IF (LST.EQ.0) GO TO 10
      T=TEMPA(LST)
      GO TO 15
   10 T=TS
   15 CONTINUE
      ARGA=C2/(WV(1)*T)
      IF (ARGA.GT.50.) GO TO 20
      BAD=C1/((WV(1)**5.)*(EXP(ARGA)-1.))
      EBLT=BAD
      RETURN
   20 CONTINUE
      BADEX=ALOG(C1)-(5.*ALOG(WV(1))+ARGA)
      BAD=EXP(BADEX)
      EBLT=BAD
      RETURN
      END
```

```
      FUNCTION SMUMU(I,J)
      REAL MU
      COMMON/AREA1/M,MU(8),A(10)
      DIMENSION A1(20)
      EXTERNAL PN
      MU(1)=0.06943184E0
      MU(2)=0.33000984E0
      MU(3)=0.66999052E0
      MU(4)=0.93056816E0
      A1(1)=2.0053
      A1(2)=1.53831
      A1(3)=0.69465
      A1(4)=0.23156
      A1(5)=0.04996
      A1(6)=0.00713
      A1(7)=0.00089
      A1(8)=0.0
      DO 10 IP=1,4
10    MU(IP+4)=-MU(IP)
      N=8
      III=I
      IF(I.LT.0)III=-I+4
      JJJ=J
      IF(J.LT.0)JJJ=-J+4
      S=1.0
      DO 20 M=1,N
      MMM=M
20    S=S+A(M)*PN(III,JJJ)
      SMUMU=S
      RETURN
      END
```

```
      FUNCTION PN(I,J)
      COMMON/AREA1/M,MU(8),A(10)
      EXTERNAL PNCOS
      PXRC=DMLIN(PNCOS,0.0,2*3.14159,1,300,0.0,0.001,IER)
      PN=1./(2.0*3.14159)*PXRC
      RETURN
      END
```

```
      FUNCTION PNCOS(K,PHI)
      COMMON/AREA1/M,MU(8),A(10)
      REAL MU,PHI(K)
      FACT(Z)=EXP(-Z)*Z**Z*SQRT(2.*3.14159*Z)
      COSTH(APHI,X,Y)=X*Y+(1.-X**2)**0.50*(1.-Y**2)**0.50*
     1  COS(APHI)
      PNC=0.0
      N=M
      NP1=N+1
      ZN=FLOAT(N)
      DO 15 MM=1,NP1
      ZM=(MM-1)/2.
   15 PNC=(-1.)**ZM*FACT(ZN)/(FACT(ZM)*FACT(ZN-ZM))*FACT(2.*ZN-2.*ZM)/
     1 (FACT(ZN)*FACT(ZN-2.*ZM))*COSTH(PHI(1),MU(I),MU(J))**(ZN-2.*ZM)
      PNCOS=(1./(2.**M))*PNC
      RETURN
      END



      SUBROUTINE RADPRM
      COMMON/BLK1/LST,TS,AS,BS,TEMPA(050),RHOA(050),YA(050),EB2(050),
     1  EB3(050),TAU2(050),TAU3(050),ZK2(050),ZK3(050)
      COMMON/BLK2/N,NP1,NP2,NP3,NEQ,NPH,KEX,KIN,KASE,KRAD,PEI,AMI,AME,
     1  DPDX,XU,XD,XP,XL,DX,INTG,CSALFA,HGS,CINF(10),PREF(10),
     2  PR(10),P(10),U(050),F(10,050),R(050),RHO(050),OM(050),V(050),
     3  DEN(050),AMU(050)
      COMMON/BLK3/KRP,MACH,KR,INDI(10),INDE(10),SUMR,AK,ALMG,BETA,
     1  ,TAUE,VINF,DELTA,TW,TINF,QS,YL,UMAX,UMIN,FR,YIP,YEM,TR,HW,
     2  HF(10),GAMA(10),AJI(10),AJE(10),SC(050),AU(050),BU(050),
     3  CU(050),A(10,050),B(10,050),C(10,50),TEMPE(050),TEMP(050),
     4  PO(050),AMACH(050),CP(050)
      COMMON/BLK5/KRI,PINF,DIFF(50),NOPT,NSKAT
      COMMON/SANJ/SIGMEX,SIGMAB,PDEN,SIZE
      DIMENSION AUX(300),TRAN2(50),TRAN3(50)
     DIMENSION EXTN2(50),EXTN3(50),AK2(50),AK3(50),ZKA2(50),ZKA3(50),
     1  EX2(50),EX3(50),AR2(50),AR3(50),AD2(50),AD3(50),
     2  BD2(50),BD3(50),ZT2(50),ZT3(50),AA(4),YD(50)
      EXTERNAL EBLT
      EXTERNAL SMUMU
      EXTERNAL AKP2
      EXTERNAL AKP3
      BEN=0.075
      IF(NSKAT.EQ.1) GO TO 3
      IF(NSKAT.EQ.3) GO TO 2
      AA(1)=.1739274
      AA(2)=.3260726
      AA(3)=.3260726
      AA(4)=.1739274
      DO 1 I=1,4
      SCN=0.0
      DO 1 J=1,4
    1 SCN=SCN+AA(J)*(AA(J)*SMUMU(I,J,
      GO TO 3
```

AD-A182 119 RADIATIVE AND CONVECTIVE HEAT TRANSFER OVER ABLATING COMPOSITE FLAT SURFA (U) ADVANCED TECHNOLOGIES AND TESTING LABS GREENSBORO NC D Y GOSWAMI 22 APR 87 2/2

UNCLASSIFIED AFOSR-TR-87-0818 F49620-86-C-0118 F/G 20/13 NL

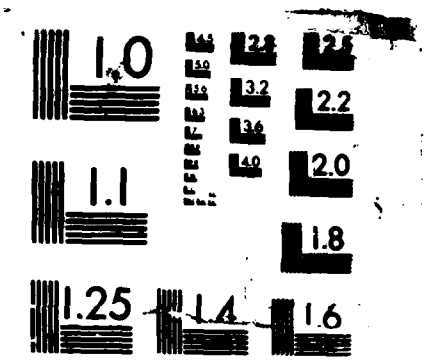

MICROCOPY RESOLUTION TEST CHART

```
      SCN=0.5
    3 DO 10 L=3,NP1
      TEMPA(L-1)=TEMP(L)
      RHOA(L-1)=RHO(L)
      YA(L-1)=Y(L)
      YD(L)=Y(L+1)-Y(L)
   10 CONTINUE
      YD(2)=(Y(3)-Y(1))/2.0
      YD(1)=YD(2)
      TEMPA(1)=TEMP(1)
      RHOA(1)=RHO(1)
      YA(1)=Y(1)
      TEMPA(NP1)=TEMP(NP3)
      RHOA(NP1)=RHO(NP3)
      YA(NP1)=Y(NP3)
      TAU2(1)=0.0
      TAU3(1)=0.0
      DO 25 L=1,NP1
      ZK2(L)=(4.37/0.03281)*((RHOA(L)/BEN)**1.009)*((TEMPA(L)*
     1 0.00018)**2.85)
      ZK3(L)=(.04985/0.03281)*((RHOA(L)/BEN)**1.205)*((TEMPA(L)*
     1 0.00018)**5.47)
      LST=L
      VFRA=F(3,L)*RHO(L)/PDEN
      NPART=VFRA*YD(L)/SIZE
      EXTN=SIGMEX*NPART+SIGMAB*VFRA
      SKA =SIGMEX*NPART
      EB2(L)=DMLIN(EBLT,.05,.135,1,300,0.0,0.001,IER)
      EB3(L)=DMLIN(EBLT,.135,20.,1,300,0.0,0.001,IER)
      ZKA2(L) = SIGMAB*VFRA+ZK2(L)*(1.0-VFRA)
      ZKA3(L) = SIGMAB*VFRA+ZK3(L)*(1.0-VFRA)
      IF(NSKAT.EQ.1) GO TO 12
      EXTN2(L)=EXTN+ZK2(L)*(1.0-VFRA)
      EXTN3(L) = EXTN+ZK3(L)*(1.0-VFRA)
      AK2(L)=(ZKA2(L)*(ZKA2(L)+2.0*SCN*SKA))**0.5
      AK3(L)=(ZKA3(L)*(ZKA3(L)+2.0*SCN*SKA))**0.5
      GO TO 15
   12 AK2(L)=ZKA2(L)
      AK3(L)=ZKA3(L)
   15 IF(L.EQ.1) GO TO 25
      TAU2(L) = (ZK2(L)+ZK2(L-1))*(YA(L)-YA(L-1))*0.5+TAU2(L-1)
      TAU3(L) = (ZK3(L)+ZK3(L-1))*(YA(L)-YA(L-1))*0.5+TAU3(L-1)
   20 CONTINUE
   25 CONTINUE
      EX2(1)=(EB2(1)+EB2(2))/2.0
      EX3(1)=(EB3(1)+EB3(2))/2.0
      AR2(1)=EB2(1)*2.0*ZKA2(1)
      DO 30 L=1,NP1
      AR2(L)=EB2(L)*2.0*ZKA2(L)
      AR3(L)=2.0*ZKA3(L)*EB3(L)
   30 CONTINUE
```

```
      DO 70 L=1,NP1
      AD2(L)=(2.*AKP2(-1.,0.,-Y(L+1),AK2(L),ZKA2(L))*EX2(L)-ZKA2(L)*
     1 AR2(L)/(AK2(L))**2*(AKP2(-1.,0.,-Y(L+1),AK2(L),ZKA2(L))-AKP2(1.,
     2  0.,-Y(L),AK2(L),ZKA2(L))))/(AKP2(-1.,1.,Y(L)-Y(L+1),AK2(L),
     3  ZKA2(L))-AKP2(1.,1.,Y(L+1)-Y(L),AK2(L),ZKA2(L)))
      AD3(L)=(2.*AKP3(-1.,0.,-Y(L+1),AK3(L),ZKA3(L))*EX3(L)-ZKA3(L)*
     1 AR3(L)/(AK3(L))**2*(AKP3(-1.,0.,-Y(L+1),AK3(L),ZKA3(L))-AKP3(1.,
     2  0.,-Y(L),AK3(L),ZKA3(L))))/(AKP3(-1.,1.,Y(L)-Y(L+1),AK3(L),
     3  ZKA3(L))-AKP3(1.,1.,Y(L+1)-Y(L),AK3(L),ZKA3(L)))
      BD2(L)=(2.*EX2(L)-AD2(L)*AKP2(-1.,0.,Y(L),AK2(L),ZKA2(L))-
     1  ZKA2(L)*AR2(L)/(AK2(L))**2.0)/AKP2(1.,0.,-Y(L),AK2(L),ZKA2(L))
      BD3(L)=(2.*EX3(L)-AD3(L)*AKP3(-1.,0.,Y(L),AK3(L),ZKA3(L))-
     1  ZKA3(L)*AR3(L)/(AK3(L))**2.0)/AKP3(1.,0.,-Y(L),AK3(L),ZKA3(L))

 32   IF(EX2(L).EQ.0.0) GO TO 35
      ZT2(L)=1.0-(0.5*AD2(L)*(AKP2(-1.,0.,Y(L+1),AK2(L),ZKA2(L))-
     1  AKP2(1.,0.,Y(L),AK2(L),ZKA2(L)))+BD2(L)*0.5*(AKP2(1.,0.,-Y(L+1)
     2  ,AK2(L),ZKA2(L))-AKP2(-1.,0.,-Y(L),AK2(L),ZKA2(L))))/EX2(L)
      TRAN2(L)=(AD2(L)*AKP2(-1.,0.,Y(L+1),AK2(L),ZKA2(L))+
     1  BD2(L)*AKP2(1.,0.,-Y(L+1),AK2(L),ZKA2(L))+
     2  ZKA2(L)*AR2(L)/(AK2(L)**2))/(2.*EX2(L))
      GO TO 40
35    ZT2(L)=0.0
      TRAN2(L)=1.0
40    IF(EX3(L).EQ.0.0)GO TO 45
      ZT3(L)=1.0-(0.5*AD3(L)*(AKP3(-1.,0.,Y(L+1),AK3(L),ZKA3(L))-
     1  AKP3(1.,0.,Y(L),AK3(L),ZKA3(L)))+BD3(L)*0.5*(AKP3(1.,0.,-Y(L+1)
     2  ,AK3(L),ZKA3(L))-AKP3(-1.,0.,-Y(L),AK3(L),ZKA3(L))))/EX3(L)
      TRAN3(L)=(AD3(L)*AKP3(-1.,0.,Y(L+1),AK3(L),ZKA3(L))+
     1  BD3(L)*AKP3(1.,0.,-Y(L+1),AK3(L),ZKA3(L))+
     2  ZKA3(L)*AR3(L)/(AK3(L)**2))/(2.*EX3(L))
      GO TO 50
45    ZT3(L)=0.0
      TRAN3(L)=1.0
50    CONTINUE
      IF(NSKAT.EQ.1)GO TO 57
      IF(L.LE.3) GO TO 55
      ZK2(L)=ALOG(1./(1.0-ZT2(L)))/((Y(L)-Y(L-1)))
      ZK3(L)=ALOG(1./(1.0-ZT3(L)))/((Y(L)-Y(L-1)))
      GO TO 60
55    ZK2(L)=ALOG(1./(1.0-ZT2(L)))/((Y(3)-Y(1))*.5)
      ZK3(L)=ALOG(1./(1.0-ZT3(L)))/((Y(3)-Y(1))*.5)
      GO TO 60
57    ZK2(L)=ZKA2(L)
      ZK3(L)=ZKA3(L)
60    CONTINUE
      M=L+1
      IF(L.EQ.1) GO TO 65
      TAU2(L)=(ZK2(L)+ZK2(L-1))*(YA(L)-YA(L-1))*0.5+TAU2(L-1)
      TAU3(L)=(ZK3(L)+ZK3(L-1))*(YA(L)-YA(L-1))*0.5+TAU3(L-1)
65    EX2(M)=EX2(M-1)*(1.-(ZK2(M-1)*(Y(M)-Y(M-1))))+ZKA2(M-1)*
     1  EB2(M-1)*(Y(M)-Y(M-1))
      EX3(M)=EX3(M-1)*(1.-(ZK3(M-1)*(Y(M)-Y(M-1))))+ZKA3(M-1)*
     1  EB3(M-1)*(Y(M)-Y(M-1))
70    CONTINUE
```

```
C       SUM2=2.0*ZKA2(1)*EB2(1)+QS*TRAN2(N)
C       SUM3=2.0*ZKA3(1)*EB3(1)+QS*TRAN3(N)
        QSW=QS*TRAN2(N)*TRAN3(N)
        DO 75 I=N,2,-1
C       SUM2=2.0*ZKA2(I)*EB2(I)*TRAN2(I-1)+SUM2
C       SUM3=2.0*ZKA3(I)*EB3(I)*TRAN3(I-1)+SUM3
        QSW=QSW*TRAN2(I-1)*TRAN3(I-1)
   75   CONTINUE
        CALL RADWAL
        SUMR=(1.0-REFT)*(SUMR-QSW)/3600.
C       SUMR=(1.0-REFT)*(SUM2+SUM3-EB2(1)-EB3(1))/3600.
        RETURN
        END


        FUNCTION AKP2(S,P,X,A,B)
        AKP2=(1.0+S*A/B)*(1.0+P*S*A/B)*EXP(2.0*A*X)
        RETURN
        END




        FUNCTION AKP3(S,P,X,C,D)
        AKP3=(1.0+S*C/D)*(1.0+P*S*C/D)*EXP(2.0*C*X)
        RETURN
        END









        SUBROUTINE RADCOM(I)
        COMMON/BLK1/LST,TS,AS,BS,TEMPA(050),RHOA(050),YA(050),EB2(050),
     1  EB3(050),TAU2(050),TAU3(050),ZK2(050),ZK3(050)
        COMMON/BLK2/N,NP1,NP2,NP3,NEQ,NPH,KEX,KIN,KASE,KRAD,PEI,AMI,AME,
     1  DPDX,XU,XD,XP,XL,DX,INTG,CSALFA,HGS,CINF(10),PREF(10),
     2  PR(10),P(10),U(050),F(10,050),R(050),RHO(050),OM(050),Y(050),
     3  DEN(050),AMU(050)
        COMMON/BLK3/KRP,MACH,KR,INDI(10),INDE(10),SUMR,AK,ALMG,BETA,TAUI
     1  ,TAUE,VINF,DELTA,TW,TINF,QS,YL,UMAX,UMIN,FR,YIP,YEM,TR,HW,
     2  HF(10),GAMA(10),AJI(10),AJE(10),SC(050),AU(050),BU(050),CU(050),
     3  A(10,050),B(10,050),C(10,050),TEMPE(050),TEMP(050),PO(050),
     4  AMACH(050),CP(050)
        COMMON/BLK4/NH,NNO,NNP,NO,NN,NO2,NN2,NE,IND(10),STO,AKS,RT,FT,
     1  AMT,DRAGC,STNO,TAUIW,QW,UGU,UGD
        DIMENSION E12(200),E13(200),E12S(200),E13S(200),DIV(200)
        DIMENSION AUX(300)
        EXTERNAL EBLT
        BEN=0.075
        M=I-1
        DELT=0.1
```

```
      TS=TEMPA(M)+DELT
      RHOS=DEN(M)*TR/TS
      ZK2S=(4.37/0.03281)*((RHOS/BEN)**1.009)*((TS*1.8E-04)**2.85)
      ZK3S=(4.985E-02/0.03281)*((RHOS/BEN)**1.205)*((TS*1.8E-04)**
     1  5.47)
      SUM2=0.0
      SUM3=0.0
      SUM2S=0.0
      SUM3S=0.0
      CALL EXPNI(E2A2,2,TAU2(M),IER)
      CALL EXPNI(E2A3,2,TAU3(M),IER)
      CALL EXPNI(E2B2,2,TAU2(NP1)-TAU2(M),IER)
      CALL EXPNI(E2B3,2,TAU3(NP1)-TAU3(M),IER)
      CALL EXPNI(E12(1),1,ABS(TAU2(M)-TAU2(1)),IER)
      CALL EXPNI(E13(1),1,ABS(TAU3(M)-TAU3(1)),IER)
      TAU2S=(ZK2S+ZK2(M-1))*(YA(M)-YA(M-1))*0.5+TAU2(M-1)
      TAU3S=(ZK3S+ZK3(M-1))*(YA(M)-YA(M-1))*0.5+TAU3(M-1)
      CALL EXPNI(E2A2S,2,TAU2S,IER)
      CALL EXPNI(E2A3S,2,TAU3S,IER)
      CALL EXPNI(E2B2S,2,TAU2(NP1)-TAU2S,IER)
      CALL EXPNI(E2B3S,2,TAU3(NP1)-TAU3S,IER)
      LST=0
      EB2S=DMLIN(EBLT,.05,.135,1,300,0.0,0.001,IER)
      EB3S=DMLIN(EBLT,.135,20.,1,300,0.0,0.001,IER)
      CALL EXPNI(E12S(1),1,ABS(TAU2S-TAU2(1)),IER)
      CALL EXPNI(E13S(1),1,ABS(TAU3S-TAU3(1)),IER)
      DO 60 L=2,NP1
      CALL EXPNI(E12(L),1,ABS(TAU2(M)-TAU2(L)),IER)
      CALL EXPNI(E13(L),1,ABS(TAU3(M)-TAU3(L)),IER)
      CALL EXPNI(E12S(L),1,ABS(TAU2S-TAU2(L)),IER)
      CALL EXPNI(E13S(L),1,ABS(TAU3S-TAU3(L)),IER)
      SUM2=(EB2(L)*E12(L)+EB2(L-1)*E12(L-1))*(TAU2(L)-TAU2(L-1))*.5+
     1  SUM2
      SUM3=(EB3(L)*E13(L)+EB3(L-1)*E13(L-1))*(TAU3(L)-TAU3(L-1))*.5+
     1  SUM3
      SUM2S=(EB2(L)*E12S(L)+EB2(L-1)*E12S(L-1))*(TAU2(L)-TAU2(L-1))
     1  *.5+SUM2S
      SUM3S=(EB3(L)*E13S(L)+EB3(L-1)*E13S(L-1))*(TAU3(L)-TAU3(L-1))
     1  *.5+SUM3S
   60 CONTINUE
      DIVRAD=2.*ZK2(M)*(E2A2*EB2(1)+E2B2*EB2(NP1)+SUM2-2.*EB2(M))
     1  +2.*ZK3(M)*(E2A3*EB3(1)+E2B3*EB3(NP1)+QS*E2B2*E2B3+
     2  SUM3-2.*EB3(M))
      DIVRAS=2.*ZK2S*(E2A2S*EB2(1)+E2B2S*EB2(NP1)+SUM2S-2.*EB2S)
     1  +2.*ZK3S*(E2A3S*EB3(1)+E2B3S*EB3(NP1)+QS*E2B2S*E2B3S
     2  +SUM3S-2.*EB3S)
      AS=(32.2*0.2162*DIVRAD/(RHO(I)*U(I)))
      BS=32.2*0.2162*((DIVRAD-DIVRAS)/DELT+DIVRAD/TEMP(I))/(RHO(I)*
     1  U(I)*CP(I))
      RETURN
      END
```

```
      SUBROUTINE RADWAL
      COMMON/BLK1/LST,TS,AS,BS,TEMPA(050),RHOA(050),YA(050),EB2(050),
     1  EB3(50),TAU2(050),TAU3(050),ZK2(050),ZK3(050)
      COMMON/BLK2/N,NP1,NP2,NP3,NEQ,NPH,KEX,KIN,KASE,KRAD,PEI,AMI,AME,
     1  DPDX,XU,XD,XP,XL,DX,INTG,CSALFA,HGS,CINF(10),PREF(10),
     2  PR(10),P(10),U(050),F(10,050),R(050),RHO(050),DM(050),Y(050),
     3  DEN(050),AMU(050)
      COMMON/BLK3/KRP,MACH,KR,INDI(10),INDE(10),SUMR,AK,ALMG,BETA,TAUI
     1  ,TAUE,VINF,DELTA,TW,TINF,QS,YL,UMAX,UMIN,FR,YIP,YEM,TR,HW,
     2  HF(10),GAMA(10),AJI(10),AJE(10),SC(050),AU(050),BU(050),CU(050),
     3  A(10,050),B(10,050),C(10,050),TEMPE(050),TEMP(050),PO(050),
     4  AMACH(050),CP(050)
      DIMENSION E2T2(200),E2T3(200)
      SUMR2=0.0
      SUMR3=0.0
      E2T2(1)=1.0
      E2T3(1)=1.0
      CALL EXPNI(E3T2,3,TAU2(NP1),IER)
      CALL EXPNI(E3T3,3,TAU3(NP1),IER)
      DO 15 K=2,NP1
      CALL EXPNI(E2T2(K),2,TAU2(K),IER)
      CALL EXPNI(E2T3(K),2,TAU3(K),IER)
      SUMR2=(EB2(K)*E2T2(K)+EB2(K-1)*E2T2(K-1))*(TAU2(K)-TAU2(K-1))
     1  *.5+SUMR2
      SUMR3=(EB3(K)*E2T3(K)+EB3(K-1)*E2T3(K-1))*(TAU3(K)-TAU3(K-1))
     1  *.5+SUMR3
   15 CONTINUE
      SUMR=2*EB2(1)-2.*EB2(NP1)*E3T2-2.*SUMR2
     1  +  2*EB3(1)-2.*EB3(NP1)*E3T3-2.*SUMR3
C     REFT=0.0
C      SUMR=(1.0-REFT)*SUMR/3600.
      RETURN
      END
```

```
      SUBROUTINE EXTRA
      COMMON/BLK2/N,NP1,NP2,NP3,NEQ,NPH,KEX,KIN,KASE,KRAD,PEI,AMI,AME,
     1 DPDX,XU,XD,XP,XL,DX,INTG,CSALFA,HGS,CINF(10),PREF(10),
     2 FR(10),P(10),U(050),F(10,050),R(050),RHO(050),OM(050),Y(050),
     3 DEN(050),AMU(050)
      COMMON/BLK3/KRP,MACH,KR,INDI(10),INDE(10),SUMR,AK,ALMG,BETA,TAUI
     1 ,TAUE,VINF,DELTA,TW,TINF,QS,YL,UMAX,UMIN,FR,YIP,YEM,TR,HW,
     2 HF(10),GAMA(10),AJI(10),AJE(10),SC(050),AU(050),BU(050),CU(050),
     3 A(10,050),B(10,050),C(10,050),TEMPE(050),TEMP(050),PO(050),
     4 AMACH(050),CP(050)
      COMMON/BLK4/NH,NNO,NNP,NO,NN,NO2,NN2,NE,IND(10),STO,AKS,RT,FT,
     1 AMT,DRAGC,STNO,TAUIW,QW,UGU,UGD
      COMMON/K/KRI
      COMMON/GC/GCON(050),AMOL(050)
      KIN=1
      NEQ=4
      KEX=2
      NPH=NEQ-1
      N=30
      NP1=N+1
      NP2=N+2
      NP3=N+3
      PINF=14.7
      TR=537.0
      UGCON=1543.0
      AMOL1=29.0
      AMOL2=29.0
      DO 113 I=1,NP3
  302 AMOL(I)=1.0/((F(2,I)/AMOL1)+(F(3,I)/AMOL2))
  113 CONTINUE
      DO 303 I=1,NP3
  303 GCON(I)=UGCON/AMOL(I)
      AMU1=1.2267334E-05
      AMU2=1.2267334E-05
      DO 301 I=1,NP3
  301 AMU(I)=(F(2,I)*AMU1/AMOL1)/(F(2,I)/AMOL1+0.3535*((1.+AMOL1/
     1 AMOL2)**(-0.5))*((1.+(AMU1/AMU2)**0.5*((AMOL2/AMOL1)**0.25))**
     2 2.))+(F(3,I)*AMU2/AMOL2)/(F(3,I)/AMOL2+0.3535*((1.+AMOL2/AMOL1
     3 )**(-0.5))*((1.+(AMU2/AMU1)**0.5*((AMOL1/AMOL2)**0.25))**2.))
      DO 304 I=1,NP3
  304 DEN(I)=PINF*144./(GCON(I)*TR)
      CP1=5990.0
      CP2=5990.0
      DO 306 I=1,NP3
  306 CP(I)=F(2,I)*CP1+F(3,I)*CP2
C     INTIAL VALUE OF AUXILIARY PARAMETERS
      TEMP(1)=TW
      DO 300 I=2,NP2
      TEMP(I)=(F(NH,I)-U(I)*U(I)/2.0)/CP(I)
  300 TEMPE(I)=TEMP(I)
      CALL DENSTY
```

```
      DO 351 I=1,NP3
      RO(I)=DEN(I)*(TR/TEMP(I))*(GCON(I)*TEMP(I)+0.5*U(I)/32.2)/144.
  351 AMACH(I)=U(I)/SQRT(1.4*32.2*GCON(I)*ABS(TEMP(I)))
C     CALCULATION OF RADII
      CALL RAD(XU,R(1),CSALFA)
      IF(CSALFA.EQ.0.OR.KRAD.EQ.0) GO TO 27
      DO 28 I=2,NP3
   28 R(I)=R(1)+Y(I)*CSALFA
      GO TO 29
   27 DO 30 I=2,NP3
   30 R(I)=R(1)
   29 CONTINUE
C     CALCULATION OF OMEGA VALUES
      OM(1)=0.
      OM(2)=0.
      DO 49 I=3,NP3
   49 OM(I)=OM(I-1)+.5*(RHO(I)*U(I)*R(I)+RHO(I-1)*U(I-1)*R(I-1))*
     1 (Y(I)-Y(I-1))
      PEI=OM(NP2)
      DO 59 I=3,NP1
   59 OM(I)=OM(I)/PEI
      OM(NP2)=1.
      OM(NP3)=1.
      IF(NEQ.EQ.1)RETURN
      DO 69 J=1,NPH
      IF(KEX.EQ.1)INDE(J)=1
      IF(KIN.EQ.1)INDI(J)=1
   69 CONTINUE
      RETURN
      END
```

END

8-87

DTIC